
# *IN SILICO* DRUG REPURPOSING AGAINST *Salmonella typhimurium* LT2 Dam PROTEIN

M.Sc. Thesis

2023

Submitted to

Central Department of Biotechnology

Tribhuvan University

Kirtipur, Kathmandu, Nepal

For partial fulfillment of the requirement for the

Master of Science in Biotechnology

By

Suja Maharjan

Supervisors

Dr. Pramod Aryal, MS-PhD

Assistant Professor Alina Shri Sapkota

Registration No: 6-2-37-2662-2016

# ACKNOWLEDGEMENT

I would like to express my special thanks gratitude to my supervisor, Dr. Pramod Aryal, for his unwavering support and guidance throughout the completion of my thesis, especially during the challenging times of the COVID-19 pandemic. His encouragement and motivation during the difficulties I faced during my thesis period was invaluable.

I am deeply grateful to the Covid-19 Crisis Management Center (CCMC) and the Nepal Army for believing and bringing us to the university premises during the pandemic to conduct the research. I would also like to extend my thanks to Achyut Basnet and Anju Baniya for providing a supportive environment to work in at Nepal Professors' Guest House.

I would like to acknowledge the Research Center for Applied Science and Technology for providing financial support throughout my thesis. I am also grateful to Pro. Dr. Narayan Prasad Adhikari, from the Central Department of Physics at TU, for introducing new technology (Gaussian Software) and providing ongoing guidance to complete my thesis.

I would like to express my gratitude to Alpha Agro Private Limited and the Ex-students of Buddhanilakantha School (400A Batch) for providing me with a computer and software.

I am also thankful to Prof. Dr. Krishna Das Manandhar, the HOD of Central Department of Biotechnology at Tribhuvan University, for allowing me to complete my thesis. I would like to acknowledge my friends Bidit Lamshal and Tikaram Bhandari, from the Central department of Physics, for their help and cooperation during the research.

I would like to extend my gratitude to my seniors Sabina Thapa Magar, Sita Ghimire, Pooja Pathak, and Ritu Kumari Oli for their assistance during my time of need. I would also like to express my thanks to my friends Bisheshta Nepal, Guheshwori Chataut, Kabita Kandel, Samiran Subedi and Siddhartha Gautam for their contributions both direct and indirect, to my thesis.

Finally, last but not the least I would like to express my utmost gratitude to my parents, my husband Suvash Chandra Gurung and my brother Sujan Maharjan for their ongoing support, help and encouragement throughout my studies and writing my thesis. Their unwavering faith in me has given me the strength and determination to complete my thesis. I am truly grateful for their love and support.

Thanks for all your support and encouragement!!!

**Suja Maharjan**

# LIST OF ABBREVATIONS

| | |
|---|---|
| ADME/Tox | Absorption, Distribution, Metabolism, Excretion, Toxicity |
| AMEs | Aminoglycoside Modifying enzymes |
| AMR | Antimicrobial resistance |
| BLAST | Basic Local Alignment Search Tool |
| CADD | Computer Aided Drug Design |
| CAM | Chloramphenicol |
| CAMD | computer-assisted molecular design |
| CATs | Chloramphenicol Acetyltransferases |
| CRE | Carbapenem- resistant Acinetobacter |
| Dam | DNA adenine methylase |
| DEG | database of essential genes |
| DFT | Density Function Theory |
| ECDC | European Centre for Disease Prevention and Control |
| EF-G | Elongation Factor G |
| EFSA | European Food Safety Authority |
| EGGS | Essential Genes on Genome Scale |
| EMA | European Medicines Agency |
| ESBLs | Extended Spectrum β-lactamases |
| FDA | Food and Drug Administration |
| GAP-AMR | Global Action Plan on Antimicrobial Resistance |
| GLASS | Global Antimicrobial Resistance Surveillance System |
| HGT | Horizontal Gene Transfer |
| LBDD | ligand based drug design |
| MD | Molecular Dynamics |
| MDR | Multi-Drug Resistance |
| MEP | Molecular Electrostatic Potential |
| MGEs | Mobile Genetic Elements |
| MRSA | Methicillin Resistant *Staphylococcus aureus* |
| MSSA | Methicillin-Sensitive *Staphylococcus aureus* |

| | |
|---|---|
| NMR | Nuclear Magnetic Resonance |
| OGEE | Online GEne Essentiality database |
| PBPs | Penicillin-Binding Proteins |
| ProSA | Protein Structure Analysis |
| QQ | Quorum Quenching |
| QS | Quorum Sensing |
| QSAR | Quantitative Structure-Activity Relationship |
| RBS | ribosome binding site |
| RCSB | Research Collaboratory for Structural Bioinformatics |
| ROF or RO5 | Rule of Five |
| SAM | S-Adenosyl methionine |
| SBDD | Structure based drug design |
| SBVS | structure-based virtual screening |
| SD | Shine-Dalgarno |
| SN | Sulphonamides |
| TPPs | Target Protection Proteins |
| UTR | untranslated region |
| VRE | Vancomycin- Resistant enterococci |
| VRSA | Vancomycin- resistant *Staphylococcus aureus* |

# LIST OF TABLES

# LIST OF FIGURES

# TABLE OF CONTENTS

# ABSTRACT

The increasing prevalence of Multidrug-Resistant (MDR) pathogens has resulted in the failure of current antibiotics to effectively treat these infections. Computer-Aided Drug Discovery (CADD) has become a crucial tool in the drug discovery process recently. It has been demonstrated to be a successful method for screening lead compounds against target proteins within a short amount of time and with optimal resources. In the present study, a computational approach, CADD tools were employed to identify novel drug candidates against *Salmonella enterica* serovar Typhimurium LT2, targeting its essential gene, *Dam*. Virtual screening of various ligand libraries was conducted. From the initial library consisting of 21,000 compounds from natural products, 10,342 compounds from indole derivatives, 1,685 compounds from Kinase Inbibitors and 3,118 compounds from Nucleoside mimetics after ADME/Tox and druglikeness filters were narrowed down the number of compounds to 205 Natural Products, 462 Indole Derivatives, 6449 Kinase Inhibitors, and 654 Nucleoside Mimetics. The final screening from molecular docking and binding energy resulted in the identification of four lead compounds, Antineoplaston A10 and Cardamonin from natural products, 5-cyclopentaneamido-1-ethyl-N-(2-methoxyethyl)-1H-indole-2-carboxamide from Indole Derivatives, 2-[[anilino(oxo)methyl]amino]-4,5-dimethoxybenzoic acid from Kinase Inhibitors and 3-[[[4-[2-(3,5-Dimethylpyrazol-1-yl)ethoxy]phenyl]methylamino]methyl]-1-(6-methylpyrimidin-4-yl)pyrrolidin-3-ol from Nucleoside Mimetics were identified as potential leads. These compounds showed higher binding affinity with the target protein and lower binding efficiency for human hMAT1A protein compared to the reference compound S-Adenosyl methionine (SAM) and S-adenosyl homocysteine (SAH). The stability and strength of protein-ligand binding were observed through protein-ligand interactions, Density Functional Theory (DFT), analysis of frontier molecular orbitals and vibrational spectra. The results suggest that these compounds may be potential candidates for further exploration against other MDR pathogens prioritized by the World Health Organization (WHO).



**Keywords:** CADD, Multidrug-Resistant, *Dam*, essential gene, lead compounds

# 1. INTRODUCTION

## 1.1 Background

The discovery and development of new drugs is a crucial process in the field of medicine, as it allows for the treatment and management of a wide range of diseases and medical conditions. Despite significant advancements in the field, the search for new and effective therapies remains ongoing, especially for diseases that are increasingly resistant to current treatments. This is largely due to the rapid development of antibiotic-resistant pathogens, which pose a significant challenge to public health. More than 50 years ago, it was already known that bacteria can develop resistance to antibiotics. By the late 1950s, most strains of *Staphylococcus aureus* had become resistant to penicillin, which was previously an effective treatment for these bacteria (Stapleton and Taylor, 2002). The World Health Organization (WHO) published a list of 12 families of bacteria that pose the greatest threat to human health in 2017. These bacteria were identified as the leading causes of severe and often deadly infections, including bacterial pneumonia, bloodstream infections, and infections in surgical wounds (Mulani *et al.,* 2019). WHO has categorized into three priority levels (critical, high, and medium) based on the urgency of need to develop new antibiotics to combat these pathogens.

Critical priority: These are bacteria that pose a high risk to human health and for which new antibiotics are urgently needed, includes- *Acinetobacter, Pseudomonas*, some Enterobacteriaceae such as: *Klebsiella pneumoniae, Escherichia coli* and *Enterobacter spp*.

High priority: This category comprises bacteria that cause a significant public health impact and have high levels of resistance to multiple antibiotics, includes- *Enterococcus faecium* and *Staphylococcus aureus* that are resistant to various antibiotics, such as vancomycin and fluoroquinolones.

Medium priority: This category includes bacteria that have a lower public health impact, but still pose a significant risk and require ongoing monitoring and research, includes- *Streptococcus pneumoniae* and *Shigella spp.* (Breijyeh *et al.,* 2020; Abdelaziz *et al*., 2021).

Antibiotic resistance is a naturally occurring phenomenon where bacteria develop resistance to antibiotics through genetic changes. However, the process is being accelerated by the overuse and misuse of antibiotics. Overuse allows susceptible bacteria to be killed, which then enables drug-resistant bacteria to spread. Further contributing factors to the spread of antimicrobial resistance include poor sanitation, poor infection control, and the use of antibiotics in farm animals (Reygaert, 2018). Additionally, new mechanisms of resistance, such as heteroresistance and mutant prevention concentration, further contribute to drug resistance. Heteroresistance is resistance to certain antibiotics by a subpopulation of resistant cells within a larger population of susceptible microorganisms. This can result in treatment failure and the spread of resistant bacteria (Andersson *et al.,* 2019).

Traditionally, the discovery and development of new drugs has relied on experimental approaches, such as laboratory testing and animal studies while these

methods have proven to be effective in many cases, they are also time-consuming, costly, and can be associated with ethical concerns. In recent years, computational methods have emerged as an alternative and complementary approach to traditional experimental methods, and have been used to discover and optimize potential drug candidates in a more efficient and cost-effective manner (Pina *et al.,* 2010). Computer aided drug discovery (CADD), also known as in silico drug discovery, involves the use of computational methods to analyze and predict the biological activity of potential drug candidates. This process typically involves the identification and evaluation of chemical compounds that show promise as treatments for specific diseases or medical conditions. It is an efficient tool for prioritizing active compounds in High-throughput Screening (HTS) in a short period of time, and can help identify potential drug candidates that might not be discovered through experimental means alone (Mallipeddi *et al.,* 2014). The cost of drug development could be reduced by up to 50% (Tan *et al.,* 2010). Additionally, it can aid in the identification of potential off-target effects and toxicity by screening compounds through parameters such as Absorption, Distribution, Metabolism, and Toxicity (ADME/Tox). These methods can help to improve the safety assessment of new compounds as well as more efficient selection of compounds that have a lower risk of adverse effects on human health, reducing both time and effort in the drug discovery process (Jorgensen, 2009).

Furthermore, CADD has been extensively used for drug repurposing as well. Examples of successfully repurposed drugs include Minoxidil, developed for hypertension and now indicated for hair loss. Viagra, which was originally prescribed for erectile dysfunction due to angina, has been successfully repurposed to treat erectile dysfunction, while Thalidomide, which was first prescribed to treat morning sickness, is now used to treat leprosy (Dudley *et al.,* 2011; Ashburn and Thor, 2004).

There are several approaches and algorithms that have been developed for the discovery of putative drugs using computational methods. One such approach is structure-based drug design, which involves the prediction of the biological activity of a compound based on its three-dimensional structure. De novo drug design and molecular docking are two SBDD techniques that use on crystal structures, Nuclear Magnetic Resonance (NMR) data, and homology models to determine the structure of the target macromolecule. Molecular docking is a computational method used in drug discovery to predict the interaction between a target protein and potential ligands. This method is used to screen large libraries of both ligands and targets and helps to identify the best-fit ligand for the target protein based on binding energy and other scoring functions. The protein structure can be obtained from Research Collaboratory for Structural Bioinformatics (RCSB) or predicted using tools like phyre2, swiss-model, modeller. Different softwares like Datawarrior, AutoDock and PyRx are used for molecular docking, scoring and determination of binding energy, to finalize the most suitable ligand for further analysis in drug discovery and drug repurposing (Chen *et al.,* 2012). Another approach is ligand-based drug design, such as quantitative structure-activity relationship (QSAR), pharmacophore modeling, molecular field analysis, and 2D or 3D similarity assessment, can offer crucial insights into the nature of the interactions between drug targets and ligands, allowing predictive models that are suitable for lead discovery and optimization to be

constructed in the absence of three-dimensional (3D) structures of potential targets (Acharya *et al.,* 2011).

Since essential genes are the crucial for the survival of the bacteria, targeting this would inhibit the metabolism, leading to death of the bacteria. Among the essential genes, Dam is one of them. Targeting Dam would be significant and valuable in the context of the development of the new antimicrobial agents.

## 1.2 Current Studies

Antimicrobial resistance (AMR) is a major concern for global health and well-being, as infections become more difficult to treat, leading to prolonged illness and potential death. The United Nations Secretary-General emphasized this in May 2019 by highlighting the negative impact that AMR has on public health, livelihoods, and the achievement of the Sustainable Development Goals (SDGs) (WHO, 2021). The World Health Organization (WHO) has been actively addressing the issue of Antimicrobial Resistance (AMR) for nearly two decades. In response to the growing concern about AMR, WHO initiated a range of activities aimed at promoting awareness and action on this issue. These activities included developing guidelines and tools for preventing and controlling AMR, as well as conducting research and advocacy initiatives. In May 2015, WHO's efforts to combat AMR culminated in the approval of the Global Action Plan on Antimicrobial Resistance (GAP-AMR) by the Sixty-Eighth World Health Assembly. The GAP-AMR outlines a comprehensive, coordinated global response to the threat of AMR and sets out a series of targets and actions for all countries to improve the use of antimicrobial medicines and reduce the spread of AMR (WHO Geneva, 2017). Furthermore, to address the AMR issue, WHO has established the Global Antimicrobial Resistance Surveillance System (GLASS) in October 2015 to establish a standardized approach for analyzing and sharing data on antimicrobial resistance (WHO Association Media Centre, 2015)

In 2011-12 hospital point-prevalence survey showed high levels of AMR in various types of bacteria. For example, 41% of *Staphylococcus aureus* isolates were resistant to meticillin, 10% of enterococci isolates were resistant to vancomycin, 33% of all *Enterobacteriaceae* isolates were resistant to third generation cephalosporins, 8% of *Enterobacteriaceae*, 32% of *Pseudomonas aeruginosa* and 81% of *Acinetobacter baumannii* isolates were resistant to carbapenems (Zarb *et al.,* 2012). In the USA and Europe, the problem of antimicrobial resistance is particularly acute and is estimated to cause 50,000 deaths each year (Teillant *et al.,* 2015). Additionally, AMR is increasingly being detected in community-acquired infections, although there is variation in the prevalence of AMR between countries. Moreover, antimicrobial resistance has also been detected in bacteria from food-producing animals. In particular, resistance to ampicillin, quinolones, tetracyclines, and sulfonamides has frequently been found in *Salmonella* and *Escherichia coli* isolates from broilers, artificially fattened turkeys, and meat. This highlights the need for better management practices in animal agriculture to reduce the spread of resistant bacteria and protect public health (Lazarus *et al.,* 2015; Le *et al.,* 2015). The report by the European Centre for Disease Prevention and Control (ECDC), European Food Safety Authority (EFSA), and European Medicines Agency (EMA) found that there is a link between the use of antibiotics in food-producing animals and the development

of antibiotic resistance in bacteria that can cause infections in humans. This connection was found through the analysis of data on antibiotic use in animals and the prevalence of antibiotic-resistant bacteria in both animals and humans. The findings showed that high levels of antibiotic use in food-producing animals can increase the risk of antibiotic resistance in bacteria that can cause infections in humans, and that these resistant bacteria can be transmitted from animals to humans through the food chain (European Centre for Disease Prevention and Control (ECDC) andEuropean Food Safety Authority (EFSA); European Medicines Agency (EMA), 2017).

The development of new antibiotics is crucial in addressing the growing threat of AMR, as many existing antibiotics are becoming less effective due to the increasing prevalence of multidrug-resistant organisms. Clinical studies and research efforts are focused on developing new, effective antibiotics to treat bacterial infections, especially those caused by critical and high-priority pathogens identified by WHO's Global Antimicrobial Resistance and Use Surveillance System (GLASS). However, the increasing need for alternative and often more expensive treatments also creates an economic burden for healthcare systems and individual patients. In 2003, despite a research expense of approximately 33 billion dollars, only 35 new compounds were registered with the Food and Drug Administration (FDA). This highlights the high cost and low return of traditional drug discovery methods. The Tufts Center for the Study of Drug Development estimated the cost of developing a prescription drug to be a staggering 2.558 billion dollars as published in the Journal of Health Economics in March 2016 (TUFTS CSDD R&D Cost Study, 2016). To overcome this challenge, efficient and cost-effective drug discovery processes are required. Computational strategies, such as virtual screening and in vitro techniques, have emerged as promising methods for assisting drug discovery and development (Lin *et al.,* 2020). Additionally, repurposing of drugs has been explored as a method for finding new drug candidates (Pushpakom *et al.,* 2019).

In this research, we mainly focused on the computational method- structure based CADD that have been developed for the discovery of putative drugs. We performed molecular docking on ligands that passed the criteria for druggability and ADME/Tox, to identify them as potential target inhibitors. Through our analysis, we hope to contribute to the ongoing efforts to identify and develop new drugs that can improve the lives of patients around the world.

## 1.3 Hypothesis

### 1.3.1 Null Hypothesis

The putative drug candidates to inhibit the Dam protein of *Salmonella enterica* serovar Typhimurium will not be identified through molecular docking techniques.

### 1.3.2 Alternative Hypothesis

The putative drug candidates to inhibit the Dam protein of *Salmonella enterica* serovar Typhimurium will be identified through molecular docking techniques.

## 1.4 Objectives

### 1.4.1 General Objective

- To identify novel lead compounds against SAM utilizing proteins of resistant pathogens prioritized by WHO to develop new drug.

### 1.4.2 Specific Objective

- To identify potential inhibitors (drug candidates) against the Dam gene of *Salmonella enteria* serovar Typhimurium from various ligand databases.
- To create ligand libraries by screening with the druggability parameters
- To perform Molecular docking against target protein and analyze protein ligand interactions.
- To evaluate the effectiveness of the identified inhibitors using in silico
- To advance the use of computer-aided methods in drug discovery and support the development of new treatments for Salmonella infection.

## 1.5 Rationale

The increasing emergence of antibiotic resistance among pathogens prioritized by the World Health Organization (WHO) highlights the urgent need for the development of novel antibiotics. To address this challenge, the current study aims to develop a more affordable and efficient technique for identifying therapeutic targets and potential drug candidates through virtual screening. This involves the determination of the binding affinity of lead molecules against the target and the stability of the ligand-protein complex analyzing using different softwares.

## 1.6 Scope of the study

The present study is focused on finding promising lead molecules for targeting Dam protein of *Salmonella enteria* serovar Typhimurium. The study involves conducting comprehensive screening and testing for antimicrobial activity.

# 2. LITERATURE REVIEW

## 2.1 Literature review related to antibiotics, antimicrobial resistance and underlying mechanisms

Antibiotics are those substances which are produced by a microorganism or similar product produced wholly (synthetic) or partially (semisynthetic) by chemical synthesis that have the ability, in low concentrations, of inhibiting the growth of or killing other microorganisms. They work by either inhibiting the growth of bacteria (bacteriostatic) or killing bacteria (bactericidal). Bacteriostatic antibiotics work by preventing bacteria from reproducing and dividing, which slows down the spread of the infection. Bactericidal antibiotics, on the other hand, actively kill bacteria and are more effective in treating serious infections. Antibiotics work by targeting specific structures or processes within bacteria. For example, some antibiotics target the bacterial cell wall, preventing it from forming or maintaining its structure, while others target bacterial protein synthesis, inhibiting the growth and division of the bacteria (Zimdahl *et al.,* 2015).

With the development of Penicillin in 1928 by Alexander Flemming, has brought the milestone change in the history to develop the antibiotics, the one that inhibits the growth of or destroys the microorganisms. But soon later, Penicillin resistance became the major problem as there was development of the resistance among the pathogens due to intrinsic and extrinsic mutations and other different parameters like- modification of the antibiotic molecule (Wilson *et al.,* 2014), decreased antibiotic uptake and efflux (Pages *et. al.*, 2008 and Machuca *et. al*., 2014), changes in target sites (Donhofer *et. al*., 2012; Li *et. al*., 2013), quorum sensing (Waters and Bassler, 2005) and biofilm formation (Hall and Mah *et. al*., 2017).

WHO defines Antimicrobial resistance (AMR) as the state of the microorganism (bacteria, viruses and parasites) that causes infection, resistant to the present available medicines (antibiotics), making the medicines ineffective, causes the severe illness and death (https://www.who.int/news-room/fact-sheets/detail/antimicrobial-resistance). The resistance is becoming one of the world's most urgent public health problems. Numerous important organizations, like the Centers for Disease Control and Prevention (CDC), Infectious Diseases Society of America, World Economic Forum, and the World Health Organization (WHO) have declared antibiotic resistance to be a "global public health concern" (Spellberg *et al.,* 2019). This can be correlated by the data given by CDC, in United States alone each year at least 2.8 million people are infected with antibiotic-resistant pathogen and 35,000 people die (CDC, 2020). Moreover, it is estimated that antibiotic resistance could result in the premature deaths of approximately 300 million people by 2050, with a potential loss of up to $100 trillion dollars to the global economy (Price, 2016). In 2019, CDC has categorized bacteria based on their threat level of antimicrobial resistance. Bacteria that pose an urgent or serious threat require a higher level of monitoring and preventive activities, while those considered concerning require less. The summary of information regarding the antimicrobial resistance bacteria is mentioned below and can be found at

https://www.cdc.gov/drugresistance/biggest-threats.html. The CDC categorizes bacteria into the following three threat levels:

Urgent Threats

These are the bacteria that pose a significant threat to public health and require immediate and aggressive action which include-

- Carbapenem- resistant Acinetobacter (CRE)
- *Candida auris*
- *Clostridioides difficile*
- Carbapenem- resistant Enterobacterales
- Drug- resistant *Neisseria gonorrhoeae*

Serious Threats

These are bacteria that pose a serious threat to public health and require increased attention and action which include-

- Drug-resistant *Campylobacter*
- Drug-resistant Candida
- Extended spectrum beta-lactamase producing Enterobacteriaceae (ESBLs)
- Vancomycin-resistant Enterococci (VRE)
- Multidrug-resistant *Pseudomonas aeruginosa*
- Drug-resistant nontyphoidal *Salmonella*
- Drug-resistant *Salmonella typhimurium*
- Drug-resistant *Shigella*
- Methicillin-resistant *Staphylococcus aureus* (MRSA)
- Drug-resistant *Streptococcus pneumoniae*
- Drug-resistant Tuberculosis

Concerning Threats

These are bacteria that pose a lower threat level, but still require monitoring and intervention, include-

- Vancomycin-resistant *Staphylococcus aureus* (VRSA)
- Erythromycin-resistant Group A *Streptococcus*
- Clindamycin-resistant Group B *Streptococcus*

The excessive use of antibiotics, both by humans and animals, is the leading factor behind the evolution of antibiotic resistance. Antibiotics, when overused, kill off the susceptible bacteria but allow the resistant pathogens to persist, multiply, and evolve through natural selection. Sir Alexander Fleming, the discoverer of penicillin, had warned of the dangers of overusing antibiotics, stating that “public will demand [the drug and] … then will begin an era … of abuses” (Spellberg and Gilbert, 2014). Other factors that contribute to the development of antibiotic resistance include inappropriate prescription practices (Lushniak, 2014), widespread agricultural use (Bartlett *et al.,* 2013) and many others.

### 2.1.1 Types of resistance to antibiotic

There are mainly four types of resistance to antibiotics which are- (i) Natural (intrinsic) resistance, (ii) Acquired resistance**,** (iii) Cross- resistance and (iv) Multi-drug resistance (Hasan and Al-Harmoosh, 2020).

#### 2.1.1.1 Natural (intrinsic) resistance

This type of resistance is not caused by the usage of the antibiotics but is associated by the bacteria's structural properties (Kadhum *et al.,* 2019). Here, the microorganism does not follow the target antibiotic structure or antibiotics as the characteristics of target and antibiotic does not match each other. For example- as there is mismatch of the characteristics of the outer membrane of gram negative bacteria, vancomycin antibiotic fail to move through the outer membrane of the gram negative bacteria, resulting bacteria naturally insusceptible to vancomycin (Antonoplis *et al.* 2019).

**Examples of bacteria with intrinsic resistance.**

| Organism | Intrinsic resistance |
|---|---|
| *Bacteroides* (anaerobes) | aminoglycosides, many β-lactams, quinolones |
| All gram positives | aztreonam |
| Enterococci | aminoglycosides, cephalosporins, lincosamides |
| *Listeria monocytogenes* | cephalosporins |
| All gram negatives | glycopeptides, lipopeptides |
| *Escherichia coli* | macrolides |
| *Klebsiella* spp. | ampicillin |
| *Serratia marcescens* | macrolides |
| *Pseudomonas aeruginosa* | sulfonamides, ampicillin, 1$^{st}$ and 2$^{nd}$ generation cephalosporins, chloramphenicol, tetracycline |
| *Stenotrophomonas maltophilia* | aminoglycosides, β-lactams, carbapenems, quinolones |
| *Acinetobacter* spp. | ampicillin, glycopeptides |

*Figure 1: Examples of bacteria with intrinsic resistance (Reygaert, 2018)*

#### 2.1.1.2 Acquired resistance

This type of resistance is due to the alteration of the genetic features of bacteria which is acquired (not affected by the antibiotics), emerge from the main chromosome or extra chromosome structures like plasmids, transposons etc. (Aljanaby *et. al.,* 2018). A chromosomal resistance occurs as a result of mutations in developing in spontaneous bacterial chromosome which may be due to some physical (UV-rays etc.) and chemical factors (Majeed *et al.,* 2019). The antibiotics like- Streptomycin, aminoglycosides, erythromycin and lincomycin are susceptible to this type of resistance (Krause *et al.,* 2016)

#### 2.1.1.3 Cross-resistance

Cross-resistance refers to the resistance of microorganisms to a particular type of antibiotics due to the similarities in their structures or mechanisms of action (Etebu and Arikekpar, 2016). For instance, bacteria that are resistant to cephalosporins may

also exhibit resistance to penicillins, and bacteria resistant to neomycin may also show resistance to kanamycin (Jahne *et al.,* 2015).

#### 2.1.1.4 Multi- drug resistance

Some microorganisms typically pathogens are not susceptible to more than one antibiotics i.e particular one or more than one drug is unable to kill or control the bacteria (pathogen), occurs as a result of inappropriate utilization of antibiotics (Dheda *et al.,* 2017). This type of resistance is induced by two mechanisms-bacteria acquiring several genes and increased expression of genes that code for multidrug efflux pumps, enzymatic inactivation, changes in the structure of the target (Salloum *et al.,* 2020).

### 2.1.2 Mechanisms of antibiotic resistance

#### 2.1.2.1 Genetic Basis of Resistance

The evolution of resistance in bacteria is facilitated by the acquisition of mobile genetic elements, such as plasmids, through processes such as transformation, transposition, and conjugation (known collectively as horizontal gene transfer or HGT), plus mutation in its own chromosomal DNA. Plasmids, transposons and integrons are the mobile genetic elements (MGEs) play crucial role in the development and the dissemination of antimicrobial resistance among clinically relevant organisms (Piddock, 1995).

**Horizontal Gene Transfer (HGT)**

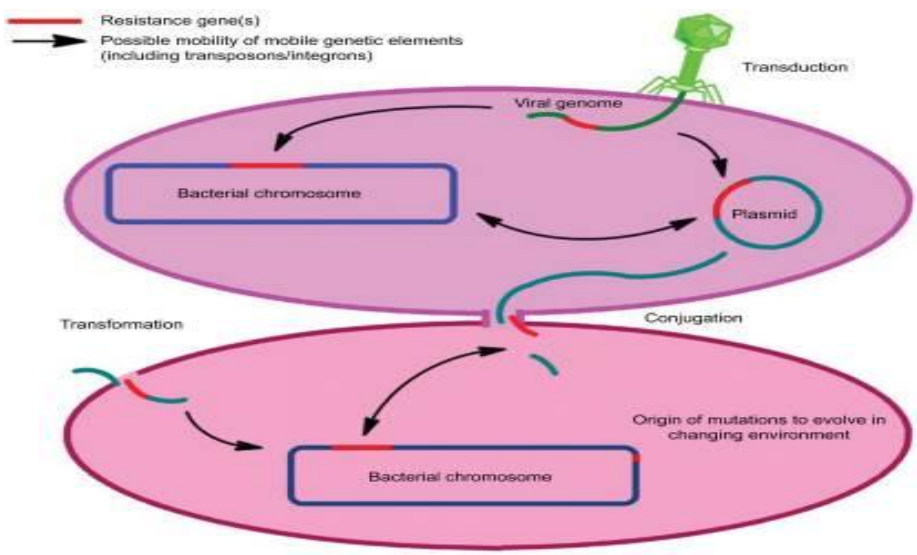


*Figure 2: Mechanism of transfer of resistance gene through horizontal gene transfer (Aslam et al., 2018)*

Horizontal gene transfer (HGT) is the exchange of genetic information between organisms. This process includes the spread of antibiotic resistance genes among bacteria (except for those from parent to offspring), resulting in Multi- Drug Resistant (MDR) development (Le Roux and Blokesch, 2018) which in turn creates the new “superbugs”. When the transferred genes and pathogens continue to evolve, often results the development of bacteria with greater resistance (McCarthy *et al*., 2014).

HGT occurs by three mechanisms-

1. Transformation: The process where bacteria acquire DNA from their environment

2. Conjugation: The process where bacteria directly transfer genes to another cell by using mainly MGEs as vehicles to share genetic information and chromosome to chromosome direct transfer has also been seen (Manson *et al.,* 2010).

3. Transduction: The process where bacteriophages transfer genes from one cell to another

Currently, there are two prevailing approaches to detect the HGT among the organisms- i) composition based approach- based on comparing base and codon usage composition across genes within a genome and ii) phylogeny based approach- based on taking higher sequence similarity and constructing their corresponding phylogeny to homologs which is encoded by more distantly related taxa compared with close relatives (Adato *et al.,* 2015).

**Mutational Resistance**

Mutation is one of the mechanisms of resistance to many antibiotics. Mutations can be occurred in different ways and shows various effects such as- point mutations in the gene encoding DNA gyrase can alter the binding efficiency of quinolones, which reduces their efficacy. Similarly, multiple point mutations lead to higher levels of resistance (Michael *et al.,* 2006). In addition, chromosomal mutations are the cause of *H. pylori*'s clarithromycin resistance (in 23S rRNA), amoxycillin (changes in penicillin binding protein 1) (Okamoto *et al.,* 2002) and so on. The bacterial populations with especially high mutation rates which are called as hypermutable strain often have higher antibiotic resistance rates than the normal mutated strains. As for instance, in a study of cystic fibrosis (CF) patients infected with *P. aeruginosa* (a major cause of sickness and death among CF patients, it was found that more than a third of all CF patients had hypermutable *P. aeruginosa* infections and were resistant to the antibiotics like aminoglycosides, quinolones B-lactams and fosfomycin (Oliver *et al.,* 2000).

### 2.1.2.2 Mechanistic Basis of Resistance

The ways to transfer the drug molecule inside the bacterial cell is diffusion through porins, bilayer or by self- uptake. Thus, the bacteria prevent the accumulation of the antimicrobials by taking various actions such as- decreased permeability, efflux pump, enzymatic modifications of antibiotics, enzymatic breakdown of antibiotics and modification in target site (Kapoor,2017).

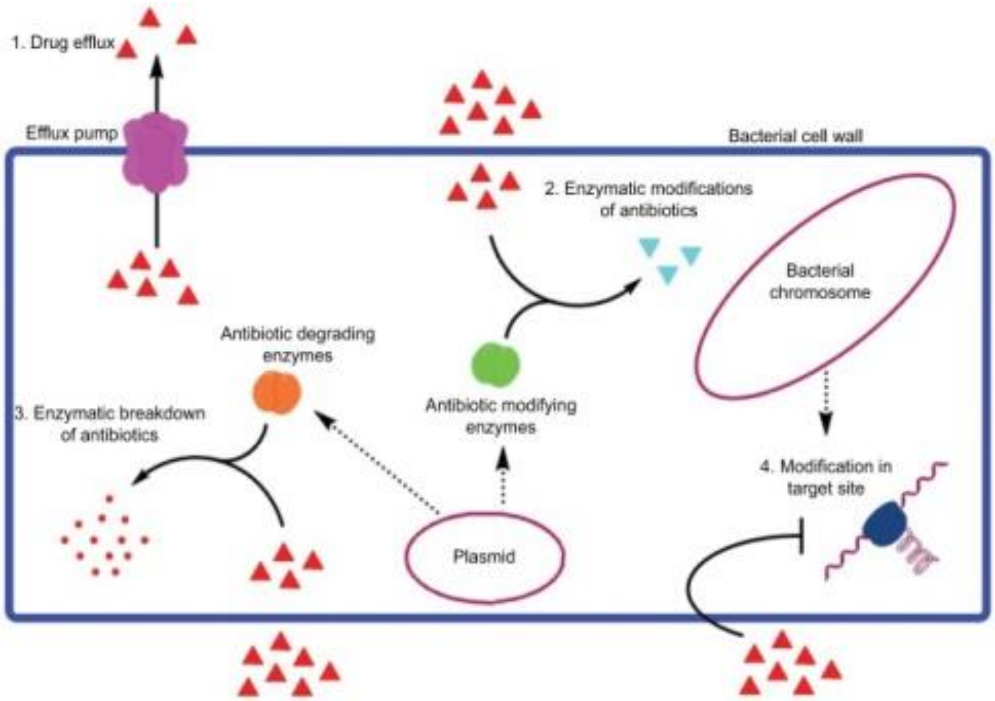


*Figure 3: Various Mechanistic basis of resistance (Aslam et al., 2018)*

**Decreased Permeability**

The small hydrophilic molecules such as- B-lactams and quinolones are transferred inside the cell by crossing the outer barrier- outer membrane via porins. Thus decrease in the number of porin channels leads to the decrease in the entry of these antibiotics which makes the cell resistance to these antibiotics (Pages *et al.,* 2008).

**Efflux pump**

Despite the presence of an outer barrier in the form of an outer membrane, some microorganisms possess the ability to eliminate antibiotics that have entered the cell through a mechanism known as efflux pumps. Efflux pumps are membrane proteins located on the cytoplasmic membrane, which help to expel antibiotics from the cell, keeping the concentration of these drugs at low levels inside the cell (Džidic *et al.,* 2008).

### 2.1.2.3 Modifications of the antibiotic molecule

To reduce the effect of antibiotics, bacteria have the ability to produce enzymes that deactivate the drugs. There are two primary methods that the bacteria use to inactivate the antibiotics: modification of the drug through transfer of chemical groups or chemical changes, and breakdown of the drug (Munita and Arias, 2016).

**I. Chemical alterations of the antibiotics**

Drug inactivation through the transfer or the alteration of the chemical group to the drug occurs through mainly three processes- (a) acetylation (chloramphenicol, aminoglycosides, streptogramins), (b) Phosphorylation (chloramphenicol, aminoglycosides) and (c) adenylation (lincosamides, aminoglycosides) (Blair *et al.,* 2015).

One of the examples of resistance via chemical alterations of the drug is the presence of aminoglycoside modifying enzymes (AMEs) which covalently modify the hydroxyl or amino groups of the aminoglycoside molecule, resulting in the alteration of chemical structure of the drug. Similarly, another example of enzymatic alteration of an antibiotic involves the modification of chloramphenicol, an antibiotic which interacts with the peptidyl-transfer center of the 50S ribosomal subunit and inhibits protein synthesis. Here the chemical modification of chloramphenicol is done by the expression of acetyltransferases known as CATs (chloramphenicol acetyltransferases). It has been reported that there is presence of multiple cat genes in both gram- both gram-positives and gram-negatives that have been classified in two main types. Type A and Type B. Type A result in high level of resistance whereas Type B result in low level of chloramphenicol resistance (Schwarz *et al.,* 2004).

**II. Destruction of the antibiotic molecule**

The production of certain enzymes such as- β-lactamases is the most common resistance mechanism used by gram negative bacteria against β-lactam drug. These enzymes inactivate or destroy the β-lactam antibiotics like- penicillin and cephalosporin by hydrolyzing a specific site in the β-lactam ring structure, causing the ring to open. Thus, the open-ring drugs are unable to bind to their target Penicillin Binding Proteins (PBP) proteins (Alekshun and Levy, 2007).

The pharmaceutical industry has successfully employed two strategies as the solution to the resistance caused by β-lactamase β-lactams: (a) the optimization of β-lactamase stable antibiotics (such as the expanded-spectrum cephalosporins and carbapenems that are resistant to hydrolysis by narrow spectrum β-lactamases or extended-spectrum β-lactamases) and (b) the development of selective β-lactamase inhibitors (BLIs) which are to be co-administered with a β-lactam antibiotic. In clinical practice it was found that the combinations of β-lactams with clavulanic acid, sulbactam, and tazobactam are intensively used to inhibit class A enzymes (Docquier and Mangani, 2018). Moreover, in March 2015, non-β-lactam β-lactamase inhibitor, avibactam in combination with ceftazidime (4:1 ratio) for the treatment of complicated urinary tract infections was successful. Avibactam efficiently inhibits most class A β-lactamases and both the chromosome and plasmid-encoded class C enzymes and several class D β-lactamases (Ehmann *et al.,* 2012). There are many other structurally-related β-lactamase inhibitors which has reached the stage of clinical development like- merck compound relebactam in combination with imipenem (Blizzard *et al.,* 2014), zidebactam (currenlty developed in combination with cefepime) and ETX2514 (Shapiro *et al.,* 2017).

### 2.1.2.4 Modification and protection of target site

One of the strategy the bacteria develop to avoid the action of the antibiotic is by interfering with their target site. This is achieved by modification and protection of the target site. The modification of the target site is done by- (i) mutations of the target site (ii) enzymatic alterations of the target site and (iii) complete replacement or bypass of the target site (Munita and Arias, 2016).

Resistance to the glycopeptide antibiotics such as- vancomycin in enterococci and in *Staphylococcus aureus* (MRSA) is one of the example of antibiotic resistance carried

out via modification of the target site. Here, resistance is mediated through the acquisition of *van* genes clusters: Van A and Van B. These gene clusters encode enzymes which produce a modified peptidoglycan precursor terminating in d-Alanyl-d-Lactate (d-Ala-dLac) instead of d-Ala-d-Ala. Thus, changes in the structure of peptidoglycan precursors cause altered pattern of intermolecular hydrogen bonding resulting low binding affinity of vancomycin (Cox and Wright, 2013).

Similarly, the drugs that target nucleic acid synthesis such as- fluoroquinolones, resistance is carried out through chromosomal mutations in both the DNA gyrase and topoisomerase IV target enzymes. In gram negative bacteria mutations occurs in DNA gyrase than in Topoisomerase IV such as- GyrA or GyrB subunits of DNA gyrase whereras in gram positive bacteria mutations occur more frequently in topoisomerase IV than DNA gyrase such as- ParC (GrlA in *Staphylococcus aureus*). These mutations cause changes in the structure of gyrase and topoisomerase that ultimately decrease or eliminate the ability of the drug to bind to these components (Redgrave *et al.,* 2014).

Furthermore, bacteria also develop resistance against antimicrobials through the protection of the target sites by target protection proteins (TPPs). This mechanism is seen in drugs like tetracycline-Tet[M] and Tet[O]), fluoroquinolones (Qnr) and fusidic acid (FusB and FusC) (Munita and Arias, 2016). TPPs mediate the antibiotic resistance three mechanisms: (a) Type I- by sterically removing drug from the target, (b) Type-II- by inducing conformational changes within the target by which the drug is dissociated from the target and (c) Type-III- by restoration of the target function despite the presence of the bound antibiotic (Wilson *et al.,* 2020).

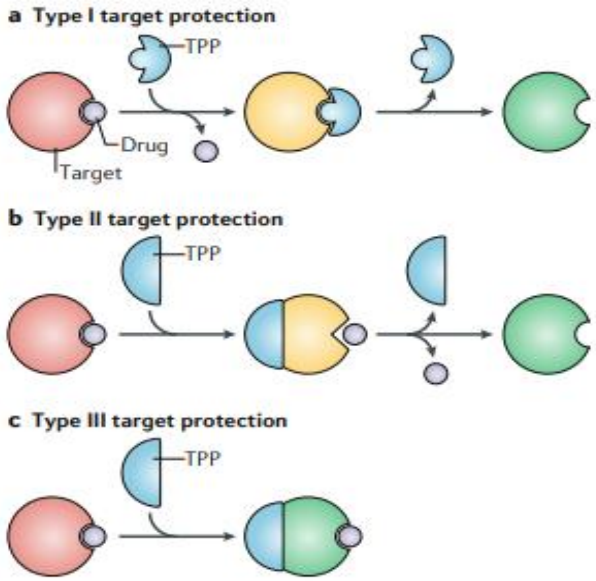


*Figure 4: Mechanism of target protection types (Wilson et al., 2020)*

One of the example of target protection mechanism carried out by bacteria is tetracycline resistance determinants Tet(M) and Tet(O). It was found that there are 20 different groups of tetracycline- resistance proteins (Roberts, 2005), among them Tet(M) and Tet(O) are best known and are paralogs of translation Elongation Factor

G (EF-G) that actively remove tetracycline from the ribosome in a GTP-hydrolysis-dependent manner (Li *et al.,* 2013).

### 2.1.2.5 Quorum sensing and Biofilm formation

Quorum sensing (QS) is a bacterial cell–cell communication at molecular level that involves the production, detection, and response to extracellular signaling molecules called autoinducers (AIs). As the bacterial population density increases, AIs accumulate in the environment, as a result bacteria changes in their cell numbers and collectively alter gene expression (Dincer *et al.,* 2020). The process of Quorum Sensing (QS) is responsible for coordinating various biological functions in bacteria, including bioluminescence, spore formation, competence, antibiotic production, tolerance to disinfectants, toxin production, drug resistance, biofilm formation, and secretion of virulence factors (reviewed in Novick and Geisinger 2008; Ng and Bassler 2009; Williams and Camara 2009).

Bofilm formation in the microorganisms is one of the reasons of the antibiotic resistance which contribute to chronic infections (Cepas *et al.,* 2019). According to the CDC over 65% of chronic hospital infections are due to biofilm formation in bacteria (Davey and O'toole, 2000) as microbial cells within biofilms are reported to have 10-1000 times more antibiotics resistance than the planktonic cells (Mah, 2012). Biofilms not only provide the protection to the microorganism from altered pH, osmolarity, nutrients scarcity, mechanical and shear forces but also block the access of bacterial biofilm communities from antibiotics and host's immune cells (Fux *et al.,* 2005). This is the reason for the additional resistance power to bacteria that makes them to not only tolerate harsh conditions but also resistant to antibiotics. Consequently, this lead to the emergence of bad bugs infections like multi drug resistant, extensively drug resistant and totally drug resistant bacteria.

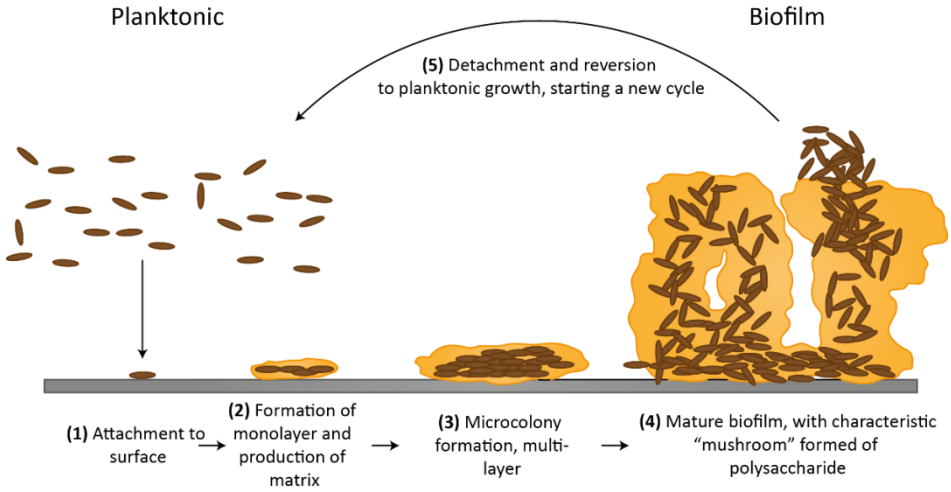


*Figure 5: Process of microbial biofilm formation (Vasudevan, 2014)*

Biofilm formation is regulated in three steps- (i) adsorption of molecules (macro and micro molecules) to surfaces; (ii) bacterial adhesion to the surface and release of extracellular polymeric substances (EPS) and (iii) colony formation and biofilm maturation (Sharma *et al,* 2019). Many pathogens often start a disease by creating organized biofilms, which increase their ability to adhere, replicate, and express their virulence. Microorganisms that form biofilms are often resistant to antibiotics

because of various factors such as: a) the formation of a polymeric matrix which restricts the diffusion of antibiotics, (b the interaction of antibiotics with the polymeric matrix which reduces their activity, (c) enzyme-mediated resistance such as β-lactamase, (d) changes in metabolic activity within the biofilm (Høiby *et al.,* 2010). Those microorganisms that form biofilm are able to collect high amounts of β-lactamases in the biofilm matrix as a defense mechanism which ultimately cause resistance to antibiotics. For example- when *Pseudomonas aeruginosa* biofilm matrix accumulates β-lactamases, it increases hydrolysis of antibiotics, such as imipenem and ceftazidime (Bagge *et al.,* 2004). Similarly, ampicillin is unable to reach the deeper layers of *Klebsiella pneumoniae* biofilms that are associated with β-lactamase activity and upon deletion of β-lactamase is found to increase the amount of ampicillin that reaches the deep layer (Anderl *et al.,* 2000).

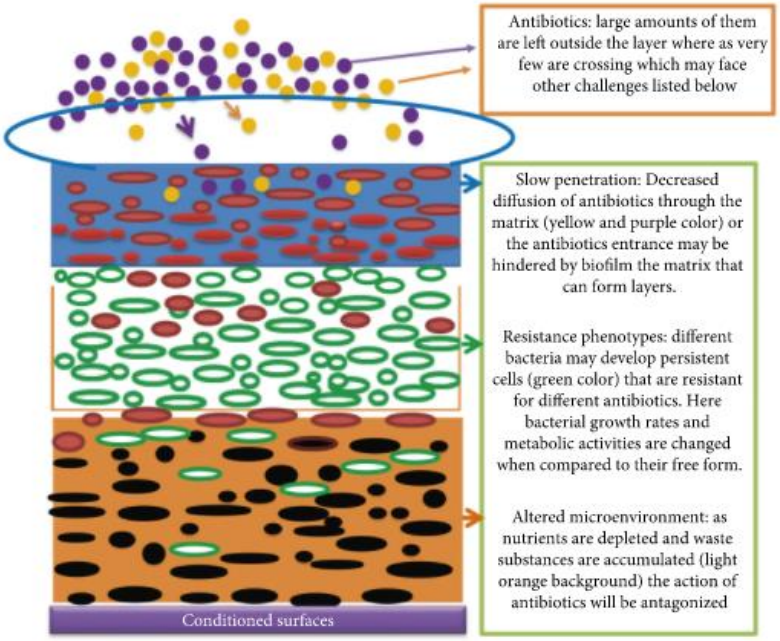


*Figure 6: Resistance shown by bacteria due to biofilm formation (Stewart et al., 2001, modified by (Gedif Meseret Abebe, 2020)*

There are many examples of biofilm infections threatening the human health, including ventilator-associated pneumonia, bronchiectasis, bronchitis, cystic fibrosis, upper respiratory airway infections (Anderson *et al.,* 2013) chronic infections of bone, cardiac tissues, middle ear, gastrointestinal tract, eye, urogenital tract, prosthetic infections and so on (Amaning *et al.,*2020). Moreover, microbial biofilms also affect indwelling medical devices such as contact lenses, central venous catheters, mechanical heart valves, peritoneal dialysis catheters, orthopedic implants and prosthetic joints, pacemakers, vascular grafts, dental diseases, urinary catheters and voice prostheses (Percival and Kite, 2007). This can lead to device failure, chronic infections and high mortality and morbidity rates (Sohns *et al.,* 2017). Furthermore, it has been estimated that the treatment of implant-associated infections removal/ replacement and antibiotic therapy cost high more than $50,000 along with high-risk surgeries.

To address the issue of microbial resistance, various approaches are being used. Some of these include: (i) Quorum quenching (QQ) which aims to interfere with the Quorum Sensing (QS) system of specific microorganisms, thereby reducing the expression of harmful factors (Wu *et al*., 2020), (ii) electrical and electromagnetic methods such as the application of DC voltage, low AC currents, pulsed electric fields, capacitive coupling treatment, and extremely low-frequency electromagnetic waves (ELF-EMF) (Freebairn *et al.* 2013), (iii) antibacterial coatings (Veerachamy *et al.,* 2014), (iv) surface modification of biomaterials, used in implantable devices to prevent the growth of bacteria (Puiu *et al.,* 2017), (v) antimicrobial photodynamic therapies, which involve the use of light absorbing compounds (photosensitizers) to produce reactive oxygen species and eradicate bacterial cells (Donelli, 2015), (vi) early diagnosis of biofilm formation using biosensors (Khatoon *et al.,* 2018).

## 2.2 Literature review related to bacterial essential gene

Essential genes are indispensable genes which are required for the survival of the organism or a cell. Studies on the bacterial essential genes are beneficial not only to understand the essence of life and reconstruct a minimal gene set artificially (Juhas *et al.,* 2014) but also to identify the effective drug targets to pathogenic bacteria and fungi (Dickerson *et al.* 2011). The experimental approaches for the identification of essential genes include single-gene knockout (Kobayashi et al., 2003), transposon mutagenesis, high-throughput sequencing and antisense RNA inhibition (Ji et al., 2001). However, these techniques are resource intensive and not feasible for all the organisms. Similarly, the pathogenic organisms are hazardous to cultivate thus require high laboratorial cost and more time consuming (Hopkins and Groom, 2002). Therefore, alternative methods have to be applied such as computational methods to overcome these problems. The computational methods like- homology modeling, protein- protein interactions are reliable.

There are various online platforms for the identification of the essential genes such as-DEG (a database of essential genes) contains number of essential and non-essential genes in archaeal, bacterial and eukaryotic organisms determined under different environments, OGEE (Online GEne Essentiality database) http://ogeedb.embl.de collects experimentally evaluated gene essentiality data and associated gene features such as expression profiles, duplication status, conservation across species, evolutionary origins and involvement in embryonic development, EGGS (Essential Genes on Genome Scale) contains microbial gene essentiality data which are acquired from genome-wide essential gene selections, CEG a database( http://cefg.cn/ceg/) contains clusters of orthologous essential genes where users can easily determine whether an essential gene is conserved in multiple bacterial species or is species- specific based on the size of the cluster (Ye *et al*., 2013) and so on.

The study of essential genes in bacteria has been greatly aided by the use of bioinformatics resources. With the increasing number of completely sequenced bacterial genomes, researchers have been able to establish essential gene databases, allowing for the in silico identification of essential genes. This has been a significant advancement in the field and has greatly facilitated the investigation of essential genes in bacteria (Zhang *et al*., 2015). Since Computational methods not

only save efforts, resources but also time, they are becoming more important in essential gene study.

## 2.3 Literature review related to Riboswitch

Riboswitches are structured elements typically found in the 5' untranslated region (UTR) regions of mRNAs, which play a crucial role in gene regulation by controlling gene expression. They consist of two structural domains: an aptamer domain and an expression platform. The aptamer domain is a folded RNA structure that specifically binds to a target metabolite, while the expression platform converts the binding events into changes in gene expression by altering the RNA folding (Breaker *et. al*., 2005).

Riboswitches have been experimentally validated for various functions in controlling gene expression. Examples of riboswitches include cobalamin riboswitch, S-Adenosyl methionine (SAM) riboswitch, tetrahydrofolate riboswitch, glutamine riboswitch, cyclic-AMO-GMP, FMN riboswitch, and others. Each of these riboswitches regulates gene expression by binding to a different metabolite and altering RNA folding, thereby controlling gene expression (Ren *et. al.,* 2015)

### 2.3.1 SAM Riboswitch

The bacterial de novo thiol metabolite SAM also known as AdoMet, is considered as vital biological methyl donor agent (Yan *et. al*., 2010). SAM is one of the second most important after ATP. It acts as co- substrate in various biochemical pathways. It plays role in methylation, aminopropylation as well as in trans sulfuration (Beri *et. al*., 2017). DNA methylation is critical for gene expression regulation and phospholipids methylation retains the membrane receptors and fluids where SAM is the methyl group donor.

SAM riboswitches or S-box leader sequences are found upstream of genes coding for biologically active proteins involved in methionine or cysteine biosynthesis. These riboswitches play a role in regulating metabolic processes through mechanisms like transcription termination, translation initiation, and antisense production. There are four types of SAM riboswitches known to date:

SAM-I riboswitch- Upon SAM binding, this riboswitch allows for the formation of an intrinsic terminator stem loop, leading to termination of transcription. In the absence of SAM-I riboswitch, an antiterminator loop structure is formed that activates transcription (Sudarsan *et. al.*,2008).

SAM-II riboswitches are typically short sequences of oligonucleotides. These type of riboswitches are mainly found in α-proteobacteria (Corbino *et. al.*, 2005). These sequences form an H-type pseudoknot after binding with SAM which is entirely distinct sequence and structural features from those of SAM-I and SAM-IV. Though, the pseudoknot ends 2nt upstream of the Shine-Dalgarno (SD) sequence, it is sufficient to occlude the ribosome binding in "off" nonfunctional state (Gilbert *et. al*., 2009).

SAM-III riboswitch- This type of riboswitch regulates gene expression by sequestrating the ribosome binding site (RBS) or SD sequence. The aptamer formed

by SAM binding with the SD sequence prevents ribosome binding to the RBS. But, it is narrowly distributed mainly in the order Lactobacillales (Fuchs *et. al.*, 2006). When SAM binds with SD sequence, aptamer is formed by base pairing of SD base sequence with an anti-SD sequence. As a result, this prevents the binding of ribosome in the ribosome binding site. The tertiary structure and binding pocket of SAM-III aptamers are distinct as compared to other SAM riboswitches (Lu *et. al.*, 2008).

SAM IV- This type of riboswitch is similar to SAM-I, but the scaffolding beneath the binding nucleotides is different. Each of these SAM riboswitches has distinct structural and binding pocket features, contributing to their specific functions in regulating gene expression and metabolic processes.

## 2.4 Literature review related to DNA adenine methylase (Dam)

### 2.4.1 The *dam* gene

The *dam* gene is a part of transcriptional unit having 834-bp which contains at least four genes or six or seven (Lyngstadass *et al.,* 1995). Dam is a single polypeptide chain of 278 amino acids having an apparent molecular size of 32kDa (Herman and Modrich, 1982). It has two SAM binding sites i.e. first a catalytic site and next one that increases specific binding to DNA which may be due to an allosteric change in the protein (Bergerat *et al.,* 1991). The optimal sequence for DNA binding and/or methyl transfer is 5'-GGGGATCAAG-3' (Peterson and Reich, 2006).

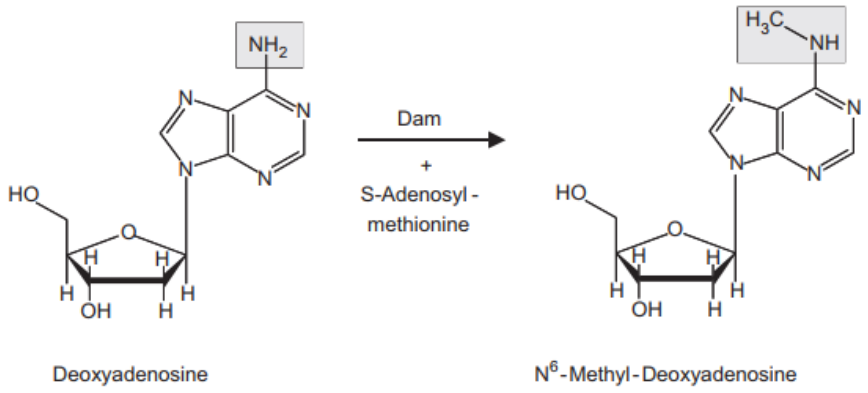


*Figure 7: Transfer of a methyl group from S-adenosylmethionine (SAM) to N6 position of adenine (Heusipp et al., 2007)*

### 2.4.2 DNA adenine methylase (Dam) as potential drug target

DNA adenine methylase (Dam) is an enzyme which adds methyl group to N-6 in adenine base of newly synthesized DNA in 5'- GATC-3', helps in several processes like- DNA replication, chromosome segregation, gene transcription, transposition and repair (Stein and Chirila, 2014).

*Dam* gene is not only necessary for viability of *E.coli* in a wild type but also required in recombination- deficient mutants such as *rec A, ruvABC* etc. (Marinus, 2000).

DNA adenine methylase is highly conserved in many pathogens such as *Vibrio cholera* (http://www.tigr.org), *Salmonella enterica* serovar Typhi

(http://www.sanger.ac.uk) , pathogenic *Escherichia coli* (Blattner, 1997), *Yersinia petis* (http://www.tigr.org) and *Haemophilus influenza* (Fleischmann *et al.,* 1995). In some studies, it was found that Dam methylation in *Salmonella enterica* serovar Typhimurium regulates the invasion genes of pathogenicity island I (SPI-1) (Balbontin *et al.,* 2006).

When Dam- mutants of *Salmonella* enterica serovar Typhimurium are attenuated in mouse model, resulted in virulence- related defects like- reduced secretion of invasion proteins, reduced cytotoxicity after infection of M cells (Garcia-del-Portillo *et al.,* 1999), sensitivity to bile and other DNA- damaging agents produced inside animal (Heithoff *et al.,* 2001 and Prieto *et al.,* 2004) and envelope instability which is enhanced by leakage of proteins, leading to activate the host immune system (Pucciarelli *et al.,* 2002)

Mutations in Dam results in the attenuation of the virulence of various pathogens hence it can be said that the DNA methylation plays a major role in the emerging the virulence (Julio *et al*., 2001). Similarly, animals that are infected with attenuated *dam* strain show resistant to superinfection by wild type, indicates the possibility of a vaccine (Dueger *et al.,* 2003 and Mohler *et al.*, 2008).

Since Dam methylase is essential for the viability and bacterial virulence in multiple gram-negative pathogens (Low *et al.,* 2001 and Heusipp *et al.,* 2007) and humans donot produce this enzyme (Mashhoon *et al.,* 2006), Dam inhibitors are the promising target for the antimicrobial drug development (Julio *et al.,* 2001). It was found that several S-adenosylmethionine analogs have the potential to inhibit Dam methyltransferase activity in approximately 10uM range (Hobley *et al.,* 2012)

## 2.5 Literature review related to computational approach in identifying new drug targets

### 2.5.1 Computer Aided Drug Discovery (CADD)

The discovery and development of new antibiotics has become crucial in light of the increasing drug resistance among pathogens. However, this process is notoriously expensive and time-consuming, with an estimated cost of $800 million and a timeline of 10 to 15 years (Dickson and Gagnon, 2004). Fortunately, advancements in computer technology have enabled researchers to employ computer-aided drug design (CADD) or computer-assisted molecular design (CAMD) to minimize cost, reduce risk, and speed up the drug discovery process. By combining biological science and chemical synthesis with computer technology, CADD has become a widely used approach for identifying promising lead compounds for the treatment of various diseases (Rio and Varchi, 2016). Computer-aided drug design (CADD) is an approach to drug discovery that uses computational techniques to design and optimize new drugs. The goal of CADD is to reduce the time and cost involved in the traditional drug discovery process, while also increasing the success rate of identifying new and effective drugs. CADD combines various techniques, such as molecular modeling, simulation, and data analysis, to predict the biological activity and potential toxicity of new drugs. CADD method has been widely used for

identifying potential lead compounds for developing the possible drug of many kinds of diseases (Baig *et al.*, 2016).

There are two methods of CADD: Structure based drug design (SBDD) and ligand based drug design (LBDD).

### 2.5.1.1Structure based drug design

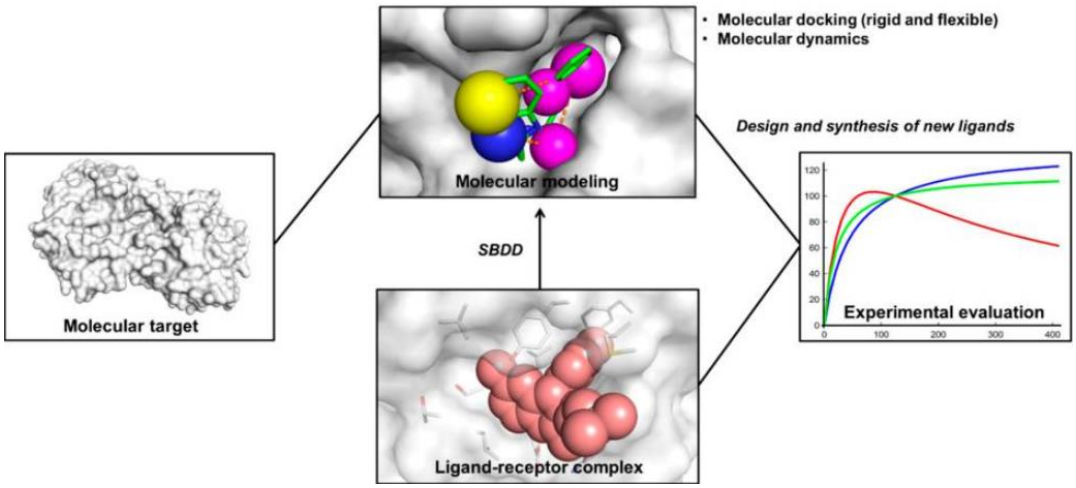


*Figure 8: General process of structure based drug design (Ferreira et al., 2015)*

Structure Based Drug Design (SBDD) is the approach which utilizes protein three-dimensional (3D) structural information of a target molecule (Lounnas *et al.*, 2013), obtained using cryo-electron microscopy (EM), NMR, X-ray crystallography and computational methods like homology modeling and molecular dynamic (MD) simulation to design new biologically active molecules (Goh *et al.*, 2016). Based on the affinity of the ligand- receptor complex the potential compounds are determined which has the necessary features for desired pharmacological and therapeutic effects. Thus, SBDD has been a promising tool to find out the lead compounds and the drugs (Wang *et al.*, 2018). The most common computational techniques used in SBDD are- structure-based virtual screening (SBVS), molecular docking, and molecular dynamics (MD) simulations. These techniques make use of the 3D structure of the target protein and knowledge about the disease at the molecular level, making the drug discovery process more specific, efficient and rapid. SBDD has been a promising approach in the field of drug discovery and optimization (Lionta *et al.*, 2014).

#### 2.5.1.1.1 Steps for structure based drug design

**(i) Identification of the target site**

The identification of an appropriate drug target is a crucial first step in the drug discovery process. The target should be closely related to human diseases and able to bind to small molecules. Target identification is the first and most important step in the drug discovery process. In drug discovery, proteins are preferred as drug

targets due to their high specificity, potency and low toxicity. The most common types of proteins selected as drug targets are kinases, proteases, and peptides. To utilize a structure-based approach for drug design, a 3-dimensional (3D) structure of the target protein is required. This 3D structure can be obtained through experimental methods such as X-ray crystallography, NMR spectroscopy or cryo-electron microscopy, and is deposited in the Protein Data Bank (PDB) database. If the 3D structure of the target protein is not available through experimental methods, there are several computational methods for predicting the 3D structure of the protein. These methods include homology modeling, protein threading or fold recognition, ab initio methods, and integrated approaches (Xiang, 2006). To assist with the prediction of the 3D structure of a protein, various online tools are available, including MODELLER, Phyre-2, Swiss-port, CPH model, PS2V2, Raptor X, etc.

**Homology modeling**

Homology modeling is the easiest and widely used method for predicting the three-dimensional structure of proteins. This approach, also known as comparative modeling, is based on the principle that proteins with similar sequences adopt similar structures. To apply this method, proteins that have more than 50% sequence similarity to the target protein are used as templates for modeling (Akhoon *et al.,* 2011). This method has been widely used to model the unknown or non resolved protein structures (Grouleff and Schiott, 2015). The process involves the following steps: (i) identification of the appropriate template through a Basic Local Alignment Search Tool (BLAST) search, (ii) sequence alignment, (iii) correction of the alignment to ensure that conserved or functionally important residues are properly aligned, (iv) optimization of the model through energy minimization, and (v) validation of the model using residues in the allowed regions of the Ramachandran plot and favorable energies (Gromiha *et al.,* 2019).

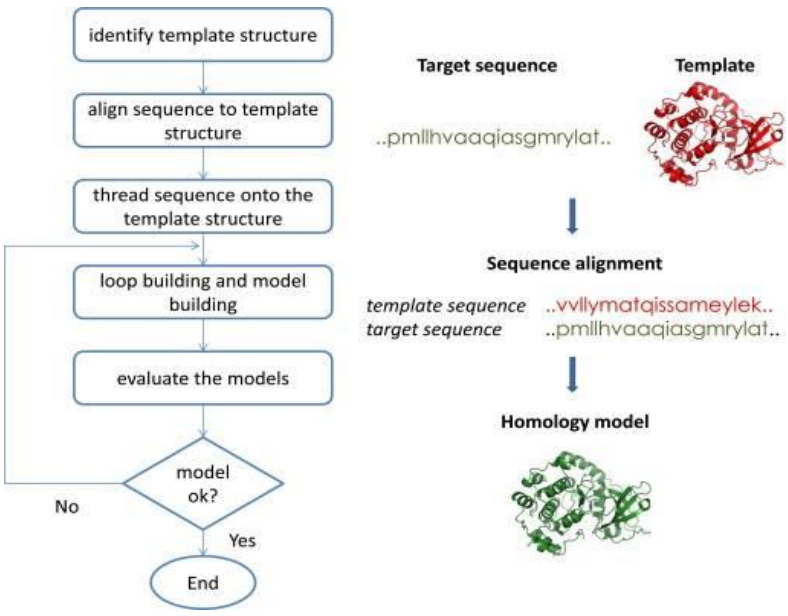


*Figure 9: Steps in homology modeling (Sliwoski et al., 2013)*

The most widely used computational method for predicting the 3D structure of protein is MODELLER (Webb and Sali, 2016).

**MODELLER**

MODELLER 10.0 is a computer program used for comparative protein modeling between the provided target and template sequences (Webb and Sali, 2016). This platform is used when the 3D crystal structure of the protein is unavailable. The program allows the user to model the target protein by aligning it with available template structures and atomic coordinates. The input target sequence is compared with the templates using a simple script file, and the program automatically generates a model of the target protein that includes all non-hydrogen atoms. Moreover, MODELLER has a variety of features that make it a useful tool in protein modeling and analysis. These features include the ability to assign protein folds, align sequences and/or structures (Marti-Renom *et al.,* 2004), perform multiple sequence alignment (Madhusudhan *et al.,* 2006 ; Madhusudhan *et al.,* 2009), calculate phylogenetic trees, and build models for loops in protein structures (Fiser *et al.,* 2000).

**PROCHECK**

PROCHECK is a software tool for the validation of protein structures, regardless of how the structures were obtained. This means that the program can be used to assess both experimental structures derived from techniques such as X-ray crystallography and NMR spectroscopy, as well as theoretical structures built by homology modeling. The program operates by analyzing the three-dimensional atomic coordinates of the protein structure and checking them against established criteria for evaluating protein structure quality. These criteria include the distribution of residues in specific regions of a Ramachandran plot, the presence of problematic secondary structure elements, and other factors. By comparing the input structure to these established standards, the PROCHECK program can provide an overall assessment of the quality of the structure, helping researchers to identify any potential issues or areas for improvement. The output of the program is a series of graphical and numerical analyses that indicate the quality of the protein structure, such as the Ramachandran Plot. The different regions of the Ramachandran plot are defined on the basis of the density of data points obtained from a database of well-refined protein structures. These regions include: core, allowed, generously allowed, and disallowed. The 'core' regions are particularly important because they are the regions where the data points tend to converge and cluster more tightly as the resolution of the protein structure improves (Laskowski *et al.,* 1993).

In the PROCHECK version, the regions of the Ramachandran plot are defined in such a way that points in the 'core' regions are considered to be of high quality and those in the 'disallowed' regions are considered to be of low quality. Points in the 'allowed' and 'generously allowed' regions are considered to be of intermediate quality. The software allows users to identify potential problems with a protein structure and to assess the quality of the structure as a whole (Morris *et al.,* 1992).

**ProSA Program**

The ProSA (Protein Structure Analysis) program is a widely used tool in the field of protein structure analysis. It utilizes web-based applications to provide an interactive platform for the refinement and validation of experimental protein structures, as well as structure prediction and modeling. The ProSA program evaluates the quality and accuracy of protein structures by calculating various energy scores and plotting them in a graphical representation, highlighting potential issues or problems in the protein structures. This tool enables scientists and researchers to assess the quality and accuracy of their experimental protein structures and make necessary adjustments, helping to improve the accuracy of predictions and models in the field of protein structure analysis (Wiederstein and Sippl, 2007). It calculates the energy of the structure by evaluating the distance-based pair potential and the solvent exposure of protein residues. The two key metrics generated by the program are the z-score and the plot of residue energies. The z-score measures the deviation of the total energy of the structure compared to a distribution derived from random conformations. If the z-score falls outside the range typical for native proteins, it indicates an erroneous structure (Sippl, 1993; Sippl, 1995). Unusual z-scores for soluble globular proteins are often associated with errors in the protein structure. In general, protein models with Z-scores that are close to 0 are considered to be of higher quality because they are more similar to the known high-quality structures in the dataset. However, it is important to note that Z-scores should not be used in isolation to validate protein structures, but rather in conjunction with other methods and considerations. ProSA-web is accessible at https://prosa.services.came.sbg.ac.at.

**(ii) Identification of active site**

Once the target protein is identified, it's crucial to locate the binding pocket, also known as the active site. This is where a ligand can bind to the target protein and is capable of inhibiting the target protein is considered as a lead compound or lead candidate. To identify the binding pocket, computational methods are used that rely on various geometric criteria and algorithmic approaches. There are several software tools available, including PyMOL (Seeliger and Groot, 2010), POCKET (Levitt and Banaszak, 1992), SURFNET (Laskowski, 1995), LIGSITE (Hendlich *et al.,* 1997), CAST (Liang *et al.,* 1998), PASS (Brady and Stouten, 2000) and others, that help in identifying the binding pockets of target proteins.

**(iii) Compound library selection**

Compound databases play a crucial role in the SBDD process. The construction of these databases involves gathering and organizing a collection of chemical compounds that can potentially serve as drug candidates. A well-structured database allows for an efficient screening process and the identification of lead compounds for further development. Ligand libraries, which are a subset of the compound database, are created by selecting compounds that possess desirable chemical and physical properties. These properties, known as drug likeness or physiochemical properties, are chosen based on the target disease or biological target of interest.

The goal of enriching these libraries is to increase the likelihood of finding compounds that can effectively interact with the target and have a positive effect on the disease. The process of virtual screening involves the use of various databases containing compounds to identify potential hits for drug discovery. These databases come in a wide range, with commercial options such as ZINC (http://zinc15.docking.org/) and PubChem (http://pubchem.ncbi.nlm.nih.gov) being widely used. ZINC is a database of compounds that have been processed to become biologically relevant and boasts an extensive library of 230 million compounds that can be purchased in 3D format. It includes a variety of forms of molecules, such as protonated, deprotonated, and tautomeric, which are classified into three different pH ranges (Irwin, 2008). Additionally, there is PubChem, which provides access to 112 million compounds. These vast collections of compounds offer a valuable resource for drug discovery efforts.

**(iv) Drug lead evaluation ( *In silico* ADME/Tox filtering for drug-likeness)**

It is a well-known fact in the pharmaceutical industry that only a small fraction of the compounds that enter the drug development process end up becoming marketed drugs. According to reports, only 10% of the compounds make it through to become commercially available drugs, while the rest fail, often due to their pharmacokinetic profile. This means that the remaining 40% of compounds are not suitable for use as drugs due to their properties related to adsorption, distribution, metabolism, excretion, and toxicity (ADME/Tox) (Prentis *et al.,* 1988). The pharmacokinetic profile is an important factor in determining the success of a drug candidate and plays a crucial role in the drug development process. Similarly, computing with millions of bioactive compounds in the libraries and finding the right compound is time consuming and waste of energy cum resources. Thus, it is necessary to know the pharmacokinetics of the bioactive compounds and their efficiency are evaluated upon adsorption, distribution, metabolism, excretion and toxicity (ADME/Tox). As oral administration is often preferred over intravenous administration, evaluating drug-like properties in the early stages of drug development is crucial. To evaluate the drug-like properties of the molecules in the early stages of drug development process Chris Lipinski and colleagues at Pfizer developed the Rule of Five (ROF or RO5), also known as the Lipinski Rules, as a simple and effective way of evaluating drug-like properties (Petit, *et al.,* 2012). The Lipinsinki rule of 5 states that the drug like compounds should have the following properties:

Table 1: Typical Range Parameters for Characteristics Associated with Drug-like Properties

| Parameters | Minimum | Maximum |
|---|---|---|
| Molecular weight (MW) in Daltons | 200 | 500 |
| clogP | -3 | 6 |
| ClogS | -4 | -2 |
| Hydrogen Bond Acceptors | 0 | 10 |
| Hydrogen Bond Donors | 0 | 5 |
| Topological Polar Surface Area (TPSA) | 0 | 120 |
| Rotatable Bonds | 0 | 10 |

Moreover, in order to increase the property of the drug likeness of a chemical compound two more conditions such as: a polar surface area and rotatable bonds (Veber *et al.,* 2002 and Chagas *et al.,* 2018) has been added.

Molecular weight

The molecular weight of a drug molecule is an important factor that determines its permeability across biological membranes, including the intestinal wall and the blood-brain barrier. The ideal range for molecular weight is considered to be between 200 and 500 Daltons for improved permeability. Compounds with higher molecular weight than this range tend to have reduced permeability and bioavailability due to their size and difficulty in crossing biological membranes. On the other hand, compounds with lower molecular weight are more likely to be rapidly excreted from the body, which can lead to poor pharmacokinetics. Therefore, compounds with molecular weight in the range of 200-500 Daltons are considered to be optimal for oral absorption and drug efficacy.

Lipophilicity (clogP)

The clogP (logarithm of partition coefficient between n-octanol and water log, $c_{octanol}/c_{water}$) is a measure of the hydrophobicity (lipophilicity) of a chemical compound, which is related to its distribution between water and oil phases. It is calculated using a theoretical model that takes into account the molecular structure, size, and polarity of a compound. The value is used as a predictor of the solubility of a compound in various solvents and biological membranes. A high ClogP value indicates a higher lipophilicity and thus a lower solubility in water and a higher permeability across biological membranes. On the other hand, a low ClogP value indicates a higher hydrophilicity and higher solubility in water but lower permeability across biological membranes. This property is important in drug design as it affects the bioavailability and efficacy of a drug, as well as its toxicity and pharmacokinetics. The range for clogP values typically falls between negative 3 to positive 6 (Egan *et al.,* 2000).

Solubility (clogS)

Aqueous solubility, the amount of a compound that can dissolve in water, is another critical factor in determining its potential for intestinal absorption. The solubility of a compound is influenced by factors such as lipophilicity and crystal lattice binding energy. Poorly soluble compounds often result in low absorption due to limited dissolution rate, leading to incomplete absorption. The solubility of a compound is influenced by factors such as lipophilicity and crystal lattice binding energy. Drugs that are both lipophilic and soluble in water are more likely to be absorbed when taken orally (Waring, 2010). Optimal oral absorption is generally achieved when a compound exhibits a balance between its lipophilicity and its aqueous solubility. The value range for solubility of the compound is between -4 to -2.

Hydrogen bond Acceptor

Hydrogen bonds are important in determining the specificity of ligand binding, membrane transport, and the distribution of drugs in biological systems. These bonds form between electronegative atoms such as nitrogen (N), oxygen (O), or fluorine (F) and a hydrogen atom that is covalently bonded to one of these electronegative atoms. The hydrogen atom acts as a partial positive charge and the electronegative atom acts as a partial negative charge, resulting in the formation of a polar covalent bond. In biological systems, hydrogen bonds play a crucial role in determining the specificity of ligand binding by allowing for selective interactions between the ligand and the target protein. In addition, they play a role in membrane transport by facilitating the transport of ions and other small molecules across the lipid bilayer. Additionally, hydrogen bonds also influence the distribution of drugs in the biological system by affecting their solubility, partitioning, and permeation across biological membranes (Kubinyi, 2007).

Hydrogen bond Donor

Hydrogen bonds play a significant role in determining the specificity of ligand binding and the distribution of drugs in a biological system. The presence of a large number of hydrogen-bond donor groups can hinder the ability of a molecule to permeate the lipophilic environment within a cellular membrane, thereby affecting its effectiveness as a drug candidate. To evaluate the hydrogen bonding ability of a molecule, it is important to measure the sum of N-H and O-H bonds in the compound. For optimal permeability and drug-like properties, it is generally recommended that the hydrogen bond donor count be less than 5 (Lipinski *et al.,* 1997).

RO5 plays the key role in earliest stage of drug development which includes compound library construction and hit-to-lead optimization programs.

**(v) Docking and scoring**

Molecular docking is a computational method that uses structural information to evaluate how well a collection of molecules, including synthesized and theoretical ones, fit into a macromolecular binding site in terms of shape and electrical interactions. It is a way to screen and rank a large number of molecules for their potential binding ability to a target protein. (Bartuzi *et al.,* 2017). It is considered one

of the most accurate methods in SBDD and is applied to examine various molecular interactions and the stability of complexes (Meng *et al.,* 2011). The docking algorithms predict binding energies and rank the ligands based on various scoring functions. The determination of the most appropriate ligand-binding conformation is dependent on two factors, the vast conformational space that defines possible binding positions, and the explicit prediction of the binding energy associated with each conformation (Kapetanovic, 2008). There are various docking algorithms and programs available, each using different scoring functions to predict the binding energy. The process is carried out through multiple iterations until the lowest energy state is achieved, which is then evaluated using different scoring functions. It is important to note that these scoring functions may be suitable for specific ligand chemotypes and target macromolecules (Kitchen *et al.,* 2004; Ferreira *et al.,* 2015).

A scoring function is a tool used in molecular docking to assess the binding affinity between a ligand and a target protein. It helps to evaluate the interaction between the two molecules, and determine the most energetically favorable binding pose. There are several types of scoring functions that are used in molecular docking, including force field, empirical, knowledge-based, and machine learning (ML) scoring functions (Huang *et al.,* 2010). Force field scoring functions estimate the intermolecular interactions between the binding partners, such as electrostatic and vdW forces. Empirical scoring functions are based on the number of atoms in the ligand and target protein and are used to predict affinity and pose. These functions take into account factors such as hydrophobic forces, hydrophilic forces, hydrogen bonding, and entropy (Guedes *et al.,* 2018). Knowledge-based scoring functions are based on statistical potentials of intermolecular interactions and assume that certain functional groups or types of atoms contribute to binding affinity (Muegge, 2006). ML scoring functions are more advanced than other types of scoring functions. These methods do not rely on predefined functional forms between structural features and binding affinity values. Instead, ML methods dynamically construct and optimize models to predict the binding pose and affinity. Different ML methods such as random forest (RF), support vector machine (SVM), and neural networks (NN) work with nonlinear dependencies among binding interactions and perform better than other methods in calculating binding energy (Li *et al.,* 2018). Similarly, consensus scoring is another scoring function that combines scores from different methods to minimize the error rate in individual scores and increase the likelihood of finding a true positive result (Sousa *et al.,* 2006).

There is a wide variety of molecular docking software programs that are utilized for drug discovery and molecular modeling, each with its own unique features and limitations. Some of the most commonly used programs include DOCK (Venkatachalam *et al.*, 2003) AutoDock (Morris *et al.,* 1998), FlexX (Rarey *et al*., 1996), Surflex (Jain, 2003), GOLD (Jones *et al*. 1997), Glide (Friesner *et al*., 2004), Cdocker, LigandFit (Venkatachalam *et al*., 2003 MOE-Dock (Corbeil *et al*., 2012), AutoDock Vina (Trott and Olson 2010), rDock (Ruiz-Carmona *et al*., 2014), UCSF Dock (Allen *et al*., 2015), and many others. These tools are used to predict the interaction between a protein (receptor) and a small molecule (ligand), which is a critical aspect of drug discovery. By using different algorithms and techniques, researchers can

compare the results from various programs and choose the best one to address a specific problem.

**(vi) Post processing (Improving selection after docking)**

Structure- based drug design is a powerful method for discovering new drug leads against important targets which can create a very promising factor for the continuation to phase I clinical trials. For this, the expert chemist is responsible for visually inspecting and analyzing the thousands of docking poses generated by molecular docking. Since, simplified scoring functions used in molecular docking can sometimes produce unrealistic results, leading to an over-estimation of binding affinity. Additionally, molecular docking may not sample the entire conformational space of a ligand, which can result in missed binding opportunities. In order to address the limitations of molecular docking and virtual screening in drug discovery, it is important to have a comprehensive understanding of the molecular interactions between ligands and targets, as well as the chemical properties and biological activity of potential compounds. This information will help make informed decisions on which compounds to prioritize for further testing, taking into account factors such as pharmacokinetics and toxicity.

### 2.5.1.2 Ligand Based Drug Design (LBDD)

Ligand-based drug design (LBDD) is a computational method used to identify new potential drug candidates. This method is based on the structural information and physical-chemical properties of already known active and inactive molecules. It utilizes the molecular similarity principle which compares the relationships between compounds in a given library and one or more known active compounds. It commonly employs two key techniques for virtual screening: QSAR and pharmacophore modeling. These methods examine the relationships between chemical structures and biological activity based on molecular similarity, utilizing a variety of molecular descriptors to describe the chemical and topological features of compounds (Acharya *et al.,* 2011). These techniques have become widely used in LBDD for their ability to efficiently screen large chemical libraries and prioritize compounds for further testing.

There are two main types of molecular descriptors used in LBDD, 1D and 2D descriptors, which encode information about the chemical nature and topological features of the compounds (Jørgensen and Pedersen, 2001; Duan *et al.,* 2010). Additionally, 3D descriptors can also be used, which describe molecular fields, shape, volume and pharmacophores. These molecular descriptors are used to perform similarity measurements, which determine the degree of similarity between the compounds in the library and the known active compounds (Abrahamian *et al.,* 2003). The goal of LBDD is to reduce the number of compounds that need to be tested experimentally, thus saving time and resources. It is a useful tool in the early stages of drug discovery, as it can quickly identify new potential drug candidates and prioritize them for further testing.

### 2.5.2 Softwares applied in this study

**i) Auto Dock**

AutoDock is a software tool that uses a combination of empirical free energy calculations and Lamarckian genetic algorithms to predict the binding of a molecule to its target with a predicted measure of its free energy of association. This helps in quickly determining the shape and energy of the complex between the molecule and its target (Morris *et al.,* 1998). AutoDock is a suite of software tools for molecular docking, which aims to predict the binding of small molecules to a receptor protein. It has been developed and improved over time, and currently includes two generations of software: AutoDock 4 and AutoDock Vina. The suite also includes an accelerated version called AutoDock-GPU, which is faster than the original single-CPU version (https://autodock.scripps.edu/). During a docking simulation, the energy of the ligand-protein interaction is evaluated using a grid-based method. In this method, the interaction energies between the ligand and the target protein structure are pre-calculated and stored as a reference in a look-up table. This allows for a rapid evaluation of the ligand-protein interaction during the simulation. However, the use of this grid-based method requires that the target protein is treated as a rigid molecule, unless specific side chains are treated outside the grid, separately. This means that the method does not take into account any changes in the structure of the target protein, except for certain side chains that are treated differently. This limitation is due to the nature of the grid-based method, which is designed for rapid evaluation of the ligand-protein interaction, rather than an accurate representation of the protein's flexibility (Cosconati *et al.,* 2010).

**Autodock Vina**

AutoDock Vina is a free and open-source software program that is used to perform molecular docking. It was created by Dr. Oleg Trott while he was working in the Molecular Graphics Lab (currently known as the CCSB) at The Scripps Research Institute. The software enables researchers to predict how small molecules interact with proteins by modeling the way they bind together (Trott and Olson 2010). The program uses a combination of algorithms to evaluate the potential binding energy between the protein and the ligand, and to search for the most energetically favorable binding pose. This information can be used to study the mechanism of drug-protein interactions and to design new drugs (https://vina.scripps.edu/).

**AutoDockTools (ADT)**

AutoDockTools (ADT) is a graphical user interface (GUI) for setting up, launching, and analyzing AutoDock runs. It is a user-friendly tool for molecular docking, which is a computational method for predicting the binding of a small molecule ligand to a target protein. The ADT provides a visual interface for preparing the input files, launching AutoDock simulations, and analyzing the results. It allows users to view molecules in 3D, rotate and scale them in real-time. It also provides the ability to add hydrogens, including non-polar hydrogens, to the molecular structures. In addition, it also allows users to assign partial atomic charges to the ligand and the macromolecule using either Gasteiger or Kollman United Atom charges. This is an important step in the molecular docking process, as it helps to accurately predict the

binding affinity between the ligand and target protein. Moreover, it provides a graphical representation of the grid box to set up the AutoGrid Parameter File (GPF), using slider-based widgets. In addition, the AutoDock Parameter File (DPF) can be set up using forms, and the AutoDock simulation can be launched directly from the ADT interface. The results of an AutoDock simulation can be read and displayed graphically, providing users with an easy-to-use and visually appealing way to analyze the results of their molecular docking experiments. ADT also provides the ability to view isocontoured AutoGrid affinity maps, which can be used to determine the binding affinity of the ligand for the target protein (https://autodocksuite.scripps.edu/adt/). AutoDockTools is provided as a part of MGLTools, for use on Linux, Mac OS X, SGL and Windows.

**ii) PyMOL**

PyMOL is widely recognized as the leading software for generating high-quality molecular structures for publication. One of the key strengths of PyMOL is its advanced rendering options, which enable users to create visually stunning molecular graphics. Additionally, PyMOL provides exceptional 3D viewing capabilities, making it an indispensable tool for structure-based drug design. These features make PyMOL a highly versatile and user-friendly software for visualizing and analyzing molecular structures. PyMOL's compatibility with several commonly used file formats for electron density maps makes it an ideal tool for crystallographers. The availability of an easy-to-use Autodock/Vina plugin for PyMOL further expands its capabilities, especially for scientists who may not be experts in docking protocols. With this plugin, users can perform molecular docking within the PyMOL environment, making it possible to combine the results of docking simulations with other PyMOL applications, such as molecular mechanics, molecular dynamics simulations, and molecular graphics (Yuan *et al*., 2017). It can be downloaded from https://pymol.org/2/.

**iii) Orisis DataWarrior**

DataWarrior is a powerful software platform that combines dynamic graphical views with chemical intelligence to provide advanced molecular analysis and visualization capabilities. The software offers various types of visual representations of data, including scatter plots, box plots, bar charts, and pie charts, which can be used to visualize numerical or categorical data. Additionally, these graphical views can show trends of multiple scaffolds or compound substitution patterns, enabling users to gain a deeper understanding of their data (López-López *et al.,* 2019). It supports a wide range of chemical descriptors that encode various aspects of chemical structures, including chemical graph, chemical functionality from a synthetic chemist's perspective, and 3-dimensional pharmacophore features. These descriptors allow for different types of molecular similarity measures, which can be applied for row filtering and customizing graphical views. The software also provides capabilities for the enumeration of combinatorial libraries, as well as the creation of evolutionary libraries, making it an indispensable tool for library design and optimization https://openmolecules.org/datawarrior/). The huge ligand library database can be optimized using ADME/Tox filters for drug like properties. Furthermore, users can cluster compounds and pick diverse subsets, and calculated

compound similarities can be used for multidimensional scaling methods, such as Kohonen nets.

DataWarrior also includes tools for calculating physicochemical properties and creating structure-activity relationship tables, as well as for visualizing activity cliffs. These features make DataWarrior a valuable tool for drug discovery and medicinal chemistry research, enabling users to gain insights into their data and make informed decisions (Sander *et al.,* 2015). It can be freely downloaded from (https://openmolecules.org/datawarrior/), compatible for all Windows, LINUX and MacOS-X.

**iv) BIOVIA Discovery Studio Visualizer**

BIOVIA Discovery Studio Visualizer is a powerful and feature-rich molecular modeling software application that enables users to visualize, share, and analyze protein and small molecule data. This software provides an interactive and user-friendly interface for exploring molecular structures and enables users to manipulate and analyze their data in real-time. The Visualizer includes a variety of molecular visualization tools, such as interactive ribbon and surface models, which provide users with a detailed understanding of molecular structures and interactions. Additionally, the software supports multiple file formats, allowing users to import and view data from a wide range of sources, including X-ray crystallography, NMR spectroscopy, and molecular dynamics simulations. It also provides advanced data analysis tools, including ligand-protein interaction analysis and molecular dynamics simulations, enabling users to investigate and understand complex biological processes and drug interactions. Furthermore, the software provides an intuitive and interactive interface for annotating and annotating molecular structures, including the ability to add labels, annotations, and notes to individual atoms, residues, and regions of the molecule. This feature enables users to effectively communicate their results and findings with others (https://www.3ds.com/products-services/biovia/products/molecular-modeling-simulation/biovia-discovery-studio/).
It can be downloaded from the source https://discover.3ds.com/discovery-studio-visualizer-download.

**v) PyRx**

PyRx is a virtual screening software that is extensively used for computational drug discovery. It is used to screen libraries of compounds against potential drug targets. This program enables medicinal chemists to perform virtual screening from any platform and provides support for each step of the process. From data preparation to job submission and results analysis, it helps users in every aspect of their drug discovery journey. Despite the fact that there is no one-size-fits-all solution in the drug discovery process, PyRx includes a docking wizard (Autodock 4 and Autodock Vina) with an easy-to-use user interface that makes it a useful tool for computer-aided drug design. Additionally, it consists of the softwares such as- python as a scripting language, AutoDock Tools, to generate input files, open Babel for importing SDF files, removing salts and energy minimization, matplotib for 2D plotting, Visualization ToolKit (VTK) by Kitware, Inc., Enthought Tool suite including Traits, for application building blocks, wxPython for cross-platform GUI. Moreover, this

software features chemical spreadsheet-like functionality and a powerful visualization engine that are crucial for structure-based drug design (http://pyrx.sourceforge.net.). Furthermore, it provides an efficient and effective way to screen compounds and to identify potential lead candidates in the drug discovery process. PyRx version 0.8 is available free from http://pyrx.sourceforge.net.

**vii) Open Babel**

Open Babel is a free, open-source chemical toolbox designed to interconvert 110 chemical file formats such as Mol, PDB, SMILES, CML, etc. It can perform various chemical tasks such as molecule conversions, structure optimization, molecular descriptor calculation, structure-activity relationship (SAR) analysis, and many more. It supports various operating systems including Windows, Linux, and macOS. Open Babel has a robust C++ library which makes it suitable for integration into other software and programs. The library provides developers with a high-level interface to perform chemical operations, making it a useful tool in computational chemistry and drug discovery (O'Boyle *et al.,* 2011). It can be obtained under an open-source license from the website http://openbabel.org.

**vii) Ligplot$^{+}$**

LigPlot$^{+}$ is a graphical interface software tool for visualizing protein-ligand interactions. It is a newer version of the original LIGPLOT program which can automatically generate schematic diagrams of protein-ligand interactions from the 3-dimensional (3D) coordinates of the protein and its bound ligand. The program uses the 3D information to identify and highlight the key interactions between the protein and ligand, including hydrogen bonds, hydrophobic interactions, and electrostatic interactions. The diagrams generated by LigPlot are designed to be intuitive and easy to interpret, providing a clear visual representation of the molecular interactions between a protein and its ligand. This information is useful for understanding the molecular basis of drug action and for predicting the binding affinity of drugs for their targets (Wallace *et al.,* 1995). The program also allows us to customize the appearance of the diagrams, including the size and color of the atoms and bonds, and to save the 2D diagrams as image files for use. Moreover, this program also generates protein- protein interaction through DIMPLOT option (Laskowski and Swindells, 2011).

**viii) Gauss View and Gaussian 03W**

Gaussian is a computational chemistry software program used for a wide range of molecular modeling and simulation tasks, including molecular dynamics, quantum chemistry calculations, and reaction modeling. Gaussian uses advanced mathematical algorithms to perform these simulations and provides a high level of accuracy and predictive ability. GaussView is a graphical user interface (GUI) for Gaussian that makes it easier to use the software and view the results of simulations. With GaussView, users can create and edit molecular structures, visualize molecular properties, and perform various types of simulations without having to enter complex command-line commands. GaussView also provides interactive graphical

tools for analyzing and interpreting simulation results, making it a useful tool for both research and teaching purposes (https://gaussian.com/gaussview6/).

Gauss View and Gaussian 03 W are utilized for predicting molecular properties such as energies and structures, vibrational frequencies, thermochemical properties, reaction pathways, orbital information, spectra, atomic charges, magnetic and optical properties, and electron densities. These programs are capable of simulating various molecular characteristics including transition states, IR and Raman spectra, bond and reaction energies, molecular orbitals, NMR shielding, vibrational circular dichroism, electron affinities, polarizabilities, and hyperpolarizabilities. Gaussian 03W was used in this study.

# 3. MATERIALS AND METHODOLOGY

## 3.1 Obtaining the 3D crystal structures of the target proteins

The target protein, Dam of *Salmonella* enterica subsp. Serover Typhimurium was selected for molecular docking and searched in the PDB (http://www.rcsb.org/) for the 3D structure but its 3D structure was not available. Thus, the crystal structure of Dam protein (uniprot ID: P0DMP3) was prepared using Modeller 9.2, a protein homology tools. The best match model was calculated through Z-score and then Ramachandran plot was made to make sure the 3D structure made was close to what experimental would give.

### 3.1.1 Homology modeling using MODELLER

The 3D crystal structure which are not available in protein data bank (PDB) are prepared by homology modeling. There are various softwares and online tools available for homology modeling such as- Phyre-2, Swiss Prot, CPH model, PS2V2, MODELLER, Raptor X etc. Here, we used MODELLER for constructing 3D structure of the target protein.

(a) Template recognition

The first step was obtaining the target sequence from NCBI or uniprot (getting the FASTA format of the protein). Once the desired sequence of the target protein was obtained then the sequence was run for a BLAST search. In order to find the structure of these sequences, it was searched in PDB. After that, the target sequence was converted into PIR format, a readable format by modeller.

(b) Sequence alignment using BLAST

Using BLAST, PsiBlast, or fold recognition techniques, the sequence of similarities were explored and aligned with known structures in PDB. The best sequence that has a high degree of similarity was found by comparing a query sequence to a database using BLAST. Each line's degree of similarity was summed up by its E-value (Expected value), which is near to zero, indicating a high degree of similarity. The first five proteins which have the maximum identity were downloaded in PDB format from RCSB. The five *E.coli* strains (4RTJ_A, 2G1P_A, 4GBE_D, 4GOL_D, 2ORE_D) showed the highest percentage identity (92.45%) thus it was chosen to carry out BLAST.

For the two sequences which have low percentage identity, one can use Multiple Sequence Alignment programs such as CLUSTALW. In homology modeling, alignment correction is a crucial step; omitting it would create a defective model.

(c) Preparation of input files

The target sequence (FASTA format) was converted to PIR format (*.ali) which is a readable format by MODELLER. All the input and output files are available in https://salilab.org/modeller/tutorial/ site which is either in zip format (for windows) or .tar.gz format (for Unix/ Linux) were downloaded and files were extracted. The pdb_95 file, converted query sequence in PIR format and reference sequence were copied in a new folder for MODELLER run. Similarly, MODELLER commands that tell MODELLER program what to perform are contained in script files were prepared.

Script files

(i) Build_profile.py

The text was copied from the tutorial (https://salilab.org/modeller/tutorial/) in notepad and TvLDH was replaced with the query protein name (Dam) then saved as script1.py and run in MODELLER by changing to the directory containing the script and the alignment files that was created earlier using 'cd' command. This generated the *.bin file.

(ii) Compare.py

The text was copied from the tutorial (https://salilab.org/modeller/tutorial/) in notepad and replaced the protein name with the referenced protein name (4RTJ_A, 2G1P_A, 4GBE_D, 4GOL_D, 2ORE_D) and saved as script2.py then the MODELLER was executed.. After successfully running in MODELLER, it is discovered that the model with low angstrom provides the optimum structure.

(iii) Align 2d.py

The content from the tutorial (https://salilab.org/modeller/tutorial/) was copied in notepad and replaced the protein name with the reference protein (2g1pA) and TvLDH with the query protein name (Dam). After that, the file was saved as script3.py and MODELLER was executed. This generated *.pap file. The PAP is used for visualization by MODELLER.

(iv) Model_build.py

Using the Automodel class, the MODELLER automatically calculates a 3D model of the target after creating the alignment of the target and the template. For this, first TvLDH was replaced with Dam and 2g1pA and saved as script4.py then MODELLER was executed. On running script4.py file generated five similar models of Dam based on structure of the template and alignment in "queryseq-2g1p.ali". The script4.log file is one of the most significant output file which includes the details of modeling input constraints, errors, warnings, summary of all built models, file name along with the scores for each model's coordinates in PDB format.

(v) Evaluate_model.py

There are various methods for choosing a good model among the recently developed models for the same target. The best model was chosen based on its lowest DOPE score and maximum GA341 score.

(d) Model validation using Ramachandran plot

Protein validation can be done using a various techniques and tools, including Ramachandran Analysis, Z-score, Energy Plot and DOPE score. Ramachandran analysis was carried out using SAVES v6.0 (https://saves.mbi.ucla.edu/) with the PROCHECK option. This feature checks the protein structure for any deviations from the expected conformations. Similarly, Z-score ( https://prosa.services.came.sbg.ac.at/prosa.php) was performed to calculate the energy separation between the native fold and the average of an ensemble of misfolds in the units of the standard deviation of the ensemble.

Moreover, DOPE score was also used to evaluate the quality of protein models by comparing them to each other. It is a statistical potential that compares pairs of atoms in order to determine how closely a model conforms to the expected structure for a given amino acid sequence. A lower DOPE score indicates a better-quality model. This score is useful for comparing different models of the same protein and can help identify the most accurate or reliable one.

Additionally, the human hMAT1A S-adenosyl methionine synthetases (PDB ID: 6SW5) was obtained from the RCSB protein data bank. After that, the pdb files of proteins were processed in PyMoL, a program for protein visualization, where cofactors, water molecules, and native ligands were removed in order to prevent hindrance during molecular docking (Kagami *et al.,* 2020) and opened in AutoDock tools. For the preparation of proteins, Hydrogen bonds were added, non-polar surface areas were combined and Gasteiger charges were calculated using AutoDock tool. S-adenosyl homocysteine (SAH) and S-adenosyl-lmethionine (SAM) were used as reference molecules, and their 3D structures, along with the screened ligands, were downloaded from PubChem (https://pubchem.ncbi.nlm.nih.gov/). These structures were then processed using the Openbabel GUI (O'Boyle *et al*., 2011) and saved as pdbqt file format, a required file format for molecular docking.

## 3.2 Ligand database preparation

The ZINC15 database (www.zinc15docking.org), consists of more than 230 million commercially accessible chemicals ready-to-dock, 3D formats for virtual screening, was used to develop the ligand library which consists of different categories such as natural product FDA, natural product biogenic-FDA, natural product in man, natural product in the world, natural product in trial, and natural product in vivo. Similarly, UROSY (https://uorsy.com/), for kinase inhibitor and ASINEX (https://www.asinex.com/nucleoside-mimetics), for nucleoside mimetics were used

to develop additional ligand library. All the selected ligands were then processed for ADME/Tox screening for docking.

## 3.3 ADME/Tox Screening

Drug research and development are duo time and money-consuming processes. Numerous promising lead compounds fail to reach the clinical stage of therapeutic research due to poor pharmacokinetic properties and toxicity issues. Hence, in order to improve absorption, distribution, metabolism, and excretion, the ligand library in *.sdf format, was screened for druggability based on Lipinski's rule of five and LogS. Using the OSIRIS data warrior program the druglikeness properties of ligands such as- molecular weight, cLogP and cLogS, druglikeness, and toxicities like mutagenicity, tumorigenicity, reproductive effects, and irritating effects based on their binding energies were calculated (Veber *et al.,* 2002 and Chagas *et al.,* 2018). The following parameters were set.

ADME/Tox

Total Molecular weight: 200-500 Daltons

cLogP : -3 to +6

cLogS : -4 to -2

Hydrogen bond acceptor : 0 to 10

Hydrogen bond donors : 0 to 5

Topological Polar surface area : 0 to 120

Drug likeliness : positive value (as default)

LE/TOx/S criteria

Mutagenesis : None

Reproductiveness : None

Tumorogenicity : None

Irritant : None

Rotable bonds: 0 to 10

## 3.4 Identification of active site of target protein

To perform molecular docking between a target protein and a ligand, it is essential to identify the ligand binding site on the protein, also referred to as the active site. This can be achieved by using PyMol, a software program for protein structure analysis and visualization. The process started by loading the protein structure, along with its native ligand, into the PyMol window. The active site was then identified by examining the amino acid residues within a 5 Å distance from the ligand and protein to determine their specific interactions. Additionally, polar interactions were also

evaluated. The information was then saved as a PDB file and visualized using Ligplot+ and Biovia Discovery Studio.

## 3.5 Molecular docking and virtual screening

Molecular docking experiments were performed using the AutoDock Vina Wizard in the PyRx 0.9.8 platform to study the binding energy of Dam with a library of natural product ligands, kinase inhibitor and nucleoside mimetics. The docking experiments were performed using specific center grid box values x= -18.775 y= -25.182 z= 33.889 and dimension values x=35.214 y= 23.529 and z= 22.425 as well as certain parameters such as numbers of exhaustiveness of 8 and number of modes of 16. The ligands were then sorted according to their binding energy, and those with higher binding energies than the native ligand, SAM, and SAH were selected for further analysis.

## 3.6 Screening with hMATs Proteins and Preference index

After a selection process, the selected ligands were tested for their potential to interact with human hMAT1A protein, which is involved in the production of SAM. This additional screening was done to ensure that the chosen drug candidate would not inhibit SAM production by these proteins, both of which are found in the liver and play important roles in human health. The ligands were docked with the hMAT1A protein to assess their potential to interfere with their function.

Molecular docking was conducted with hMAT1A protein and a set of primarily screened ligands. The center grid box and dimension values for the hMAT1A protein were x: 31.096, y: -0.571, z: 24.983 and x: 27.625, y: 57.151, z: 32.622, respectively. The final selection of the lead molecule was based on its high binding energy against the target protein, high preference index, but low binding energy against human hMAT1A protein, which is involved in the synthesis of SAM. To further refine the selection of the lead molecule among the screened ligands one parameter was added called preference index was calculated using the hydrogen bond acceptor and donor capabilities and the number of rotatable bonds of the pharmacophore.

The formula for calculating the preference index was as follows:

{(H-acceptor + H-donor + Rotatable bonds count) * 5}/ 25.

## 3.7 Visualization of interaction of Protein-ligand

The protein-ligand interactions were visualized using PyMOL and Ligplot. These tools allowed for the analysis and visualization of the binding between proteins and ligands, providing insights into the nature of the interactions and the spatial arrangement of the molecules. Additionally, the binding energy between each docked ligand and the target protein was calculated in KJ/mol. This value reflects the strength of the interaction between the ligand and the protein and can be used to evaluate the potential of the ligand as a drug candidate.

(a) Using Ligplot

The protein and ligand pdb file (made while visualizing active sites) was opened in ligplot+ for visualization of 2D interactions. By using this tool, the hydrogen bonds and hydrophobic bonds were determined which are responsible for the higher binding energy. These interactions gave a more detailed understanding of the specific interactions taking place between the protein and the ligand which contribute to their binding.

(b) Using Biovia Discovery Studio

The protein and ligand pdb file was opened in BioVia Discovery Studio, a computational tool that allows for the identification of various types of bonds between atoms of a protein and a ligand. This tool was used to identify other types of interactions such as alkyl bonds, pi-alkyl bonds, pi-pi t-shaped bonds, pi-sigma bonds, carbon-hydrogen bonds, etc. and the residues of the protein and the ligand that are involved in those interactions. Additionally, the bond distances, which provide information about the strength of the interactions, were also calculated. This information further helped to understand the affinity and specificity of the binding of ligand to the protein.

## 3.8 Predicting properties of the molecule using Gauss view and Gaussian 03

The properties and the reactions of the molecules were visualized by using Gauss view and Gaussian 03. The Density Functional Theory (DFT) method, named Becke, 3-parameter, Lee-Yang-Parr (B3LYP) and 6-31G basis set was selected as method to gain a deeper understanding of the electronic properties of the ligand and its interactions with the protein, the electronic structure, equilibrium geometry and quantum chemical calculations as well as to interpret Highest Occupied Molecular Orbital (HOMO) and Lowest Unoccupied Molecular Orbital (LUMO) analysis in their optimized structures(i.e. at the minimum potential energy. These calculations were performed using Gaussian 03. Furthermore, the electronic properties of the compound, frontier molecular orbital studies and molecular electrostatic potential maps (MEP) were prepared and visualized using Gauss view.

Gaussian input file was prepared for DFT calculations in PyMol by adding hydrogen atoms in PDB file of the docked ligand structure. Parameters were set for the Gaussian calculator, such as job type options for optimization and frequency calculations as well as Raman computations. After creating the Gaussian input file, it was opened in Gaussian 03 and were used for visualizing and preparing the molecular electrostatic potential map (MEP) and observing vibrations, as well as for performing the Frontier orbital studies to obtain the highest occupied molecular orbital (HOMO) and the lowest occupied molecular orbital (LUMO) and the HOMO-LUMO energy gap. The Gaussian output file was also studied to observe the charge distribution, which provides information about the regions of positive and negative electrostatic potential.

# 4. RESULTS AND DISCUSSION

## 4.1 Target protein selection

Protein target identification is the most important factor for the development of the new drug. Targeting the essential genes or proteins which are involved in biosynthesis of essential metabolites, required for the survival of the cell, and by inhibiting their function, the drug can effectively kill or inhibit the growth of the targeted pathogen. It was found that DNA adenine methylase, also known as Dam, is a conserved enzyme in many pathogenic bacteria, including Vibrio *cholera*, *Salmonella enterica* serovar Typhi, pathogenic *E. coli*, *Yersinia pestis* and *Haemophilus influenza* (Fleischmann *et al.,* 1995). This enzyme plays a key role in DNA methylation serves several important functions in the bacteria including, regulating gene expression, protecting the genome from foreign DNA, maintenance of the chromosomal structure and integrity of the bacterial cell (Sánchez-Romero *et al.,* 2020). In some studies, researchers have found that Dam methylation in *Salmonella enterica* serovar Typhimurium plays a role in regulating the invasion genes of pathogenicity island I (SPI-1) (Balbontin *et al.,* 2006), which is a genetic element that contributes to the bacteria's ability to cause infections in host cells. This suggests that Dam methylation could be a target for developing new drugs to combat infections caused by *Salmonella enterica* serovar Typhimurium and other pathogens that rely on Dam methylation to regulate the expression of genes involved in pathogenesis. Additionally, *dam* gene is found to be the essential gene for bacterial survival. Thus, here dam protein was taken as the target. Since, the 3D crystal structure was unavailable in RCSB, its 3D structure was made through Homology Modeling by using MODELLER.

DNA methyltransferases (Dam) transfer the methyl group from SAM to specific residues in double-stranded DNA i.e it uses SAM. Similarly, hMAT1A (PDB ID: 6SW5) are the enzymes that produce S-adenosylmethionine (SAM), which is a critical metabolite for liver health. In order to develop new drugs targeting the bacterial DNA adenine methylase (Dam), it is important to identify compounds that do not inhibit hMAT1A. Therefore, the protein structure of hMAT1A was retrieved from the RCSB database and used as a target for molecular docking studies to screen for molecules that do not inhibit the activity of hMAT1A. This way it is possible to identify drug candidates that target Dam in bacteria without affecting the activity of hMAT1A and therefore minimizing potential side effects on human liver health.

## 4.2 Homology modelling using MODELLER

Homology modeling, also known as comparative modeling, is a method for predicting the structure of a protein based on the structure of a related protein with known structure. It is a useful technique when experimental methods for determining a protein structure, such as X-ray crystallography or NMR spectroscopy, are not feasible. Here, the 3D crystal structure of Dam protein was unavailable in PDB. Thus, its structure was made by homology modeling using MODELLER. The process typically involved three main steps:

Identification of a suitable template structure: The first step was to find a protein structure with a similar sequence to the target protein. This was done by performing a sequence alignment between the target protein and known structures in databases such as the Protein Data Bank (PDB) by using BLAST. The template structure which had a high degree of sequence similarity (92.45%)) to the target protein was with *E.coli* strain. Thus, *E.coli* strain was chosen as a template structure.

Building the model: Once a suitable template structure had been identified, the next step was to use the coordinates of the template structure to generate a model of the target protein which was done by superimposing the target protein sequence onto the template structure and adjusting the coordinates of the template structure to match the sequence of the target protein.

Model evaluation: The final step was to evaluate the quality of the model. This was done by comparing the modeled structure with the known structure of the template, and by evaluating the stereochemistry of the model and the energy of the model. Several assessment softwares was used to evaluate the model like ProSA, Ramachandran plot, ERRAT, etc.

Table 2: Evaluation of different model using different softwares

| **Model no.** | **Ramachandran Aanalysis** | | **Z-score** | **DOPE score** | **ERRAT** |
|---|---|---|---|---|---|
| | **Most favored** | **Disallowed** | | | **Overall quality factor** |
| dam.B99990001 | 88.8 | 1.2 | -7.95 | -32446.86328 | 73.034 |
| dam.B99990002 | 87.6 | 0.8 | -8.52 | -31949.17773 | 63.019 |
| dam.B99990003 | 84.4 | 1.6 | -7.98 | -31974.81055 | 68.773 |
| dam.B99990004 | 87.6 | 0.4 | -7.93 | -31972.24414 | 71.161 |
| dam.B99990005 | 90.8 | 0.4 | -8.29 | -32854.00000 | 85.338 |

When evaluating protein structure models, among several methods and criteria one of the methods is Ramachandran plot (Ramachandran and Sasisekharan, 1968). It is a graphical representation that shows the distribution of the dihedral angles phi and psi in a protein structure. The plot visualizes the regions that are energetically favorable and unfavorable for the peptide backbone conformations which is based on the chemical properties of the peptide bond and experimental data. When evaluating protein structure models, particularly those generated by homology modeling, a Ramachandran plot can be used to identify potential problems with the structure. If a high number of dihedral angles fall in the forbidden regions of the Ramachandran plot, it indicates that the model is of poor quality and that there may be errors in the structure. This is because such deviations are unusual in experimental structures and indicate that something is wrong with the structure.

These deviations can be caused by errors in the alignment, errors in the model building, or other factors (Sobolev *et al.,* 2020). In this case, it was noted that the model dam.B99990005 had a high percentage of residues (90.8%) in the favored region and low percentage of residues (0.4%) in the disallowed region of the plot, which is an indication of a good quality model. On the other hand, the model dam.B99990004 also had a similar low percentage of residues (0.4%) in the disallowed region of the plot, but it was rejected because it had a lower percentage of residues (87.6%) in the favored region of the plot than model dam.B99990005. This suggests that even though both models had a similar level of errors or deviations in the dihedral angles, but the model dam.B99990005 still had a higher number of residues within the expected or allowed region, making it a better model.

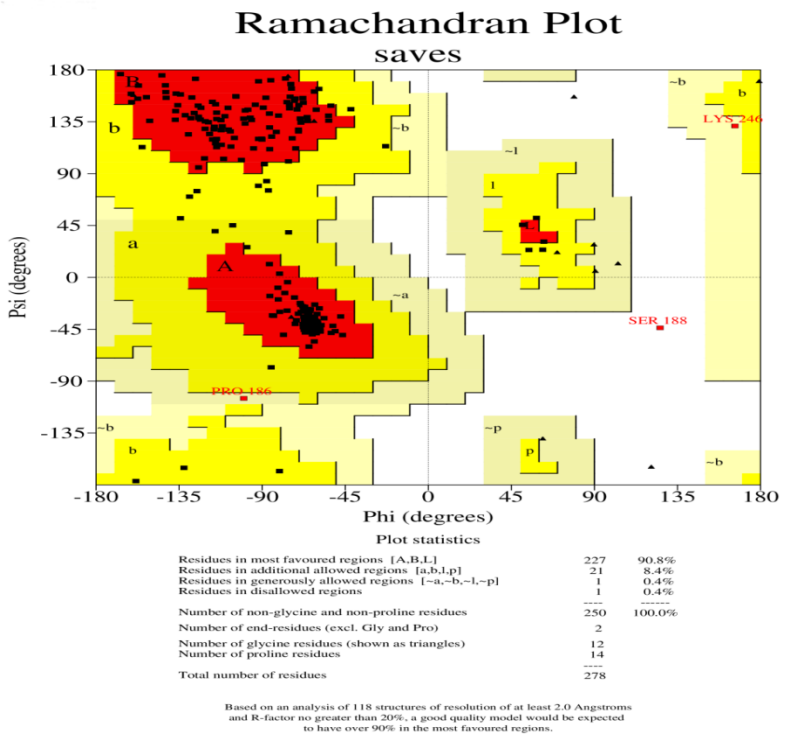


*Figure 10: Ramachandran plot of selected dam.B99990005 model*

Another method for evaluating the protein structure is through ProSA (Protein Structure Analysis) (https://prosa.services.came.sbg.ac.at/prosa.php) program where Z-score is calculated. ProSA is a web-based tool that can be used to evaluate the quality of protein structures and to identify errors in the structure, it's based on a scoring function that calculates a total energy score for a given protein structure and compares it to a set of experimental data and physical principles (Wiederstein and Sippl, 2007). Z-score is based on the concept of energy separation, the difference in energy between the native fold of a protein and the average energy of an ensemble of misfolded structures. The energy separation is then normalized by the standard deviation of the ensemble, to get the Z-score. The standard deviation serves as a measure of the spread of the ensemble and gives an indication of the confidence that can be placed in the Z-score value (Sippl, 1993 ).

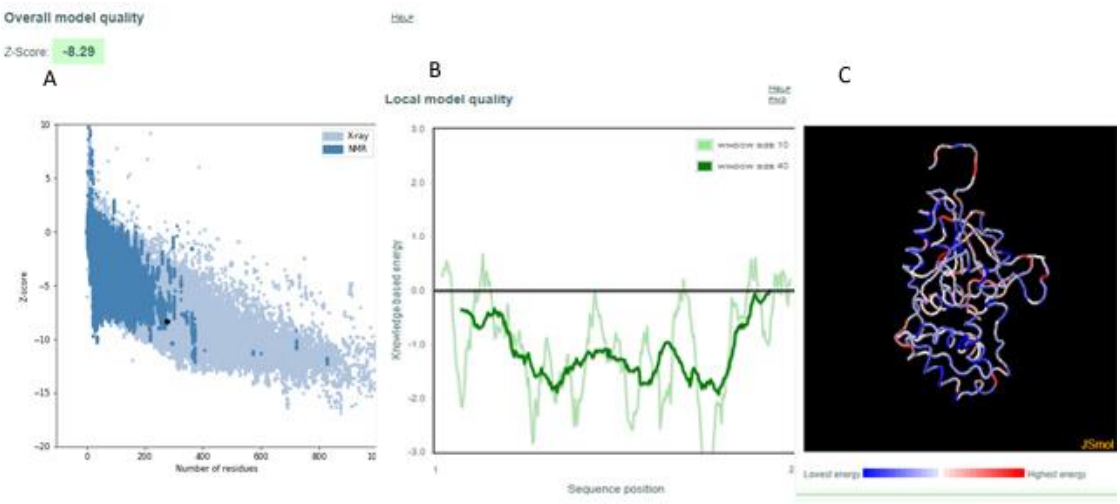


*Figure 11: Z-score result of dam.B99990005 model A) black spot represents the value of Z-score of the selected model B) energy plot diagram C) 3D diagram of selected model showing highest and lowest energy in blue and red respectively.*

ERRAT is another method, used to check the accuracy of protein structures that have been determined through crystallography (Colovos and Yeates,1993). Higher the overall quality factor in ERRAT the more accurate is the structure. Here, model dam.B99990005 showed higher overall quality factor (85.338).

Similarly, another used method is the DOPE (Discrete Optimized Protein Energy) score. It is a statistical potential that is calculated for each residue in a protein structure and is used to assess the quality of the model. A lower DOPE score generally indicates a better quality model, as it means that the model has a more favorable energy state. In this case, model dam.B99990005 had the lowest DOPE score among the four other models so it could be considered as the best among the models. Additionally, the Ramachandran analysis of this model also suggests that it is of high quality, with a high percentage of favored conformations (90.8%) and the ERRAT analysis also showed an overall high quality for this model. Based on these observations, it was concluded that the model dam.B99990005 is likely to be the best model among the four models considered.

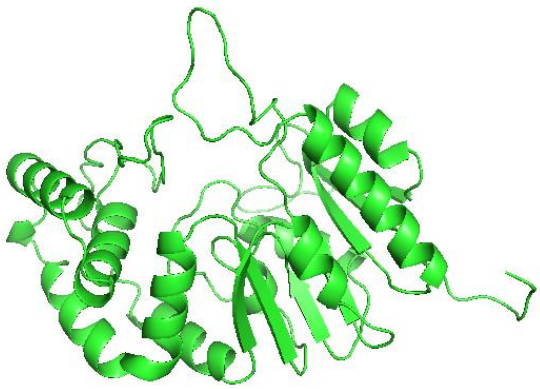

*Figure 12: Final model of Dam protein observed in PyMol*

## 4.3 Preparation and selection of Ligand Library

Ligands were prepared from various ligand library such as ZINC15 (www.zinc15docking.org) for natural products which consists of different categories such as- FDA, Biogenic-FDA, in Man, in World, in Trial and *in vivo*, UORSY database (https://uorsy.com/) for kinase inhibitors, indole derivatives and ASINEX (https://www.asinex.com/nucleoside-mimetics), for nucleoside mimetics.

Natural products have a long history of use in traditional medicine and have played a key role in the development of modern pharmaceuticals. Many natural products, such as plants and microorganisms, contain compounds that have medicinal properties. These compounds can be isolated and studied to determine their potential therapeutic uses. It is estimated that about 40% of all medicines are either natural products or their semisynthetic derivatives. This is due in large part to the diversity of chemical compounds found in natural products, which can provide a rich source of potential drug candidates. As for instance, Vincristine, irinotecan, etoposide, and paclitaxel are plant-derived compounds that are used in cancer treatment. Dactinomycin, bleomycin, and doxorubicin are anticancer agents that come from microbial sources. Citarabine is an anticancer agent that is derived from a marine source (da Rocha *et al.,* 2001). Similarly, Natural products also have structural diversity making them to avoid potential drug-drug interactions that can arise when drugs have similar structures. Furthermore, natural products have been found to have a high degree of specificity and selectivity in their biological activity, hence can target specific receptors or enzymes without affecting other biological systems, reducing the risk of unwanted side effects. Thus, the diverse range of compounds found in natural products, as well as their specificity and selectivity in biological activity, make them an attractive option for drug development.

ZINC database was used to develop the natural product library which consists of 21,000 molecules. 205 natural compounds were narrowed down after ADME/Tox filteration and carried out for docking.

In addition, kinase inhibitors from UORSY database were selected as the potential therapeutic targets as they can compete with S-adenosyl methionine (SAM) due to the adenosine moiety they possess. Similarly, they can also act as inhibitors because they mimic the hydrogen bond interactions that are normally formed by the adenosine ring of ATP. It was found that several S-adenosylmethionine analogs have the potential to inhibit Dam methyltransferase activity in approximately 10uM range (Hobley *et al*., 2012). Here, out of 6,449 kinase inhibitors processed for ADME/Tox filters for docking through OSIRIS, 1,685 molecules were narrowed down and carried out for molecular docking.

Nucleoside analogues are a class of compounds that have a similar structure to nucleosides, which are the building blocks of nucleic acids such as DNA and RNA. These compounds have a nucleoside-like core, which often includes an adenosine moiety, and have been shown to have antibacterial activity. These compounds target cell-wall biosynthesis, which is an essential process for bacterial growth and survival.

By inhibiting cell-wall biosynthesis, these compounds can disrupt the integrity of the bacterial cell wall and ultimately lead to the death of the bacteria. The adenosine moiety in these compounds makes them similar in structure to SAM. A ligand library of nucleoside mimics containing 3118 molecules was obtained from ASINEX and a final library of 654 molecules was prepared after filtering through the OSIRIS filter.

Indole derivatives have long been used as drug targets in many pharmaceutical research studies. These compounds have a structural similarity with the adenosine moiety of SAM, which makes them a potential target for SAM-utilizing bacterial genes, such as –Dam. A ligand library of 462 molecules including indole derivatives was prepared after filtering a library of 10342 molecules through the OSIRIS ADME/Tox filter.

## 4.4 *In-silico* ADME/Tox tests

In drug discovery, it is important to select ligands (compounds) that have the potential to be developed into drugs. To do this, it is necessary to evaluate the ligands for certain essential parameters that are relevant to drug molecules. One way to do this is to use a program such as OSIRIS, which can analyze the druglikeness and pharmacokinetics properties of the ligands using a list of parameters. One such parameter that is commonly used is Lipinski's rule of five (also known as the "Rule of 5"), which states that a drug candidate should have no more than five hydrogen bond donors, no more than 10 hydrogen bond acceptors, a molecular weight of less than 500 kdaltons, and a partition coefficient (logP) between -5 and 5.

For a drug to be effective, it needs to be properly absorbed into the body. Molecular size is also an important factor that affects the absorption of drugs. Smaller molecules are able to cross the cell membrane more easily than larger molecules. This is because small molecules are able to fit through the protein channels in the cell membrane, while larger molecules are too big to pass through. The molecular size should be between 200-500 kdaltons since small drug molecules are able to cross the membrane more easily than larger molecules.

The number of hydrogen bonds in a drug molecule can affect its ability to cross biological membranes. A compound that has more hydrogen bonds will have a higher affinity for water and will have to break more bonds to cross the membrane. This can make it more difficult for the drug molecule to cross the membrane, which can affect its absorption and distribution in the body. Therefore, it is generally considered unfavorable for a compound to have a high number of hydrogen bonds, as it can make it more difficult for the drug molecule to cross the biological membrane and enter the body. On the other hand, compounds with fewer hydrogen bonds will have less interaction with water, which allows the molecule to cross the membrane more easily. This can increase the absorption and distribution of the drug in the body, which is important for its effectiveness. Thus, the optimal number of hydrogen bond acceptor is less than 10 and hydrogen bond donor is less than 5.

Similarly, cLogS is a measure of the aqueous solubility of a molecule. The solubility of a drug in water is an important factor that affects its absorption and distribution characteristics in the body.The aqueous solubility of a drug significantly affects its ability to be absorbed by the body and to reach the site of action. Drugs that are highly soluble in water are more likely to be absorbed and distributed throughout the body, while drugs that are poorly soluble in water are less likely to be absorbed and may be eliminated before entering circulation consequently do not exhibit pharmacological activity.

Moreover, the cLogP value is a measure of a compound's hydrophilicity which is used to predict the behavior of a compound in an aqueous environment and its ability to cross biological membranes. In general, compounds with a lower cLogP value are more hydrophilic and are more likely to dissolve in water, while compounds with a higher cLogP value are more hydrophobic and are more likely to dissolve in fats and oils. This is important because the ability of a drug molecule to cross biological membranes is dependent on its solubility. Lipid-soluble drugs are more likely to cross the cell membrane than water-soluble drugs. It has been shown that compounds with a cLogP value greater than 5.0 have a lower probability of being well absorbed. This is because compounds with a high cLogP value are more likely to be hydrophobic and less likely to dissolve in water. This makes it more difficult for the drug molecule to cross the hydrophobic cell membrane, which can affect its absorption and distribution in the body.

Further screening of the ligands was done using Veber's rule which is based on the two main criteria- the rotatable bond count and the topological polar surface area (TPSA).The rotatable bond count is the number of bonds in a molecule that can rotate freely. It is believed that molecules with a low rotatable bond count no more than 10 are more likely to have good oral bioavailability because they are less flexible and less likely to become trapped in a particular conformation that makes it difficult to cross biological membranes. The second criterion, TPSA, is a measure of the polar surface area of a molecule. It is believed that molecules with a low TPSA, less than 120 A are more likely to have good oral bioavailability because they are less polar and less likely to be attracted to the polar environment of biological membranes. These criteria were applied as an additional filter to the ligands to ensure that the selected compounds have a higher probability of crossing biological membranes and having good oral bioavailability.

Furthermore, the ligands were also screened for their druglikeness and toxicity such as- mutagenicity, tumorigenicity, reproductive effects and irritant effects through ORISIS. The ORISIS tool provides a comprehensive assessment of the ligand's safety profile. By filtering the ligands through this process, it ensures that the compounds selected for further development have a lower risk of causing harmful effects on human health. This is an important step in the drug development process as it helps to identify compounds that may have a high probability of success and help to reduce the risk of negative effects on human health (Beaumont *et al.,* 2014).

Hence, the ligands that pass these initial screens are more likely to be safe and effective drugs. Finally, after ADME/Tox screening, the ligand library was converted into pdbqt format.

## 4.5 Active sites prediction and molecular docking

To find out the putative drug against *Salmonella typhimurium,* the target specific proteins that are essential for the survival of the pathogen needs to be identified. The Dam protein is one such protein that is crucial for the survival of *Salmonella*. By blocking the formation of the Dam protein, the survival of the pathogen can be inhibited. For identification of the active sites of the Dam protein, molecular docking and molecular dynamics simulations can be used. Here, we used molecular docking for this task. This method predicted the binding pose of potential inhibitors, and the interactions between the inhibitors and the protein, ultimately helped to design new molecules that can bind to the active site of the Dam protein and inhibit its activity.

To carry out molecular docking, the verified 3D structure, made through MODELLER in PDB format was converted to pdbqt format in PyRx. Total Gasteiger charge 6.0016 was added. These charges are important for accurately modeling the electrostatic interactions between atoms, which is crucial for understanding the behavior of molecules in a wide range of chemical processes. Gasteiger charges are calculated using the SetPartialCharge algorithm, calculates charges based on the concept of electronegativity equilibration. In the SetPartialCharge method, all hydrogen atoms are explicitly included in the calculation of the partial charges, rather than being treated as a single entity. The explicit representation of hydrogens is important for accurately modeling the electrostatic interactions between atoms, particularly for hydrogen bonding interactions which are important in biological systems. Similarly, the algorithm takes into account the electronegativity of each atom in the molecule and distributes the electrons in a way that results in electronegativity equilibrium. This means that the electrons are distributed in a way that balances the electronegativity of each atom and results in a stable electron distribution (Rafael and Vinícius, 2018).

For maintaining the consistency in the experimental conditions for each ligand library being studied, a grid box was set up to cover the active sites of the target protein during the docking process. This grid box was kept constant for each docking process with all ligand libraries, allowing for unbiased comparison of the outcomes. This ensured that any differences in the results were due to the properties of the ligand libraries and not variations in the experimental setup. The center grid box values x= -18.775 y= -25.182 z= 33.889 and dimension values x=35.214 y= 23.529 and z= 22.425 as well as certain parameters such as numbers of exhaustiveness of 8 and number of modes of 16 were set up.

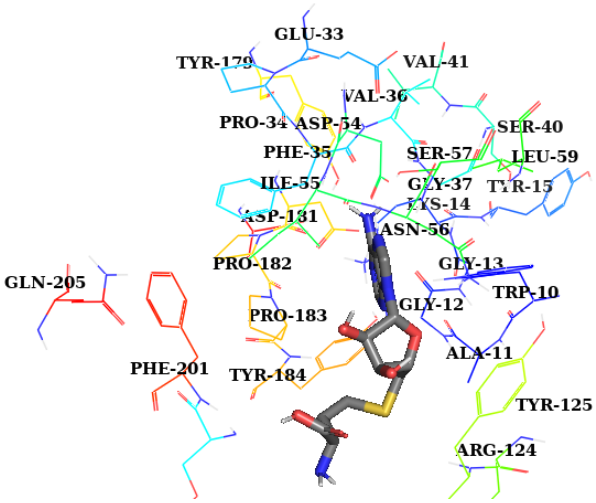


*Figure 13: Binding sites prediction within 5Å with native ligand (SAH) with Dam protein*

The active sites of Dam protein which were used for docking are mentioned in the table 3 below

Table 3: Active binding sites of Dam protein obtained by PyMol

| Residues | Amino Acid | Residues | Amino Acid |
|---|---|---|---|
| 10 | TRP | 54 | ASP |
| 11 | ALA | 55 | ILE |
| 12 | GLY | 56 | ASN |
| 13 | GLY | 59 | LEU |
| 14 | LYS | 163 | GLU |
| 15 | TYR | 164 | SER |
| 33 | GLU | 165 | TYR |
| 34 | PRO | 179 | TYR |
| 35 | PHE | 181 | ASP |
| 36 | VAL | 182 | PRO |
| 37 | GLY | 183 | PRO |
| 39 | GLY | 184 | TYR |
| 40 | SER | 201 | PHE |
| 41 | VAL | 205 | GLN |

## 4.6 Screening with hMATs Proteins and Preference Index and its significance

S-adenosylmethionine (SAM) is a critical molecule for human health that is primarily produced in the liver through the catabolism of methionine, a process catalyzed by the enzyme methionine adenosyltransferase (MAT). There are two different genes that encode for MAT, MAT1A and MAT2A, which are responsible for producing the enzymes hMAT1A and hMAT2A, respectively. These enzymes are responsible for biosynthesis of SAM in liver and extra-hepatic tissues. In order to find potential drug

candidates that could specifically target the target protein, while avoiding inhibition of human hMAT1A and hMAT2A. First, the ligands that had high binding affinity for the target protein, Dam, were selected as the best candidates for further analysis. After that these ligands were docked with and those which had lower binding affinity with human enzymes were selected. Thus, the ligands that had higher binding affinity for Dam than for the human enzymes were considered as potential drug candidates, as they have a higher binding affinity towards the bacterial Dam and lower binding affinity towards human SAM biosynthesizing enzymes. This is crucial because the drug targets discovered should not degrade human health and must be safe for human consumption. The ligands that passed this screening were then studied further for their potential as drug candidates. The active sites of hMAT1A (PDB: 6SW5) binding with SAM are mentioned in the table 4.

Table 4: Active sites of hMAT1A (PDB: 6SW5) binding with SAM obtained from PyMol

| **Residues** | **Amino acid** |
|---|---|
| 55 | ALA |
| 70 | GLU |
| 112 | GLN |
| 114 | SER |
| 117 | ILE |
| 133 | GLY |
| 134 | ASP |
| 289 | LYS |
| 291 | ASP |

The center grid box values in A x= 31.096 y= -0.571 z= 24.983 and dimension values x= 27.625 y= 57.151 and z= 32.622 for hMAT1A (PDB: 6SW5) was set up.

Furthermore, to select the most promising ligands for drug development, an empirical formula was used to calculate a preference index. The formula was based on the number of H-bond acceptors, H-bond donors, and rotatable bond counts in the ligands.

{(H-acceptor + H-donor + Rotatable bonds count) * 5}/ 25.

The reason for using this formula is that, for a drug to be effective, it needs to be able to cross biological membranes and reach its target protein. Hydrogen bonds play a crucial role in the partitioning of biologically active compounds and their interactions with target proteins. H-bond acceptors are atoms or groups of atoms that can accept a hydrogen bond, while H-bond donors are atoms or groups of atoms that can donate a hydrogen bond. In the aqueous environment of the body, drug molecules must be able to break hydrogen bonds in order to cross biological membranes and reach their target proteins. The number of H-bond acceptors and donors in a ligand can affect its ability to partition across membranes and interact with its target protein.

Rotatable bonds are chemical bonds that allow a molecule to rotate around a specific axis, which can affect its flexibility and ability to bind to a target protein. A molecule with more rotatable bonds may be more flexible and able to bind to a target protein in different orientations, which can increase its binding affinity.

## 4.7 Protein- Ligand Interaction

The molecular docking of natural products, indole derivatives, kinase inhibitors and nucleoside mimetics were carried out along with native ligand SAM and SAH against Dam protein in PyRx.

### 4.7.1 Analyzing virtual screening of natural products

A virtual screening of natural products against the Dam protein of *Salmonella typhimurium* was performed using the PyRx software. Among the 205 natural products that were screened, 5 compounds were selected based on their binding energy and preference index with Dam and hMAT1A. The screening process involved evaluating the binding affinity of the ligands to the Dam protein, as well as comparing their binding affinity with hMAT1A, a human protein. The ligands that showed higher binding affinity with Dam and lower affinity with hMAT1A were chosen for further analysis.

The binding energy and preference index of the selected 5 compounds were analyzed, and it was found that two compounds, ZINC000001590366 and ZINC000004716487, had the highest binding energy with Dam at -8.5 kJ/mol and -8.1 kJ/mol respectively, and the highest preference index of 2. Additionally, these compounds showed better binding affinity towards Dam as compared to binding energy against Dam to -7.8 kJ/mol of SAM and -8kJ/mol of SAH. The compound ZINC00005729706 had a higher binding energy of -8.5 kJ/mol, but it was not selected as it had a lower preference index.

These results suggest that the two compounds ZINC000001590366 and ZINC000004716487 have the potential to be developed as drugs that specifically target the Dam protein of *Salmonella typhimurium*, as they showed higher binding affinity with Dam and lower affinity with hMAT1A.

Table 5: Summary of top hits Natural Product compounds after molecular docking against Dam

| Natural Products | Molecular Characters | | | | | | Binding energy (kJ/mol) | | |
|---|---|---|---|---|---|---|---|---|---|
| Database ID | cLogP | cLogS | H-Acceptors | H-Donors | Polar Surface Area | Druglikeness | Dam | hMAT1A | Preference Index |
| ZINC000001590366 | 0.2123 | -2.099 | 5 | 2 | 75.27 | 3.5451 | -8.5 | -7.2 | 2 |
| ZINC000004716487 | 2.5424 | -3.266 | 4 | 2 | 66.76 | 0.21902 | -8.1 | -6.9 | 2 |
| ZINC000001319234 | 2.6104 | -3.097 | 4 | 1 | 45.59 | 0.87864 | -8.1 | -6.6 | 1.8 |
| ZINC000003831404 | 2.6104 | -3.097 | 4 | 1 | 45.59 | 0.87864 | -8.1 | -7.2 | 1.8 |
| ZINC000057297068 | 2.9248 | -3.576 | 4 | 1 | 45.33 | 2.3478 | -8.5 | -7.1 | 1.6 |

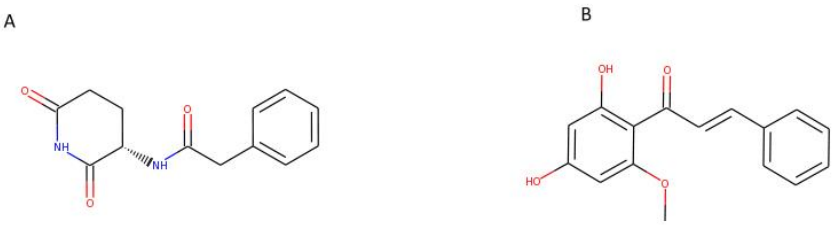


*Figure 14: Molecular structures of the selected Natural Product molecules that could be the putative drug against Salmonella typhimurium (A) ZINC000001590366 (B) ZINC000004716487*

Compound ZINC000001590366 was identified as Antineoplaston A10 in Pubchem (https://pubchem.ncbi.nlm.nih.gov/)**.** This compound is a mixture of peptides, amino acid derivatives, and organic acids that are believed to be part of a natural defense system against human cancers and other diseases (Buckner *et al.,* 1999). The active compound was found to be 3-phenylacetylamino-2,6-piperinedione, thus named as Antineoplaston A10 (Revelle *et al.,* 1996). It was first isolated from human urine. This compound has been proposed as a cancer treatment by Dr. Stanislaw Burzynski. According to Dr. Burzynski, antineoplastons bind to specific receptors on cancer cells and cause them to differentiate or undergo programmed cell death, leading to the regression of the cancer (Burzynski *et al.,* 2006). It is being used in the trails studying

the treatment of Sarcoma, Lymphoma, Lung Cancer, Liver Cancer, and Kidney Cancer (https://www.drugbank.ca/drugs/DB11702).

Compound ZINC000004716487 was identified as Cardamonin (https://zinc15.docking.org/substances/ZINC000004716487/). Cardamonin, also known as Dihydroxymethoxychalcone, is a naturally occurring flavonoid compound that belongs to a class of compounds called chalcones (https://pubchem.ncbi.nlm.nih.gov/compound/641785). It is found in various plant species, including the plant family Zingiberaceae, which includes ginger and cardamom. The compound has been found to have a wide range of biological activities, including anti-inflammatory, antioxidant, antimicrobial, and anticancer properties (Chavan *et al.,* 2016). Zhang *et al* discovered that methoxy chalcones have the potential to be developed as a treatment for acute inflammatory diseases (Zhang *et al.,* 2016). A study found that a specific subgroup of chalcones compounds, called methoxy-4'-amino chalcones, demonstrated strong antimicrobial properties in vitro against *Escherichia coli*, *Staphylococcus aureus* and *Candida albicans* (Gomes *et al.,* 2017). Some chalcones have been successfully developed as drugs for the treatment of digestive system diseases, cancer, cardiovascular diseases, and viral infections (Ni *et al.,* 2004; Katsori *et al.,* 2011). Chalcones have been found to inhibit the growth of cancer cells and induce cell death in various types of cancer cells. They are also reported to inhibit the formation of new blood vessels in tumors, which is important for the treatment of cancer (Orlikova *et al*., 2011; Zhong *et al*., 2015). Thus, these studies show cardamonin as the potential drug against pathogens.

### 4.7.2 Analyzing virtual screening of indole derivatives

A large library of indole derivatives containing a total of 10,345 ligands were screened for their ADME/Tox properties, and narrowed down to 462 ligands. These 462 ligands were then analyzed using molecular docking in the PyRx platform with the Dam protein. Based on the binding affinities with Dam and hMAT1A, as well as preference index, three compounds were selected for further analysis. The native ligand SAM and SAH had binding energies of -7.8 kJ/mol and -8 kJ/mol with the Dam protein, respectively. Similarly, the binding energy of SAM with hMAT1A was -7.4 kJ/mol. The compound with the highest binding energy with Dam compared to SAM and SAH, and low binding affinity with hMAT1A was selected for further analysis. The compound v029-3617 had a binding energy of -8.7 kJ/mol with Dam and -6.8 kJ/mol with hMAT1A, which met the criteria. Additionally, this compound had the highest preference index of 3 among the other compounds. The compound p935-1675, despite having high binding energy with Dam and low binding affinity with hMAT1A, was not selected as it had a low preference index.

Table 6: Summary of top hits indole derivative compounds after molecular docking against Dam

| Indole derivatives (kJ/mol) | Molecular Characters | | | | | | Binding energy | | |
|---|---|---|---|---|---|---|---|---|---|
| Database ID | cLogP | cLogS | H-Acceptors | H-Donors | Polar Surface Area | Druglikeness | Dam | hMAT1A | Preference Index |
| v029-3617 | 2.1939 | -3.157 | 6 | 2 | 72.36 | 1.5223 | -8.7 | -6.8 | 3 |
| p091-0204 | 2.8102 | -3.47 | 5 | 1 | 46.5 | 2.2271 | -8.8 | -6.8 | 2.4 |
| p935-1675 | 2.3374 | -2.123 | 5 | 1 | 49.74 | 3.4187 | -9 | -6.8 | 2.2 |

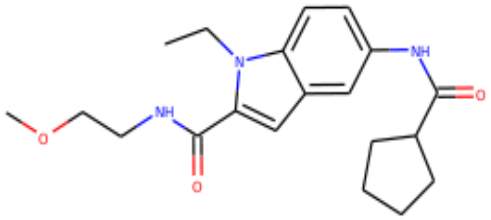


*Figure 15: Molecular structures of the selected indole derivative molecule (v029-3617) that could be the putative drug against Salmonella typhimurium*

The compound v029-3617 was found to be 5-cyclopentaneamido-1-ethyl-N-(2-methoxyethyl)-1H-indole-2-carboxamide (https://pubchem.ncbi.nlm.nih.gov/). This compound consists of important functional groups such as- indole and carboxamide. The indole moiety is a six-membered heterocyclic ring that is found in a variety of natural products and synthetic compounds. It has attracted significant interest in the field of drug development due to its structural similarity to several biologically active compounds, and its ability to interact with a wide range of target proteins. Indole derivatives exhibit antimicrobial, anti-cancer, anti-diabetic, anti-tubercular, anti-malarial, anti-HIV and anti-inflammatory properties (Caruso *et al.,* 2014; Guerra *et al.,* 2011; Saini *et al.,* 2015; Alsayed *et al.,* 2021). Some studies have shown that 5-(4-methylpiperazin-1-yl)-3-propyl-2-(1H-pyrrolo[2,3-b]pyridin-3-yl)-3H-imidazo[4,5-b]-
83 pyridine (X12) demonstrated anti-inflammatory properties both in vitro and in vivo to 84 inflammatory diseases. The compound was able to inhibit the production

of inflammatory cytokines, such as TNF-alpha, IL-1beta, and IL-6, in response to LPS stimulation, a component of the cell walls of gram-negative bacteria that can trigger the production of pro-inflammatory cytokines (Chen *et al.,* 2013). Moreover, the study found that this compound was able to reduce the severity of inflammation in a mouse model of sepsis, a severe systemic inflammatory response caused by bacterial infection in vivo (Liu *et al.,* 2016). Similarly, Dai *et al.,* created two analogs of compound X12 and those compounds demonstrated effective in attenuating LPS-induced pulmonary edema, reducing lung pathological changes, reducing the infiltration of inflammatory cells into the lungs and the expression of pro-inflammatory cytokines in vivo (Dai *et al.,* 2018). Additionally, the researchers have discovered a series of small molecule inhibitors which includes a 1H-indole-2-carboxamide hinge scaffold, showed therapeutic effects on DSS (Dextran sulfate sodium)-induced UC (a mouse model of Ulcerative Colitis), by acting as an ASK1 (Apoptosis Signal-regulating Kinase 1) small molecule inhibitor with anti-inflammatory properties (Hou *et al.,* 2021). Hence, based on these studies It can be concluded that compound v029-3617 (5-cyclopentaneamido-1-ethyl-N-(2-methoxyethyl)-1H-indole-2-carboxamide) having both indole and carboxamide together as the potential drug target.

### 4.7.3 Analyzing virtual screening of kinase inhibitors

A ligand library from UORSY kinase inhibitor from 6449 ligands 1685 ligands were narrowed down using ADME/Tox filter from OSIRIS datawarrior. Six compounds were finalized based on their binding affinity with target protein, Dam and hMAT1A as well as preference index. Out of six compounds the compound, pb56907280 was chosen for further analysis. The compounds showed a better binding affinity towards Dam than the reference compounds SAM binding energy of -7.8 kJ/mol and SAH of -8kJ/mol, with binding energies of -9kJ/mol. Furthermore, the compound had a lower binding affinity towards hMAT1A than the other compounds in the library, with binding energiy of -6.9kJ/mol. Similiarly, the preference index (3) was high with this compound than rest of the compounds. Based on these results, the compound pb56907280 was chosen as the putative drug for further analysis that would effectively target Dam protein of *Salmonella typhimurium*.

Table 7: Summary of top hits uorsy kinase inhibitor compounds after molecular docking against Dam

| Kinase inhibitors | Molecular Characters | | | | | | Binding energy (kJ/mol) | | |
|---|---|---|---|---|---|---|---|---|---|
| Database ID | cLogP | cLogS | H-Acceptors | H-Donors | Polar Surface Area | Druglikeness | Dam | hMAT1A | Preference Index |
| pb28367209 | 3.0013 | -3.991 | 3 | 2 | 44.89 | 0.96835 | -9.8 | -7.4 | 1.4 |
| pb30240174 | 3.9129 | -3.144 | 5 | 0 | 94.31 | 6.3259 | -9.6 | -7.3 | 1.8 |
| pb26780487 | 0.3008 | -2.313 | 7 | 2 | 89.02 | 4.4893 | -9.4 | -7.3 | 3 |
| pb1220506044 | 1.3884 | -2.27 | 6 | 2 | 70.25 | 7.6812 | -9 | -6.7 | 2.8 |
| pb56907280 | 2.1461 | -3.693 | 7 | 3 | 96.89 | 0.20255 | -9 | -6.9 | 3 |
| pb1190699900 | 1.3737 | -3.095 | 7 | 1 | 80.49 | 0.37992 | -8.8 | -6.9 | 2.6 |

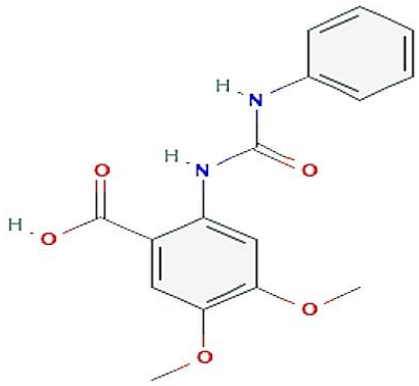

*Figure 16: Molecular structure of the selected kinase inhibitor molecule (pb56907280) that could be the putative drug against Salmonella typhimurium*

The compound pb56907280 was found to be 2-[[anilino(oxo)methyl]amino]-4,5-dimethoxybenzoic acid (https://pubchem.ncbi.nlm.nih.gov/).. This compound consists of some important functional group such as- aniline and benzoic acid. Aniline is used as a starting material for the synthesis of a variety of pharmaceuticals, including analgesics (paracetamols), anti-inflammatory drugs and anti-tumor drugs (Bicalutamide, Nilutamide etc). It was found that aniline derivative was identified as inhibitors of influenza A virus subtype H1N1 (Leiva *et al.,* 2018). Benzoic acid and its derivatives are commonly used as a preservative in a wide range of products, such as food, cosmetics, hygiene products, and medicines (oral, parenteral, and topical) as they have the ability to inhibit the growth of bacteria and fungi (SCCNFP, 2011). It was found that 3,5-Dihydroxybenaldehyde showed bactericidal activity against *Salmonella enterica* ($BA_{50}$=0.65) and *Campylobacter jejuni* ($BA_{50}$=0.088) (Friedman *et al.,* 2003). Studies have shown that benzoic acid can exhibit antiviral activity against picornaviruses, a family of viruses that includes bovine enterovirus type 1 (BEV-1) (EU Regulation 528/2012, 2013). Benzoates have been proposed as a potential therapeutic approach in the treatment of schizophrenia by inhibiting the activity of

D-amino acid oxidase (DAAO), an enzyme that is involved in the metabolism of D-amino acids. The inhibition of DAAO by benzoates may lead to an increase in the levels of D-serine in the brain, which in turn may lead to an improvement in the symptoms of schizophrenia, including cognitive deficits (Lane *et al.,* 2013). Thus, the screened kinase inhibitor compound could be suggested as the potential drug target to develop as antibiotics.

### 4.7.4 Analyzing virtual screening of Nucleoside mimetics

After conducting a virtual screening of 653 nucleoside mimetics compounds, six were selected based on their binding affinity with target proteins Dam and hMAT1A, as well as their preference index. Among these compounds, las_52127683 was found to have the highest binding affinity towards Dam, with a binding energy of -9.7 kJ/mol. This is significantly higher than the binding energies of -7.8 kJ/mol and -8 kJ/mol for the reference compounds SAM and SAH, respectively. Additionally, this compound had low binding affinity towards hMAT1A, with a binding energy of -7.5 kJ/mol compared to -7.9 kJ/mol for SAM. Furthermore, the preference index for las_52127683 was -3.8. In contrast ligand las_52139647 had highest preference index of 4.2 but it was not selected as drug target since it had low binding affinity with target protein Dam i.e. -8.7kJ/mol as well as high binding affinity with hMAT1A (-7.6kJ/mol) as compared to selected ligand las_52127683. These results suggest that las_52127683 is a promising compound for further consideration as a drug target.

Table 8: Summary of top hits Nucleoside mimetic compounds after molecular docking against Dam

| Nucleoside Mimetics | Molecular Characters | | | | | | Binding energy (kJ/mol) | |
|---|---|---|---|---|---|---|---|---|
| Database ID | cLogP | cLogS | H-Acceptors | H-Donors | Polar Surface Area | Druglikeness | Dam | hMAT1A | Preference Index |
| las_52127683 | 1.3605 | -3.203 | 8 | 2 | 88.33 | 6.7454 | -9.7 | -7.5 | 3.8 |
| las_52141662 | 1.9905 | -3.142 | 7 | 2 | 73.75 | 3.8818 | -9.1 | -7.5 | 3.6 |
| bdh_34041315 | 2.2819 | -3.396 | 9 | 2 | 94.06 | 5.9519 | -9 | -7.6 | 4 |
| bdh_34041301 | 2.3394 | -2.909 | 8 | 1 | 82.03 | 5.7108 | -9 | -7.6 | 3.4 |
| las_52141017 | 0.8265 | -2.253 | 8 | 2 | 82.98 | 4.2055 | -8.9 | -7.6 | 3.8 |
| las_52139647 | 1.0184 | -2.716 | 9 | 2 | 86.22 | 4.0605 | -8.7 | -7.6 | 4.2 |

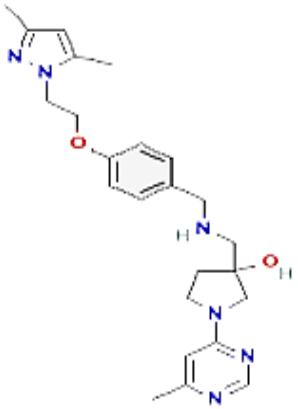

*Figure 17: Molecular structure of the selected Nucleoside mimetic molecule (las_52127683) that could be the putative drug against Salmonella typhimurium*

The compound las_52127683 was found to be 3-[[[4-[2-(3,5-Dimethylpyrazol-1-yl)ethoxy]phenyl]methylamino]methyl]-1-(6-methylpyrimidin-4-yl)pyrrolidin-3-ol (https://pubchem.ncbi.nlm.nih.gov/). This compound consists of several functional groups such as- pyrrolidinone, pyrimidine and pyrazole. Pyrrolidinone is a natural product found in *Ascochyta medicaginicola* and *Microtropis japonica*. It was found that Pyrrolidine carboxamide as a InhA inhibitors, gene *inhA* is a key catalyst in mycolic acid biosynthesis in *Mycobacterium tuberculosis,* showing an IC50 of 10.05 µM (He *et al.,* 2006). Similarly, Pyrimidine is one of the two main classes of nitrogen-containing bases that make up nucleic acids (DNA and RNA), the other being purines. Examples of pyrimidine bases found in DNA and RNA are cytosine, thymine, and uracil. Pyrimidine compounds are used as drugs to treat cancer and viral infections. As for instance cytarabine (Ara-C), a pyrimidine nucleoside analog, has been proven to be one of the most effective antineoplastic agents for treating leukemia, lymphoma as well as neoplastic meningitis. The drug works by interfering with the replication of cancer cells and preventing them from dividing and growing. It is converted into an active form within the cancer cells and incorporated into the DNA, which causes the cancer cells to die. (Burnett *et al.,* 2011; Friedberg, 2011). Additionally, 5-fluorouracil (5-FU) also one of the pyrimidine analog used to treat colorectal cancer (Blondy *et al.,* 2020).

Pyrazole has a wide range of biological activities, including antimicrobial, anticancer, cytotoxic, analgesic, anti-inflammatory, antihypertensive, and central nervous system (CNS) activities such as antiepileptic and antidepressant effects. Derivatives of pyrazole have also been found to have important pharmacological activities. They have been used as useful materials in drug research because of their potential to target specific biological pathways and molecules. One of the key areas where pyrazole derivatives have been found to be particularly useful is in the treatment of cancer. These compounds have been shown to have good inhibitory activities against a number of cancer-related targets, including BRAFV600E, EGFR, telomerase, ROS Receptor Tyrosine Kinase, and Aurora-A kinase. These are all proteins that are involved in the growth and spread of cancer cells, and by inhibiting their activity, pyrazole derivatives may be able to slow or stop the growth of cancerous tumors (Küçükgüzel *et al.,* 2015).

## 4.8 Analysis of protein ligand interactions

The lead compounds that have been identified as potential drug candidates based on their binding affinity to a target protein were screened for their protein-ligand interactions using PyMol, Discovery studio and ligplot. The interactions between the lead compounds and the protein were then analyzed in detail. Different amino acid residues in the protein can be involved in these interactions and they can interact via different types of bonding, such as hydrogen bonding, hydrophobic interactions, and electrostatic interactions. The specific amino acid residues involved and the type of interactions they form can provide important information about how the lead compound binds to the protein, which can be useful for understanding the mechanism of action of the compound and for optimizing its binding affinity.

### 4.8.1 Using Pymol

PyMol is a molecular visualization software that can be used to create detailed 3D models of protein-ligand complexes. Here we can visualize the interactions between the lead compound and the protein, including hydrogen bonding interactions, hydrophobic interactions and electrostatic interactions which is useful for identifying the specific residues and groups involved in the interaction and for understanding the structural basis of the binding.

In this case, five lead compounds were selected as the best candidates that had the highest predicted binding affinity to the protein as determined by the docking simulation. The interactions of these five lead compounds with the protein were then analyzed in more detail by studying the binding mode of the lead compounds to the protein, and identifying the specific amino acid residues involved in the interaction. Additionally, the interactions of native ligand (SAM and SAH) to the protein were also observed. This provided a baseline of how the native ligand interacts with the protein, which was useful for understanding the mechanism of action of the protein and for comparing the binding mode of the lead compounds to the native ligand. The specific interactions of these lead compounds with the protein were also visualized, such as hydrogen bonding interactions, hydrophobic interactions and electrostatic interactions. The interactions of native ligand with the protein provided us as a reference point to identify the regions of the protein that are important for binding, and to compare the binding mode of the lead compounds to the native ligand. The following Figure 35 and Figure 36 show the interactions of protein Dam with native ligand SAM and SAH respectively.

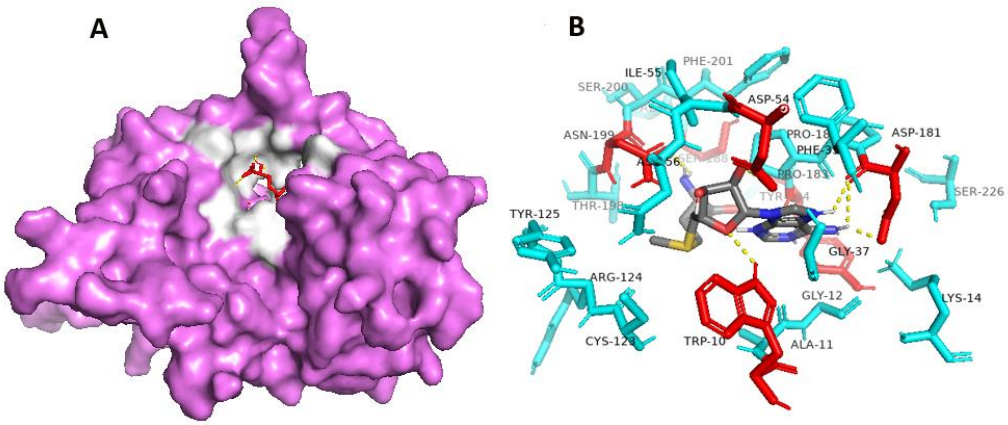


*Figure 18: Visualization of Protein ligand interaction A) Dam and SAM complex (protein ligand complex) Dam protein in pink color, ligand in red color, active binding sites of ligand in white color B) Polar and Non- polar amino acids of ligand interacting with Dam within 5Å, polar amino acids in red color, yellow lines showing H-bond, non- polar amino acids in blue color*

SAM showed nine polar contacts with six amino acid residues, TRP-10, ASP-54, ASP-181, TYR-184, SER-188 and ASN-199. It formed two polar contacts with ASP-54 and three polar contacts with ASP-181. The polar residues form hydrogen bonds with the lead compound. Hydrogen bonds are a specific type of polar interaction that can occur between the hydrogen atom of a polar group in the lead compound and the oxygen or nitrogen atom of a polar group in the protein. These interactions can be particularly important in the binding of the lead compound to the protein, as they can provide additional stability to the binding (Pang and Zhou, 2017). In addition, charge-charge interactions can be strong even at a distance of 5-10 Å. These "long-range" interactions can also play a crucial factor in determining the rate constants of proteins binding with small and macromolecular partners. These interactions can occur through electrostatic interactions, which are mediated by the Coulombic forces between the charges. The strength of these interactions can depend on the distance between the charges, as well as on the dielectric constant of the solvent. Long-range interactions can also provide specificity to the binding of the lead compound to the protein, as they can help to orient the lead compound in the correct position for binding (Schreiber *et al.,* 2009). Similarly, there are fifteen non-polar residues of SAM with Dam such as- ALA-11, GLY-12, LYS-14, PHE-35, GLY-37, ILE-55, ASN-56, CYS-123, PRO-182, PRO-183, ALA-189, THR-198, SER-200, PHE-201 and SER-226. These non-polar residues interact with the lead compound through hydrophobic interactions which are also important for the folding stability of proteins, as they help to bring nonpolar regions of the protein together in a way that minimizes the exposure of these groups to the aqueous environment. In proteins, the hydrophobic interactions occur between the nonpolar side chains of amino acids such as alanine, valine, leucine, and other hydrophobic residues. These residues tend to be buried inside the protein, away from the aqueous environment, where they interact with each other to form a stable hydrophobic core. This core helps to maintain the correct conformation of the protein, and to prevent the protein from unfolding (Nick *et al.*, 2014). The hydrophobic interactions are driven by the fact that

water is a polar solvent and nonpolar groups are not attracted to it. In order to minimize the contact with water, nonpolar groups tend to come together and form a hydrophobic core that is buried inside the protein. This way, the nonpolar residues can avoid the polar solvent and interact with each other in a more favorable environment. Additionally, the hydrophobic interactions are enthalpically favorable, meaning that they release energy when they occur. This energy release helps to stabilize the protein structure and to prevent the protein from unfolding (Baldwin, 2007).

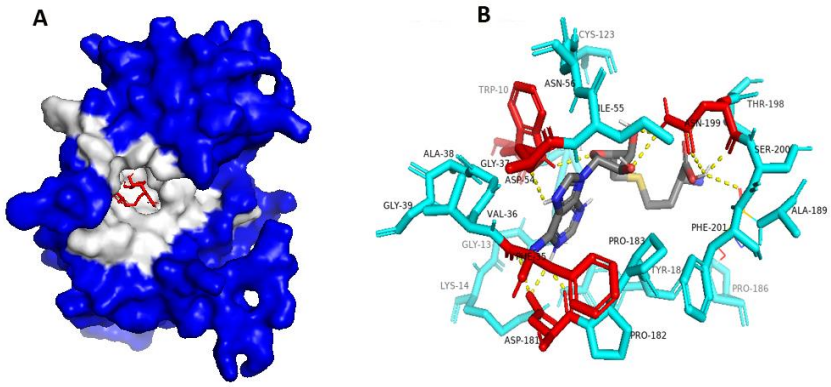


*Figure 19: Visualization of Protein ligand interaction A) Dam and SAH complex (protein ligand complex) Dam protein in blue color, ligand in red color, active binding sites of ligand in white color B) Polar and Non- polar amino acids of ligand interacting with Dam within 5Å , polar amino acids in red color, yellow lines showing H-bond, non- polar amino acids in blue color*

SAH showed eleven polar contacts with five amino acid residues, TRP-10, PHE-35, ASP-54, ASP-181 and ASN-199. It formed three polar contacts with ASP-181, five polar contacts with ASN-199. Similarly, there are eighteen non-polar residues of SAH with Dam such as- ALA-11, GLY-13, LYS-14, VAL-36, GLY-37, GLY-39, ALA-38, ASN-56, CYS123, PRO-182, PRO-183, TYR-184, PRO-186, ALA-189, THR-198, ASN-199, SER-200 and PHE-201.

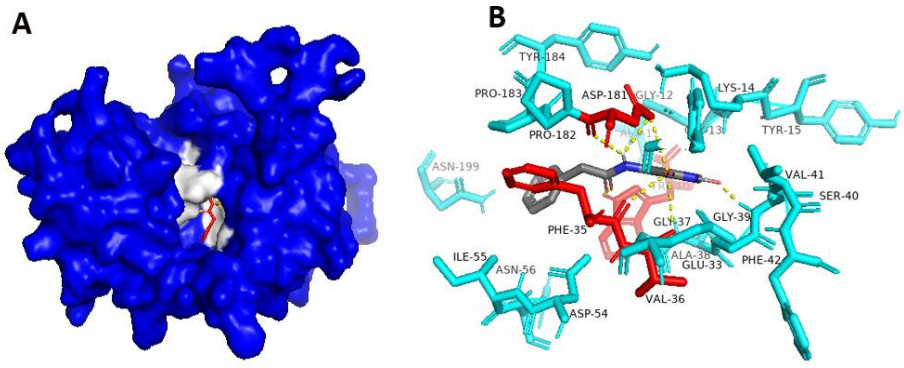


*Figure 20: Visualization of Protein ligand interaction A) Dam and Antineoplaston A10 complex (protein ligand complex) Dam protein in blue color, ligand in red color, active binding sites of ligand in white color B) Polar and Non- polar amino acids of ligand interacting with Dam within 5Å , polar amino acids in red color, yellow lines showing H-bond, non- polar amino acids in blue color*

Antineoplaston A10 showed eleven polar contacts with five amino acid residues, TRP-10, PHE-35, VAL-36, SER-40 and ASP-181. It formed three polar contacts with ASP-181. Similarly, there are seventeen non-polar residues of Antineoplaston A10 with Dam such as- TRP-10, ALA-11, GLY-12, GLY-13, LYS-14, TYR-15, GLU-33, ALA-38, GLY-39, SER-40, VAL-41, PHE-42, TYR-179, PRO-182, PRO-183, TYR-184 and ASN-199.

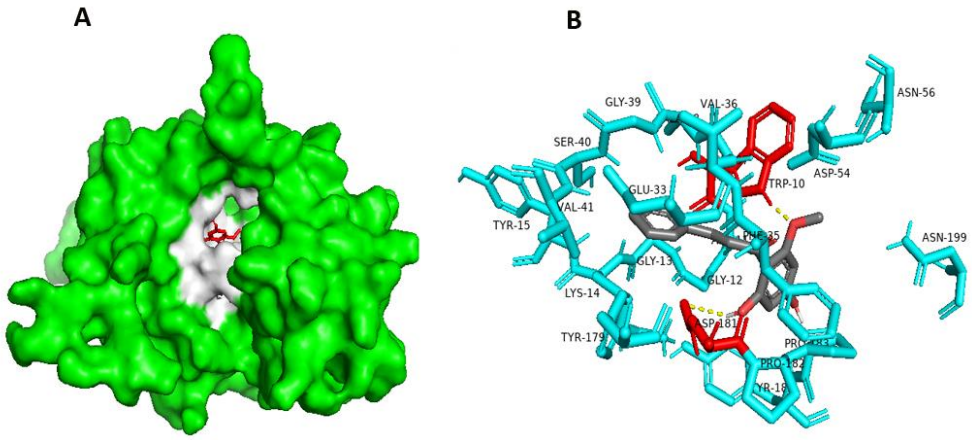


*Figure 21: Visualization of Protein ligand interaction a) Dam and Cardamonin complex (protein ligand complex) Dam protein in green color, ligand in red color, active binding sites of ligand in white color b) Polar and Non- polar amino acids of ligand interacting with Dam within 5Å , polar amino acids in red color, yellow lines showing H-bond, non- polar amino acids in blue color*

Cardamonin showed two polar contacts with two amino acid residues, TRP-10 and ASP-181 Similarly, there are nineteen non-polar residues of cardamonin with Dam such as- ALA-11, GLY-12, GLY-13, LYS-14, TYR-15, GLU-33, PHE-35, VAL-36, ALA-38, GLY-39, SER-40, VAL-41, ASP-54, ASN-56, TYR-179, PRO-182, PRO-183, TYR-184 and ASN-199.

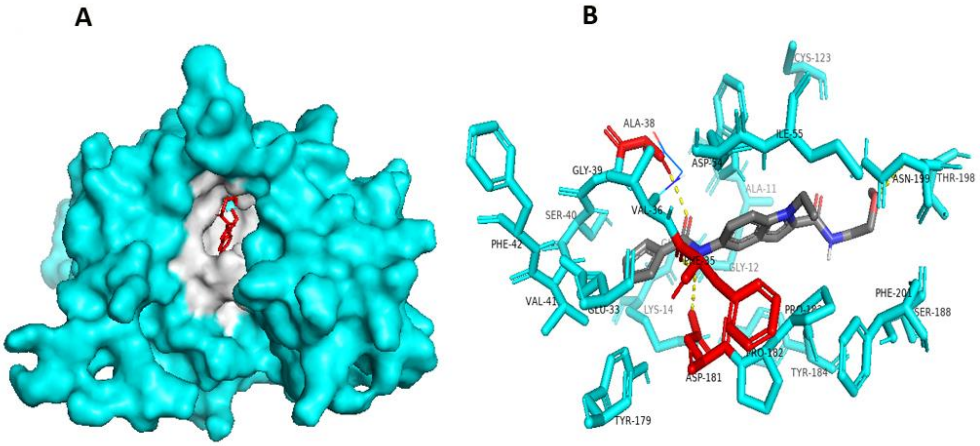


*Figure 22: Visualization of Protein ligand interaction A) Dam and indole derivative (5-cyclopentaneamido-1-ethyl-N-(2-methoxyethyl)-1H-indole-2-carboxamide) complex (protein ligand complex) Dam protein in blue color, ligand in red color, active binding sites of ligand in white color B) Polar and Non- polar amino acids of ligand interacting with Dam within 5Å , polar amino acids in red color, yellow lines showing H-bond, non- polar amino acids in blue color*

Indole derivative (5-cyclopentaneamido-1-ethyl-N-(2-methoxyethyl)-1H-indole-2-carboxamide) showed four polar contacts with four amino acid residues, PHE-35, ALA-38, ASP-181 and ASN-199. Similarly, there are eighteen non-polar residues such as- ALA-11, GLY-12, LYS-14, GLU-33, VAL-36, GLY-39, SER-40, VAL-41, PHE-42, ILE-55, CYS-123,TYR-179, PRO-182, PRO-183, TYR-184, SER-188, THR-198 and PHE-201.

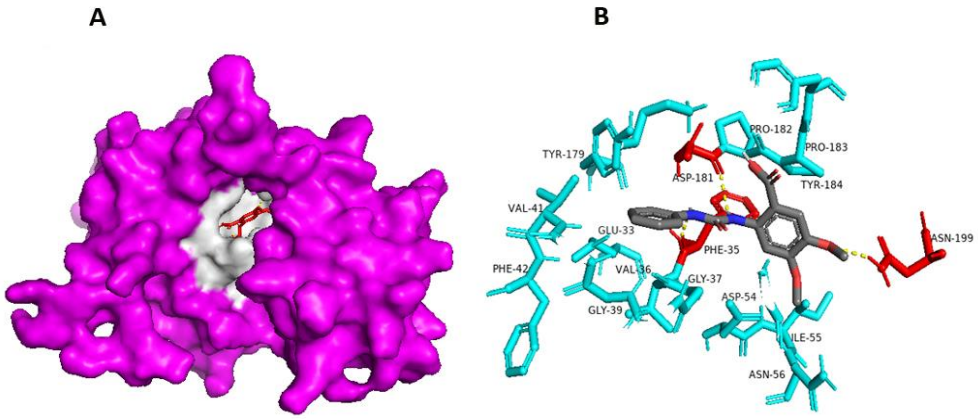


*Figure 23: Visualization of Protein ligand interaction A) Dam and Kinase inhibitor (2-[[anilino(oxo)methyl]amino]-4,5-dimethoxybenzoic acid) complex (protein ligand complex),Dam protein in pink color, ligand in red color, active binding sites of ligand in white color B) Polar and Non- polar amino acids of ligand interacting with Dam within 5Å , polar amino acids in red color, yellow lines showing H-bond, non- polar amino acids in blue color*

Kinase inhibitor (2-[[anilino(oxo)methyl]amino]-4,5-dimethoxybenzoic acid) showed three polar contacts with three amino acid residues, PHE-35, ASP-181 and ASN-191. Similarly, there are nineteen non-polar residues such as- TRP-10, ALA-11, GLY-12, GLY-13, LYS-14, GLY-30, GLU-33, VAL-36, GLY-37, ALA-38, SER-40, ASP-54, ILR-55, ASN-56, CYS-123, TYR-179, PRO-182, PRO-183 and TYR-184.

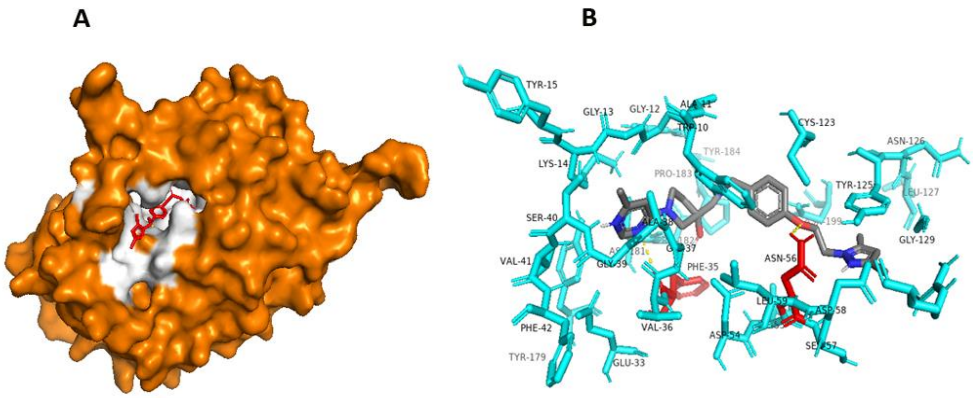


*Figure 24: Visualization of Protein ligand interaction A) Dam and , Nucleoside Mimetics (3-[[[4-[2-(3,5-Dimethylpyrazol-1-yl)ethoxy]phenyl]methylamino]methyl]-1-(6-methylpyrimidin-4-yl)pyrrolidin-3-ol) complex (protein ligand complex), Dam protein in orange color, ligand in red color, active binding sites of ligand in white color B) Polar and Non- polar amino acids of ligand interacting with Dam within 5Å , polar amino acids in red color, yellow lines showing H-bond, non- polar amino acids in blue color*

Nucleoside Mimetics (3-[[[4-[2-(3,5-Dimethylpyrazol-1-yl)ethoxy]phenyl]methylamino]methyl]-1-(6-methylpyrimidin-4-yl)pyrrolidin-3-ol) showed two polar contacts with two amino acid residues, PHE-35 and ASN-56. Similarly, there are twenty-six non-polar residues of such as- TRP-10, ALA-11, GLY-12, GLY-13, LYS-14, TYR-15, GLU-33, SER-40, VAL-41, PHE-42, ASP-54, ILE-55, ASN-56, SER-57, ASP-58, LEU-59, ARG-107, CYS-123, TYR-125, ASN-126, LEU-127, ASP-181, PRO-183, TYR-184 and ASN-199.

### 4.8.2 Using Discovery studio

Discovery Studio is a software package that can be used to generate 2D and 3D interaction maps of protein-ligand interactions. These maps provide detailed information on the specific protein residues and groups involved in the interaction, as well as the types of bonds that are formed and the distance between the interacting groups. It also allows to identify the residues that interact more often in a protein-ligand interaction. The orientation and stereochemistry of the individual amino acids and groups can also be visualized, which can provide insight into the specific mechanisms of the interaction. This can be useful for understanding the structural basis of protein-ligand interactions and for drug design. The different types of bonds are formed during protein-ligand interactions. The bonds can be both covalent and non-covalent bonds. Non-covalent interactions include pi-alkyl, pi-pi T shaped, and pi-sulphur interactions. In a pi-alkyl interaction, the pi electron cloud of an aromatic group interacts with the electron group of an alkyl group. In a pi-pi T shaped interaction, the pi electron cloud of two aromatic groups interact in a T-shaped manner. In a pi-sulphur interaction, the pi electron cloud of an aromatic ring interacts with the lone pair of electrons of a sulphur atom. These interactions play an important role in the binding of the ligand to the protein and affect the overall binding energy.

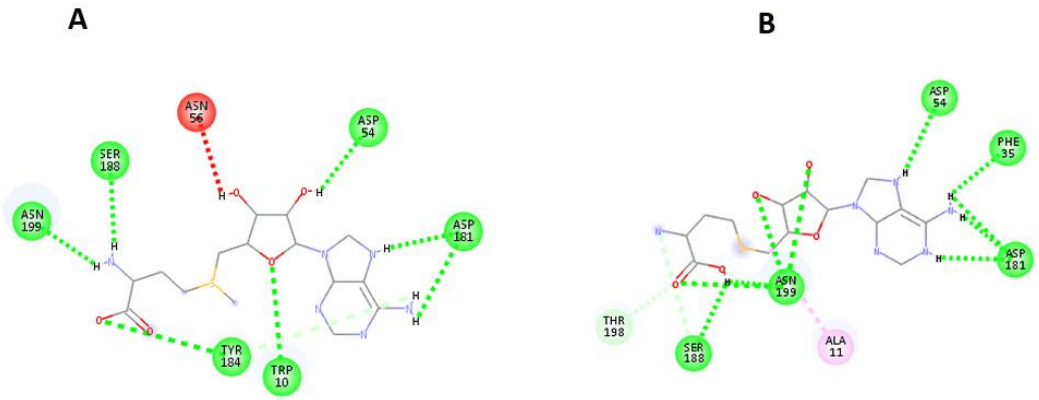


*Figure 25: 2D Visualization of Protein ligand interaction between SAM and Dam (A) and SAH and Dam (B) in Discovery Studio*

When visualizing the interactions between the native ligand SAM and Dam, it was found that seven amino acid residues- TRP-10, ASP-54, TYR-184, SER-188 ASN-199 and ASP-181 formed Conventional Hydrogen bond with the ligand, each forming single conventional H-bond whereas ASP-181 formed two Conventional Hydrogen bond. In this case, the hydrogen atoms of the SAM molecule are forming bonds with

the oxygen atoms of the specified amino acid residues of Dam. Each of these amino acids residues is forming a single conventional hydrogen bond with the ligand, suggesting ASP-181 playing a more significant role in the binding of the ligand to Dam. Likewise, TYR-184 formed Pi-Donor Hydrogen bond with the ligand. This type of interaction is less common than conventional hydrogen bonds and is generally weaker. Hydrogen bonding is a type of chemical interaction in which a hydrogen atom, which is covalently bonded to one atom, forms a weak bond with a second atom that has a lone pair of electrons. Similarly, one Unfavorable Donor-Donor bond was also observed with amino acid ASN-56. This type of interaction is less favorable because it involves the sharing of two electrons between atoms. The amino acid TYR-184 also formed Vander waals with the ligand.

Additionally, it was found that five specific amino acid residues, PHE-35, ASP-54, SER-188, ASP-181, and ASN-199 formed conventional hydrogen bonds with the native ligand SAH in the interaction between the protein Dam and SAH. Specifically, the amino acid ASN-199 formed four conventional hydrogen bonds and ASP-181 formed two conventional hydrogen bonds with the ligand. Similarly, the amino acids SER-188 and THR-198 formed Carbon Hydrogen Bond whereas ALA-11 formed Alkyl bond with the ligand.

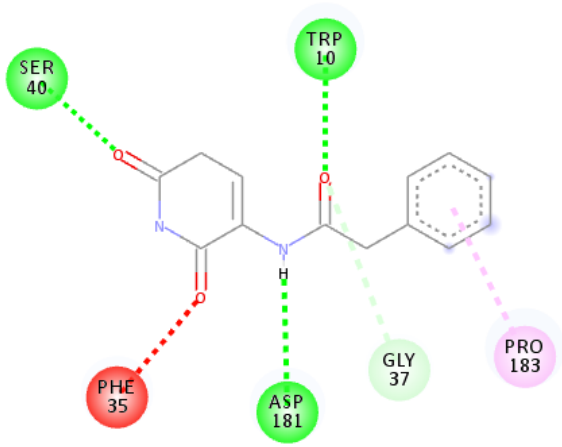


*Figure 26: 2D Visualization of Protein ligand interaction between Antineoplaston A10 and Dam in Discovery Studio*

Table 9: Summary of Protein-ligand interaction between Antineoplaston A10 and Dam

| Amino acid | Bond type | Bonded with | Bond length |
|---|---|---|---|
| TRP-10 | Conventional H-bond | Amide | 2.36 |
| GLY-37 | Carbon H-bond | Amide | 3.32 |
| PHE-35 | Unfavorable Acceptor- Acceptor | Oxygen group of Piperidine | 2.87 |
| SER-40 | Conventional H-bond | Oxygen group of Piperidine | 1.91 |
| ASP-181 | Conventional H-bond | Amino | 2.44 |
| PRO-183 | Pi-Alkyl | Benzene | 4.40 |

The protein ligand interaction between Dam and Antineoplaston A10 showed presence of three types of bond. TRP-10, SER-40 and ASP-181 showed conventional Hydrogen bond with the ligand while GLY-37 formed Carbon Hydrogen (C-H) bond. The C-H and C-H···O hydrogen bonds are typically weaker than heteroatom-hydrogen bonds, such as N-H···O or O-H···O, because of the weaker electronegativity of carbon atoms as compared to nitrogen or oxygen atoms. However, when a C-H group is activated by an electron-withdrawing group, the strength of the C-H···O hydrogen bond can become similar to that of heteroatom-hydrogen bonds. This is because the electron-withdrawing group causes the C-H bond to become more polarized, making the hydrogen atom more positive and the carbon atom more negative. This increased polarity makes the hydrogen atom more attractive to the electron-rich oxygen atom of the O-H bond, resulting in a stronger interaction between the two atoms (Adhikari and Scheiner, 2013). Similarly, PHE-35 showed Unfavorable Acceptor- acceptor bond and PRO-183 formed Pi-Alkyl bond with the ligand.

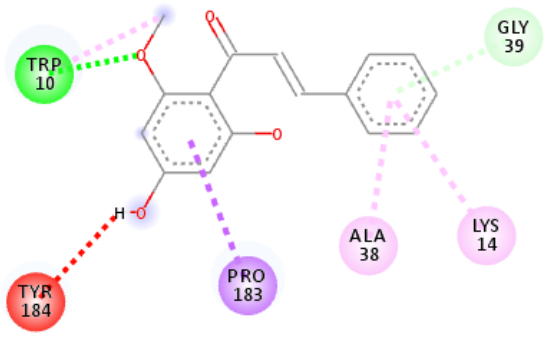


*Figure 27: 2D Visualization of Protein ligand interaction between Cardamonin and Dam in Discovery Studio*

Table 10: Summary of Protein-ligand interaction between Cardamonin and Dam

| Amino acid | Bond type | Bonded with | Bond length |
|---|---|---|---|
| TRP-10 | Conventional H-bond | Oxygen atom of methoxy group | 1.82 |
| TRP-10 | Pi-Alkyl | Hydrogen of methoxy phenyl | 5.24 |
| TRP-10 | Pi-Alkyl | Hydrogen of methoxy phenyl | 4.86 |
| LYS-14 | Pi-Alkyl | Benzene | 4.38 |
| ALA-38 | Pi-Alkyl | Benzene | 4.92 |
| GLY-39 | Pi- Donor H-bond | Benzene | 3.12 |
| PRO-183 | Pi-sigma | Phenyl group | 3.80 |
| TYR-184 | Unfavorable Donor- Donor | Hydrogen of phenyl group | 2.39 |

Considering all analyses, ligand Cardamonin mostly interacted with TRP-10, LYS-14, ALA-38 residues by forming Pi- Alkyl bond and with GLY-39 residue by Pi-Donor H-bond. TRP-10 formed Conventional H-bond as well. Similarly, PRO-183 and TYR-184 formed Pi-sigma and unfavorable Donor-Donor bond by accepting proton, respectively with the ligand.

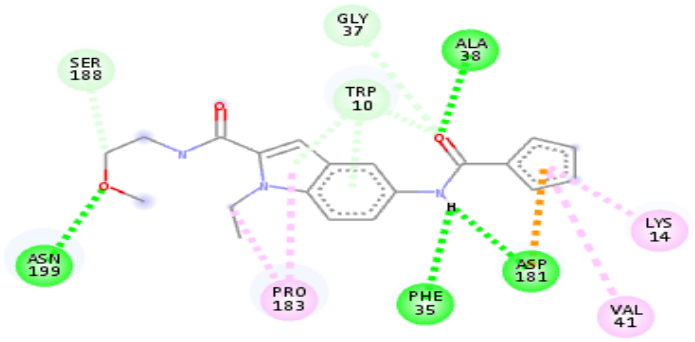


*Figure 28: 2D Visualization of Protein ligand interaction between indole derivative (5-cyclopentaneamido-1-ethyl-N-(2-methoxyethyl)-1H-indole-2-carboxamide) and Dam in Discovery Studio*

Table 11: Summary of Protein-ligand interaction between indole derivative (5-cyclopentaneamido-1-ethyl-N-(2-methoxyethyl)-1H-indole-2-carboxamide) and Dam

| Amino acid | Bond type | Bonded with | Bond length |
|---|---|---|---|
| TRP-10 | Pi- Donor H-bond | Indole | 2.80 |
| TRP-10 | Carbon H-bond | Amide | 3.27 |
| TRP-10 | Pi- Donor H-bond | Indole | 3.00 |
| LYS-14 | Pi-Alkyl | Cyclopentane | 4.16 |
| PHE-35 | Conventional H-bond | Hydrogen of amide group | 2.68 |
| GLY-37 | Carbon H-bond | Amide | 3.16 |
| ALA-38 | Conventional H-bond | Amide | 2.40 |
| VAL-41 | Pi-Alkyl | Cyclopentane | 5.28 |
| ASP-181 | Pi-Anion | Cyclopentane | 3.85 |
| ASP-181 | Conventional H-bond | Hydrogen of amide group | 2.77 |
| ASP-181 | Conventional H-bond | Hydrogen of amide group | 3.02 |
| PRO-183 | Pi-Alkyl | Indole | 5.03 |
| PRO-183 | Alkyl | Amino of indole | 4.93 |
| SER-188 | Carbon H-bond | Hydrogen | 3.72 |
| ASN-199 | Conventional H-bond | Methoxy ethyl | 2.67 |
| ASN-199 | Conventional H-bond | Methoxy ethyl | 2.85 |

During the interaction of the ligand, an indole derivative, with the protein Dam, a variety of bonds were observed between the amino acid residues of Dam and the various functional groups of the ligand. These include conventional hydrogen bonds, which were formed by residues PHE-35, ALA-38, ASP-181 and ASN-199 with the amide group of the ligand. Additionally, residue TRP-10 formed a carbon H-bond and two pi-donor H-bonds with the amide and indole moiety of the ligand respectively. Other residues, such as GLY-37 and SER-188, formed carbon H-bonds, while LYS-14, VAL-41 and PRO-183 formed pi-alkyl bonds. PRO-183 also formed an alkyl bond. Lastly, an additional Pi-anion bond was formed by ASP-181 residue. Pi-anion interactions are a type of electrostatic interactions that occur between an anion and an aromatic ring. These interactions involve an anion positioned over the centroid of an aromatic ring, where the anion's negative charge is attracted to the ring's pi

electrons. The strength of a Pi-anion interaction is determined by the electron density of the aromatic ring, the size and shape of the anion, and the distance between the anion and the ring. Pi-anion interactions have been found to be important in various biological systems, such as in the binding of anions to proteins and in the regulation of enzyme activity. These interactions can also be exploited in the design of new drugs, as they allow for the selective binding of anions to specific sites on a protein, which can help to modulate its activity. Furthermore, they also play an important role in the transport of anions across biological membranes (Watt *et al.,* 2013). In this context, Pi-anion interactions are thought to facilitate the binding of anions to transmembrane proteins, which can then transport the anions across the membrane.

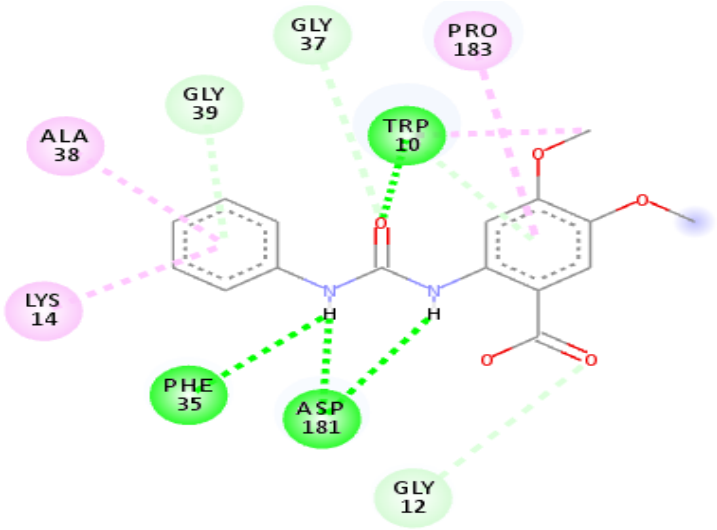


*Figure 29: 2D Visualization of Protein ligand interaction between Kinase inhibitor (2-[[aniline (oxo) methyl]amino]-4,5-dimethoxybenzoic acid) and Dam in Discovery studio*

Table 12: Summary of Protein-ligand interaction between Kinase inhibitor (2-[[anilino(oxo)methyl]amino]-4,5-dimethoxybenzoic acid) and Dam

| Amino acid | Bond type | Bonded with | Bond length |
|---|---|---|---|
| TRP-10 | Conventional H-bond | Oxygen of Amide | 2.97 |
| TRP-10 | Pi-Donor H-bond | Benzoic acid | 3.06 |
| TRP-10 | Pi-Alkyl | Methoxy group | 5.13 |
| GLY-12 | Carbon H-bond | Dimethoxybenzoic acid | 3.57 |
| LYS-14 | Pi-Alkyl | Aniline | 4.40 |
| PHE-35 | Conventional H-bond | Amide | 2.20 |
| GLY-37 | Carbon H-bond | Oxygen of Amide | 3.49 |
| ALA-38 | Pi-Alkyl | Aniline | 5.06 |
| GLY-39 | Pi-Donor H-bond | Aniline | 3.16 |
| ASP-181 | Conventional H-bond | Amide | 2.32 |
| ASP-181 | Conventional H-bond | Amide | 3.04 |
| PRO-183 | Pi- Alkyl | Benzoic acid | 4.90 |

In the interaction between the protein Dam and the ligand Kinase inhibitor (2-[[anilino(oxo)methyl]amino]-4,5-dimethoxybenzoic acid), four types of bonds were

observed. These include conventional hydrogen bonds, pi-donor hydrogen bonds, pi-alkyl bonds, and pi-donor H-bond. The residues TRP-10, PHE-35 and ASP-181 formed conventional hydrogen bonds with the amide group of the ligand. TRP-10 also formed pi-donor hydrogen bonds and pi-alkyl bonds. Additionally, GLY-39 formed pi-donor hydrogen bonds and LYS-14, ALA-38 and PRO-183 formed pi-alkyl bonds.

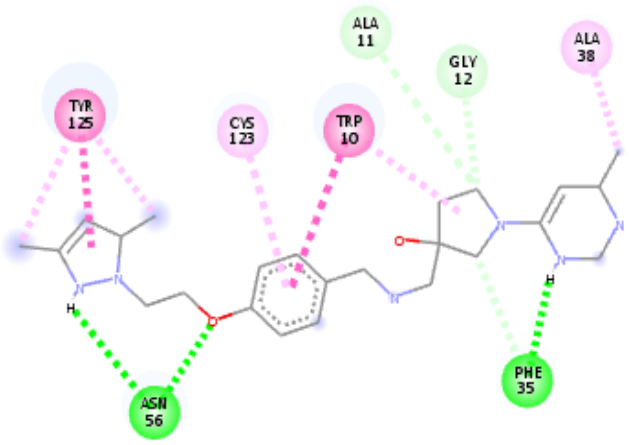


*Figure 30: 2D Visualization of Protein ligand interaction between Nucleoside Mimetics (3-[[[4-[2-(3,5-Dimethylpyrazol-1-yl)ethoxy]phenyl]methylamino]methyl]-1-(6-methylpyrimidin-4-yl)pyrrolidin-3-ol) and Dam in Discovery studio*

Table 13: Summary of Protein-ligand interaction between Nucleoside Mimetics (3-[[[4-[2-(3,5-Dimethylpyrazol-1-yl)ethoxy]phenyl]methylamino]methyl]-1-(6-methylpyrimidin-4-yl)pyrrolidin-3-ol) and Dam

| Amino acid | Bond type | Bonded with | Bond length |
|---|---|---|---|
| TRP-10 | Pi-Pi T-shaped | Phenol | 5.20 |
| TRP-10 | Pi-Alkyl | Pyrrolidin | 5.05 |
| ALA-11 | Carbon H-bond | Pyrrolidin | 3.61 |
| GLY-12 | Carbon H-bond | Pyrrolidin | 3.65 |
| PHE-35 | Conventional H-bond | Hydrogen of Pyrimidine | 2.14 |
| PHE-35 | Carbon H-bond | Pyrrolidin | 3.49 |
| ALA-38 | Alkyl | Methyl of Pyrimidine | 3.37 |
| ASN-56 | Conventional H-bond | Hydrogen of Pyrazol | 2.67 |
| ASN-56 | Conventional H-bond | Oxygen of phenol | 2.20 |
| CYS-123 | Pi-Alkyl | Phenol | 5.08 |
| TYR-125 | Pi-Alkyl | Methyl of Pyrazol | 4.21 |
| TYR-125 | Pi-Pi Stacked | Pyrazol | 3.76 |
| TYR-125 | Pi-Alkyl | Methyl of Pyrazol | 4.78 |

It was observed that six types of bonds were formed in protein ligand interaction of between Nucleoside Mimetics (3-[[[4-[2-(3,5-Dimethylpyrazol-1-yl)ethoxy]phenyl]methylamino]methyl]-1-(6-methylpyrimidin-4-yl)pyrrolidin-3-ol) and Dam. Here, the amino acid residues ALA-11, GLY-12 and PHE-35 formed a Carbon H-bond with the pyrrolidin moiety. PHE-35, in addition to forming this bond, also formed a Conventional H-bond with the hydrogen atom of the pyrimidine

moiety. Furthermore, PHE-35 and ASN-56 formed conventional hydrogen bonds. TYR-125, TRP-10, CYS-123, TYR-125 and ALA-38 formed Pi-Alkyl and Alkyl bond respectively. TYR-125 and TRP-10 formed Pi-Pi Stacked and Pi-Pi T-shaped bonds. These are non-covalent interactions between the pi electron clouds of two aromatic groups. The Pi-Pi Stacked bond is formed when the pi electrons of two aromatic rings are aligned in parallel and in close proximity, resulting in a strong interaction. The Pi-Pi T-shaped bond is formed when the pi electrons of two aromatic groups interact in a T-shaped manner. Pi-pi interactions are particularly important in protein-ligand binding because they can lead to the formation of strong, non-covalent bonds between the aromatic ring of the ligand and the aromatic residues in the protein. These interactions are relatively specific, giving a high degree of specificity to the binding (Zhou *et al.,* 2012). In addition, Pi-Pi interactions are also able to contribute to the overall stability of the protein-ligand complex, by providing a favorable enthalpy change, which results in a positive binding energy.

From the above summaries of all protein ligand interactions of Dam with all selected screened ligands, it was found that benzene and benzene-containing frameworks are commonly found to be involved in pi-alkyl interactions in protein-ligand binding. This is because the pi electron cloud of the aromatic ring in benzene is able to interact with the electron group of an alkyl group, which can lead to a strong binding interaction. In the case of lead compounds, these interactions have been found to occur with various amino acids, which further strengthens the binding between the ligand and the protein.

### 4.8.3 Using Ligplot

Ligplot is one of the software tools that is used to analyze hydrogen bond interactions and hydrophobic interactions between the ligand and the protein. Hydrogen bond interactions are relatively strong and highly directional, which makes them useful for conferring specificity to the binding of the ligand to the protein. On the other hand, hydrophobic interactions that occur between nonpolar groups in a protein are short-range attractive, meaning that they occur between atoms or groups that are in close proximity to each other and that they tend to bring these groups together. These interactions play an important role in the binding of ligands to receptors, as they contribute to the overall binding affinity between the ligand and the receptor. The interactions between native ligand SAM, SAH and lead compounds with the target protein, Dam were observed using Ligplot.

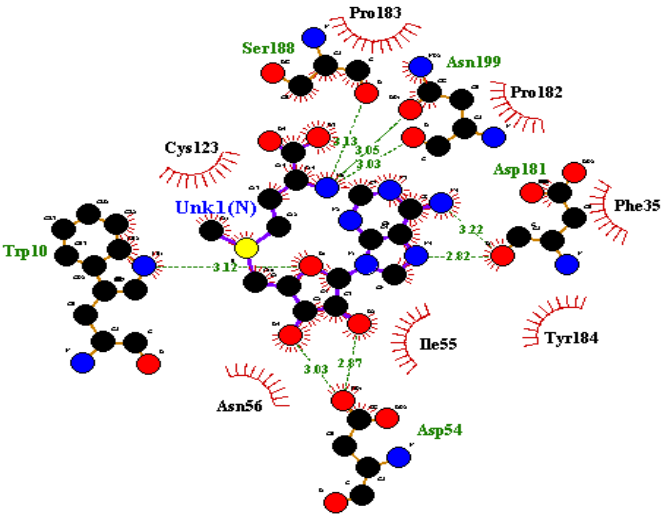


*Figure 31: Ligplot visualization of ligand binding interaction between SAM and Dam*

The protein and ligand interaction between SAM and Dam exhibited both hydrogen bonds and hydrophobic interactions. The amino acids PHE-35, ILE-55, ASN-56, CYS-123, PRO-182, PRO-183, and TYR-184 were found to be involved in hydrophobic interactions. Similarly, SER-188 and TRP-10 formed Hydrogen bond with bond lengths of 3.13 and 3.12 A respectively. Moreover, ASN-199, ASP-181 and ASP-54 formed two Hydrogen bonds with ligand. The bond lengths formed by ASN-199 were 3.05 and 3.03 whereas by ASP-181 were 3.22 and 2.82. Furthermore the bond lengths formed by ASP-54 were 3.03 and 2.87.

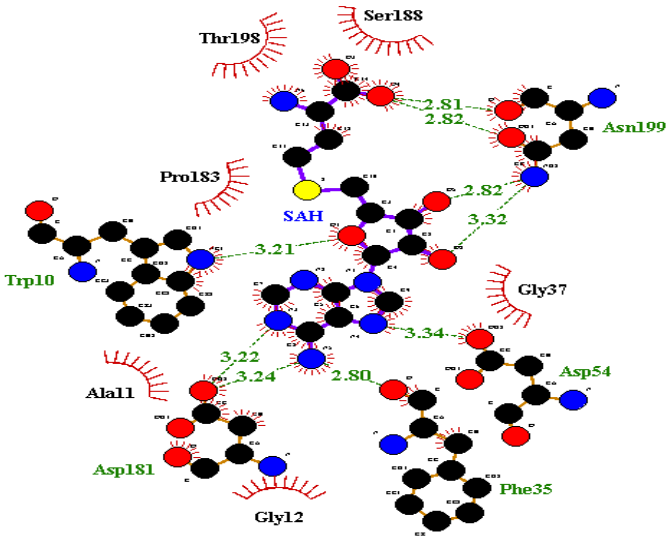


*Figure 32: Ligplot visualization of ligand binding interaction between SAH and Dam*

The interaction between the native ligand SAH and the protein Dam involved both hydrogen bond interactions and hydrophobic interactions. Specifically, the amino acids ALA-11, GLY-12, GLY-37, TYR-184, SER-188 and THR-198, were found to be involved in hydrophobic interactions with the ligand. Additionally, TRP-10, PHE-35

and ASP-54 formed hydrogen bonds with the ligand, with bond lengths of 3.21, 2.80 and 3.34 Angstroms respectively. Furthermore, ASP-181 formed two hydrogen bonds with bond lengths of 3.22 and 3.24 whereas ASN-199 formed four hydrogen bonds with the ligand, with bond lengths of 2.81, 2.82, 2.82 and 3.32 Angstroms. This information provides insights into the specific interactions that the ligand has with the protein, which can be useful for understanding the mechanism of action of the ligand and for optimizing its binding affinity to the protein.

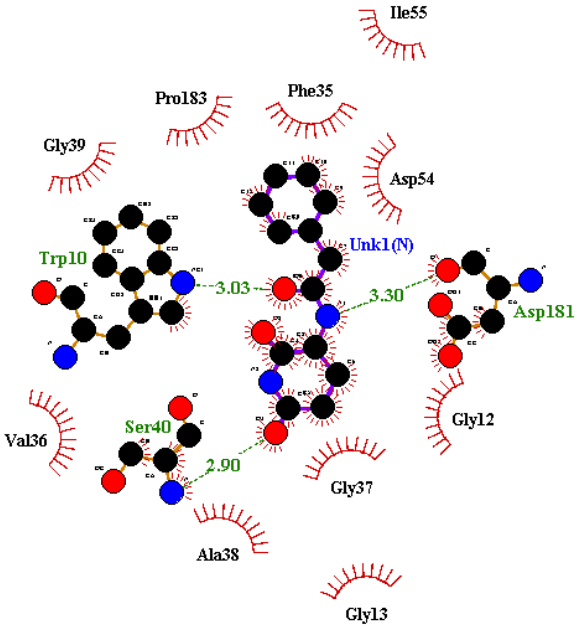


*Figure 33: Ligplot visualization of ligand binding interaction between Dam and Antineoplaston A10*

Both the hydrophobic and Hydrogen interactions were seen between the target protein Dam and natural product ligand Antineoplaston A10. Particularly, the amino acids that involved in hydrophobic interactions were-GLY-12, GLY-13, PHE-35, VAL-36, GLY-37, ALA-38, GLY-39, ASP-54, ILE-55 and PRO-183. TRP-10, SER-40 and ASP-181 formed Hydrogen bonds with the bond length of 3.03, 2.90 and 3.30 respectively. Thus, this information provides us knowledge of how the ligand interacts with the protein which is helpful for comprehending the ligand's mode of action for optimizing its affinity for binding to the protein.

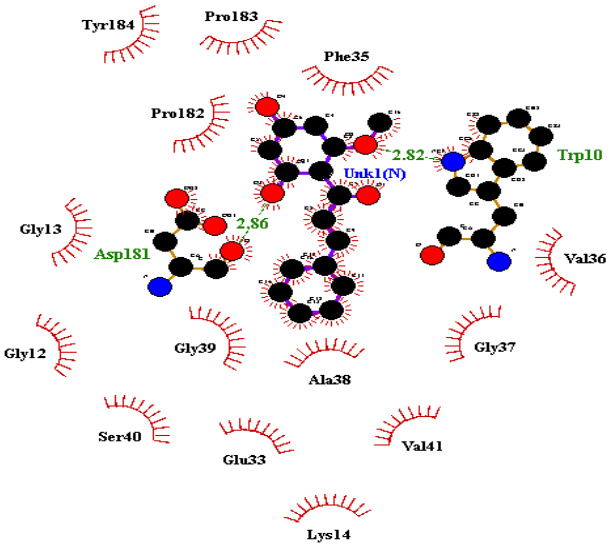


*Figure 34: Ligplot visualization of ligand binding interaction between Dam and Cardamonin*

By visualizing ligplot map, it was found that the protein, Dam and ligand, cardamonin interaction involved both Hydrogen and Hydrophobic interactions. The amino acid residues- TRP-10 and ASP-181 formed Hydrogen bonds with the ligand of bond length of 2.82 and 2.86 Angstrom respectively. Similarly, amino acid residues- GLY-12, GLY-13, LYS-14, GLU-33, PHE-35, VAL-36, ALA-38, GLY-39, SER-40, VAL-41, PRO-182, PRO-183 and TYR-184 formed Hydrophobic interactions.

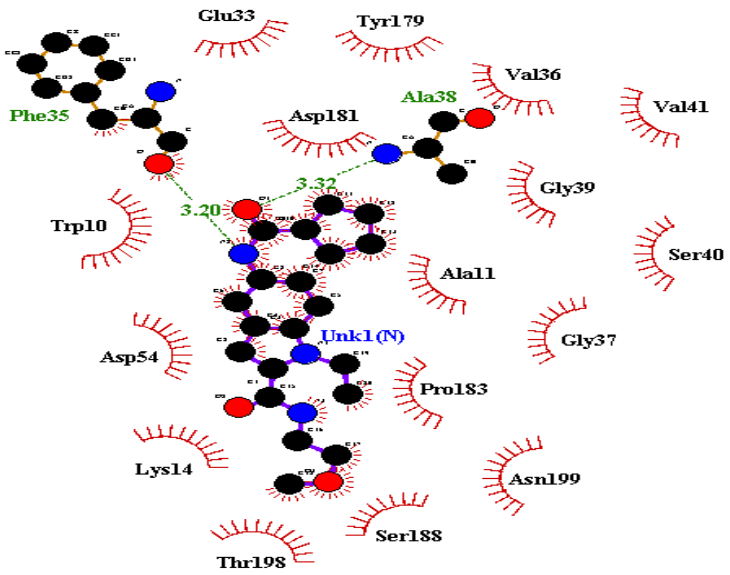


*Figure 35: Ligplot visualization of ligand binding interaction between Dam and indole derivative (5-cyclopentaneamido-1-ethyl-N-(2-methoxyethyl)-1H-indole-2-carboxamide)*

The interaction between the protein Dam and the indole derivative ligand (5-cyclopentaneamido-1-ethyl-N-(2-methoxyethyl)-1H-indole-2-carboxamide) when observed in ligplot software was found to involve both hydrogen and hydrophobic interactions. The two amino acid residues- PHE-35 and ALA-38 formed Hydrogen

bonds with the ligand of bond length 3.20 and 3.32 Angstrom respectively. Furthermore, it was found that sixteen amino acid residues- TRP-10, ALA-11, LYS-14, GLU-33, VAL-36, GLY-37, GLY-39, SER-40, VAL-41, ASP-54, TYR-179, ASP-181, PRO-183, SER-188, THR-198 and ASN-199 formed hydrophobic interaction with the ligand.

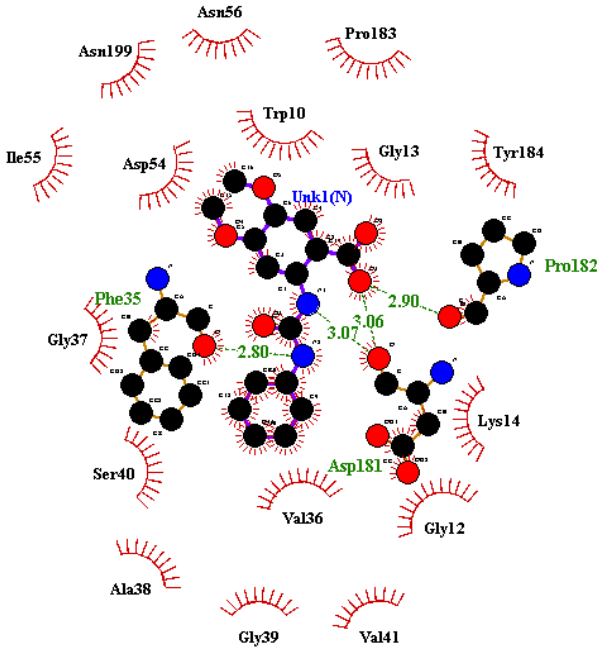


*Figure 36: Ligplot visualization of ligand binding interaction between Dam and Kinase inhibitor (2-[[anilino(oxo)methyl]amino]-4,5-dimethoxybenzoic acid)*

The protein- ligand interaction of Dam and and screened Kinase inhibitor ligand (2-[[anilino(oxo)methyl]amino]-4,5-dimethoxybenzoic acid) revealed hydrophobic interactions between TRP-10, GLY-12, GLY-13, LYS-14, VAL-36, GLY-37, ASP-54, ALA-38, GLY-39, SER-40, VAL-41, ASP-54, ILE-55, ASN-56, PRO-183, TYR-184 and ASN-199. Hydrogen bond interactions were also observed in three amino acid residues- PHE-35, PRO-182 and ASP-181. ASP-181 formed two hydrogen bonds of bond lengths of 3.06 and 3.07 with the ligand whereas PHE-35 and PRO-182 formed Hydrogen bonds of bond lengths of 2.80 and 2.90 respectively.

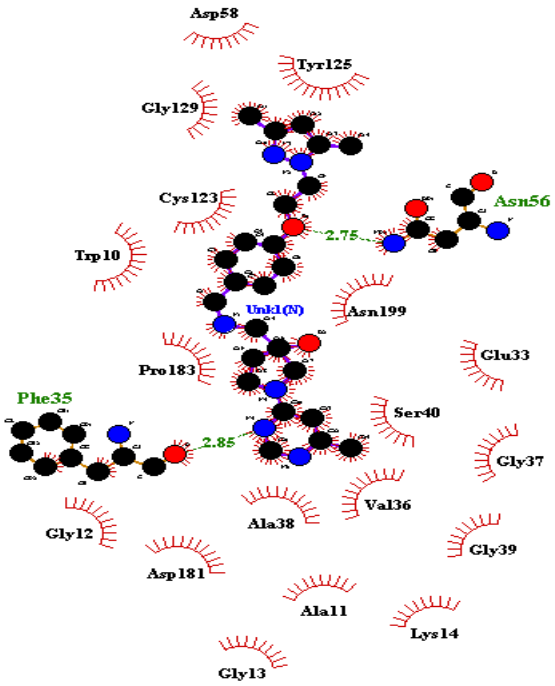


*Figure 37: Ligplot visualization of ligand binding interaction between Dam and Nucleoside Mimetics(3-[[[4-[2-(3,5-Dimethylpyrazol-1-yl)ethoxy]phenyl]methylamino]methyl]-1-(6-methylpyrimidin-4-yl)pyrrolidin-3-ol)*

The ligplot map of protein ligand interaction between Dam and selected final compound Nucleoside Mimetics (3-[[[4-[2-(3,5-Dimethylpyrazol-1-yl)ethoxy]phenyl]methylamino]methyl]-1-(6-methylpyrimidin-4-yl)pyrrolidin-3-ol) showed both hydrogen interaction and hydrophobic interactions involvement. The amino acid residues that were involved in hydrophobic interactions with the ligand were-TRP-10, ALA-11, GLY-12, GLY-13, LYS-14, GLU-33, VAL-36, GLY-37, ALA-38, GLY-39, SER-40, ASP-58, CYS-123, GLY-129, TYR-125, ASP-181, PRO-183 and ASN-199. Similarly, PHE-35 and ASN-56 formed hydrogen bonds of bond length of 2.86 and 2.75 respectively.

## 4.9 Density Function Theory Analysis (DFT)

Density Functional Theory (DFT) is a powerful computational tool used to understand the electronic structure of a variety of physical systems, including atoms, molecules, and solids. In this study, we used DFT to analyze the top-performing compounds identified and the interactions between the compounds and their receptors. The calculations were performed using the B3LYP (Becke3-Lee-Yang-Parr) method, which is a widely-used approximation for the exchange-correlation energy of the electrons in the system, and the 631G basis set, which provides a comprehensive description of the electron orbitals. Additionally, DFT was also used to study the vibrational spectra and frontier molecular orbitals of the compounds. The optimized structure of the compounds was found to have a singlet spin and zero charge, and the parameters were calculated using the B3LYP method with the Optimization+ Frequency job type. The calculated parameters for the top screened compounds-

Antineoplaston A10 (a), Cardamonin (b), indole derivative(5-cyclopentaneamido-1-ethyl-N-(2-methoxyethyl)-1H-indole-2-carboxamide) (c), Kinase inhibitor (2-[[anilino(oxo)methyl]amino]-4,5-dimethoxybenzoic acid)(d) and Nucleoside Mimetics(3-[[[4-[2-(3,5-Dimethylpyrazol-1-yl)ethoxy]phenyl]methylamino]methyl]-1-(6-methylpyrimidin-4-yl)pyrrolidin-3-ol) (e) are given below:

Table 14: Calculated parameters of the selected compounds

| Compound | Total Energy (in (kJ/mol)) | Dipole moment (in Debye) | RMS Gradient norm (in a.u) |
|---|---|---|---|
| a) | -2197055.47858125 | 4.3043 | 0.00000189 |
| b) | -2414871.21899625 | 5.0551 | 0.00000132 |
| c) | -3057970.56119625 | 2.0744 | 0.00000153 |
| d) | -2899693.8116475 | 3.3905 | 0.00000447 |
| e) | -3711716.43948 | 3.8032 | 0.00000284 |

Understanding the charge distribution within the molecule and the potency of the interactions between molecules can both be accomplished through the analysis of the dipole moment of the compounds. Dipole moment is a vector quantity that describes the separation of positive and negative charges within a molecule and is typically measured in Debye units (D). Values of the dipole moment can be used to describe how charge moves through molecules. The stability of the compounds can be affected by the strength of the dipole-dipole interactions between the molecules, which increase with increasing dipole moment. It was found that compound (b) i.e. Cardamonin had the highest dipole moment of 5.0551 Debye. A molecule is often thought to be more stable if it has more attracting forces and fewer repulsive forces. The potential energy of the molecule is decreased by attractive forces while its potential energy is increased by repulsive forces. In other words, more stable molecules are those with lower potential energy. All of the molecules selected displayed negative energy values, demonstrating the stability of the complexes.

The RMS gradient norm is calculated as the square root of the mean of the squares of the gradients of the energy with respect to the coordinates of the atoms in the system. It is a measure of how much the energy of the system changes as the coordinates of the atoms are changed. Here, in computational chemistry, the RMS gradient norm is used to determine the convergence of a geometry optimization, during which the coordinates of the atoms are adjusted to minimize the energy of the system. A lower RMS gradient norm indicates that the optimization has converged, meaning that the energy of the system is at a local minimum. The RMS gradient norm is usually given in atomic units (a.u.) and the typical convergence criteria are values less than or equal to 0.0001 a.u. In all the above compounds all had the value less than 0.0001 a.u., signifying the energy of the system is at a local minimum.

### 4.9.1 Frontier Molecular Orbital Analysis

Frontier molecular orbitals refer to the highest occupied molecular orbital (HOMO) and the lowest unoccupied molecular orbital (LUMO) in a compound, as these are the orbitals where chemical reactions occur. The HOMO represents the highest energy orbital occupied by an electron in a compound, and its energy level can be used as an indicator of a compound's electron-donor ability. In general, the higher the energy of the HOMO, the greater the electron-donating ability of a compound. The LUMO, on the other hand, represents the lowest energy orbital that is unoccupied by an electron in a compound, and its energy level can be used as an indicator of a compound's electron-acceptor ability. In general, the lower the energy of the LUMO, the greater the electron-accepting ability of a compound.

The energies of the HOMO and LUMO are commonly used as chemical reactivity indices, and they are often correlated with other indices such as electron affinity and ionization potential. Electron affinity is a measure of how strongly an atom or a molecule will accept an electron, while ionization potential is a measure of how easily an electron can be removed from an atom or a molecule. The relationship between the HOMO and LUMO energies and these other indices can provide valuable insights into the chemical reactivity and stability of a compound. Furthermore, the HOMO-LUMO gap, energy gap is also used to determine the chemical reactivity, optical polarizability, and chemical hardness-softness of a molecule. The greater the HOMO-LUMO gap, the more stable the molecule is and the less reactive it is. The greater the gap, the more stable the molecule is and the less reactive it is. On the other hand, the smaller the gap, the less stable the molecule is and the more reactive it is. This is because a larger gap means that it takes more energy to excite an electron from the HOMO to the LUMO, making it less likely for a chemical reaction to occur (Kosar and Albayrak, 2011).

The (HOMO-LUMO gap) energy gap of the screened compounds- Antineoplaston A10 (a), Cardamonin (b), indole derivative(5-cyclopentaneamido-1-ethyl-N-(2-methoxyethyl)-1H-indole-2-carboxamide) (c), Kinase inhibitor (2-[[anilino(oxo)methyl]amino]-4,5-dimethoxybenzoic acid)(d) and Nucleoside Mimetics(3-[[[4-[2-(3,5-Dimethylpyrazol-1-yl)ethoxy]phenyl]methylamino]methyl]-1-(6-methylpyrimidin-4-yl)pyrrolidin-3-ol) (e) are calculated in the given table 15.

Table 15: Calculated energy differences (LUMO-HUMO) of the selected screened compounds

| Compound | HOMO (in kJ/mol) | LUMO (in kJ/mol) | Energy Gap (in kJ/mol) |
|---|---|---|---|
| a) | -0.21707 | -0.04587 | 0.1712 |
| b) | -0.22334 | -0.02639 | 0.19695 |
| c) | -0.19899 | -0.04192 | 0.15707 |
| d) | -0.20985 | -0.04789 | 0.16196 |
| e) | -0.08308 | -0.00822 | 0.07486 |

Here, the energy gap value was found to be in decreasing order as: cardamonin (b)> antineoplaston A10 (a)> Kinase inhibitor (2-[[anilino(oxo)methyl]amino]-4,5-dimethoxybenzoic acid)(d)> indole derivative(5-cyclopentaneamido-1-ethyl-N-(2-

methoxyethyl)-1H-indole-2-carboxamide)(c)> Nucleoside Mimetics(3-[[[4-[2-(3,5-Dimethylpyrazol-1-yl)ethoxy]phenyl]methylamino]methyl]-1-(6-methylpyrimidin-4-yl)pyrrolidin-3-ol)(e). This order indicates that Nucleoside Mimetics(3-[[[4-[2-(3,5-Dimethylpyrazol-1-yl)ethoxy]phenyl]methylamino]methyl]-1-(6-methylpyrimidin-4-yl)pyrrolidin-3-ol) is the most reactive among the compounds, followed by indole derivative(5-cyclopentaneamido-1-ethyl-N-(2-methoxyethyl)-1H-indole-2-carboxamide)(c), Kinase inhibitor (2-[[anilino(oxo)methyl]amino]-4,5-dimethoxybenzoic acid)(d), Antineoplaston A10 (a) and then cardamonin (b).

Furthermore, the molecular properties of a molecule can be determined by evaluating its ionization potential (IP), electron affinity (EA), chemical potential (μ), hardness (η), softness (S), electronegativity (χ) and electrophilicity index (ω), using the energy values of its highest occupied molecular orbital (HOMO) and lowest unoccupied molecular orbital (LUMO) frontier molecular orbitals (FMOs). These properties are used to understand the chemical reactivity of a molecule and its chemical behavior. Global reactivity descriptors can be obtained by applying Koopman's theorem (Govindarajan *et al.,* 2012). The equation is given below:

Chemical Potential (μ)= -(IP+EA)/2

Hardness (η)= (IP-EA)/2

Softness (S)= 1/2η

Electronegativity (χ)= (IP+EA)/2

Global electrophilicity index (ω)= μ^2/2η

Where IP= $-E_{HOMO}$ and EA=$-E_{LUMO}$

Table 16: Calculated chemical reactivity of the selected compounds

| Compounds | Electronegativity (χ) (eV) | Hardness (η) (eV) | Softness(S) ($eV^{-1}$) | Chemical Potential(μ) (eV) | Electrophilicity index (ω) (eV) |
|---|---|---|---|---|---|
| a) | 0.13147 | 0.0856 | 5.8411 | -0.1315 | 0.1009 |
| b) | 0.1249 | 0.0985 | 5.0761 | -0.1249 | 0.0792 |
| c) | 0.1204 | 0.0785 | 6.3694 | -0.1204 | 0.0923 |
| d) | 0.1289 | 0.0809 | 6.1805 | -0.1289 | 0.1027 |
| e) | 0.0456 | 0.0374 | 13.3689 | -0.0456 | 0.0278 |

The hardness of a molecule is a measure of its resistance to deformation of its electron cloud under small perturbations encountered during chemical processes. A molecule with a large HOMO-LUMO gap is considered a hard molecule, and one with a small HOMO-LUMO gap is considered a soft molecule, which is more reactive. Soft systems are large and highly polarizable, while hard systems are relatively small and less polarizable. The local hardness provides information about intermolecular reactivity, and the intrinsic global hardness provides information about the stability of the molecule (Kosar and Albayrak, 2011). In this context, the magnitude of chemical hardness (0.0856, 0.0985, 0.0785, 0.0809 and 0.0374 eV) supported by HOMO-LUMO gap suggests that the molecules being discussed are relatively stable

and less reactive, meaning that they are resistant to changes in their electron cloud under small perturbations. Furthermore, the electrophilicity of a molecule is related to its ability to acquire additional electronic charge and its resistance to exchange electronic charge with the environment. The electrophilicity index (ω) is a quantum chemical descriptor that provides information about both electron transfer (chemical potential) and stability (hardness) of a molecule. A high electrophilicity index value indicates that a molecule has a strong tendency to acquire additional electronic charge and is therefore more nucleophilic (nucleophiles are electron-rich species that are attracted to electron-deficient species or electrophiles). This index is important in determining the toxicity of molecules and the site selectivity of drug-receptor interactions, and thus, it can be used to quantify the biological activity of drug-receptor interactions. In this context, the electrophilicity index values ω (0.1009, 0.0792, 0.0923, 0.1027 and 0.0278 eV) for the five compounds mentioned suggest that they have high nucleophility power, meaning that they have a high tendency to donate electrons to electrophilic species.

Moreover, the chemical potential, also known as the electron affinity which is a measure of the energy required to add an electron to a neutral atom or molecule. A negative chemical potential means that the molecule or atom is able to release electrons, suggesting that it is stable and does not undergo decomposition into its individual elements. In the case of all the five compounds mentioned, with negative chemical potential values of -0.1315, -0.1249, -0.1204, -0.1289 and -0.0456, it indicates that these compounds are stable and do not decompose easily. This suggests that these compounds have a low tendency to lose electrons and are less reactive, which is an indicator of stability.

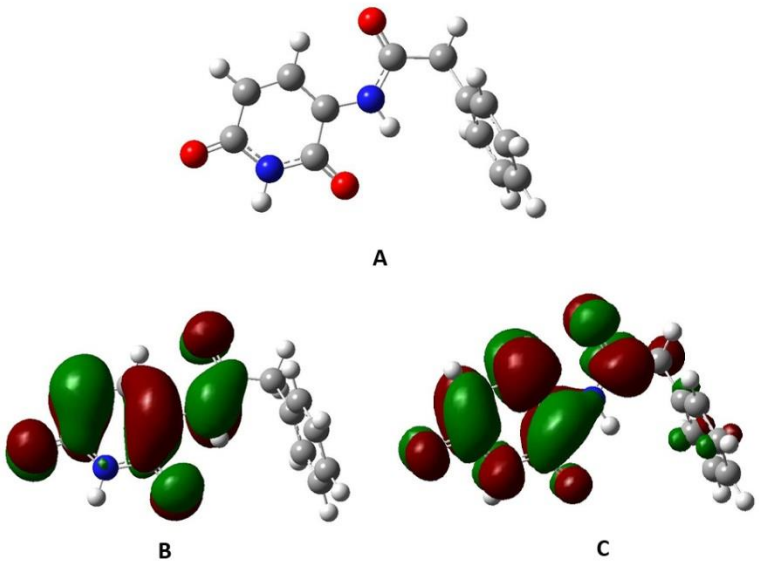


*Figure 38:Structure of Antineoplaston A10 and its frontier molecular orbitals; HOMO and LUMO A) Optimized geometry of Antineoplaston A10 B) HOMO structure of Antineoplaston A10 C) LUMO structure of Antineoplaston A10*

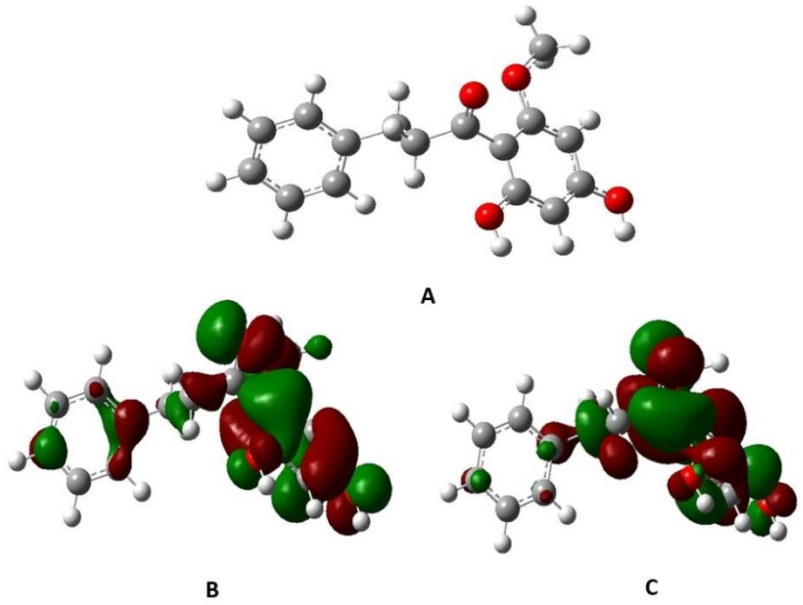


*Figure 39: Structure of Cardamonin and its frontier molecular orbitals; HOMO and LUMO A) Optimized geometry of Cardamonin B) HOMO structure of Cardamonin C) LUMO structure of Cardamonin*

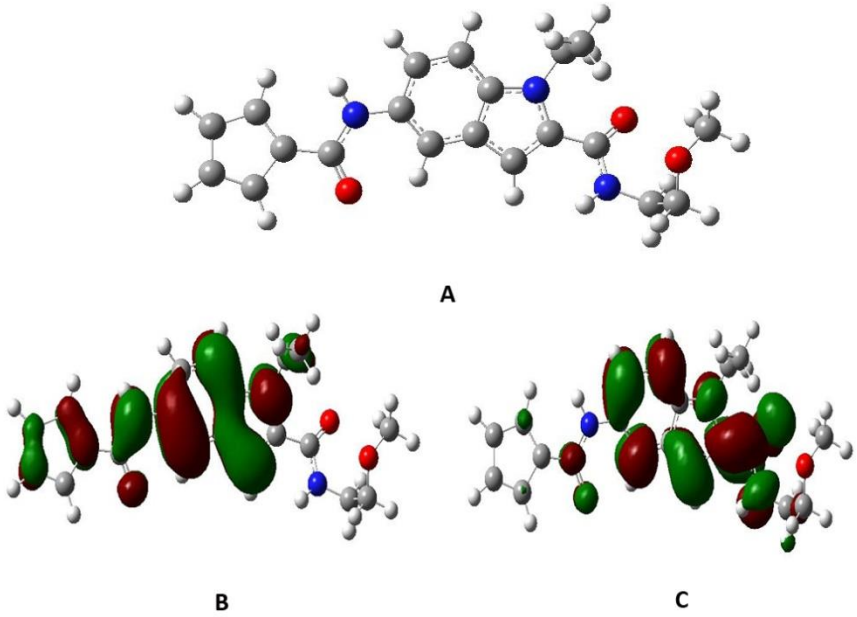


*Figure 40: Structure of indole derivative (5-cyclopentaneamido-1-ethyl-N-(2-methoxyethyl)-1H-indole-2-carboxamide) and its frontier molecular orbitals; HOMO and LUMO A) Optimized geometry of indole derivative B) HOMO structure of indole derivative C) LUMO structure of indole derivative*

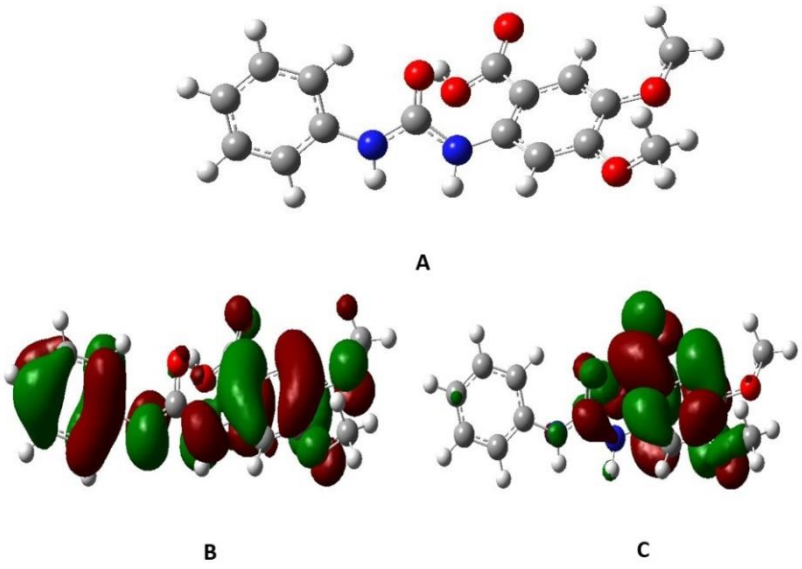


*Figure 41: Structure of Kinase inhibitor (2-[[anilino(oxo)methyl]amino]-4,5-dimethoxybenzoic acid)and its frontier molecular orbitals; HOMO and LUMO A) Optimized geometry of Kinase inhibitor B) HOMO structure of Kinase inhibitor C) LUMO structure of Kinase inhibitor*

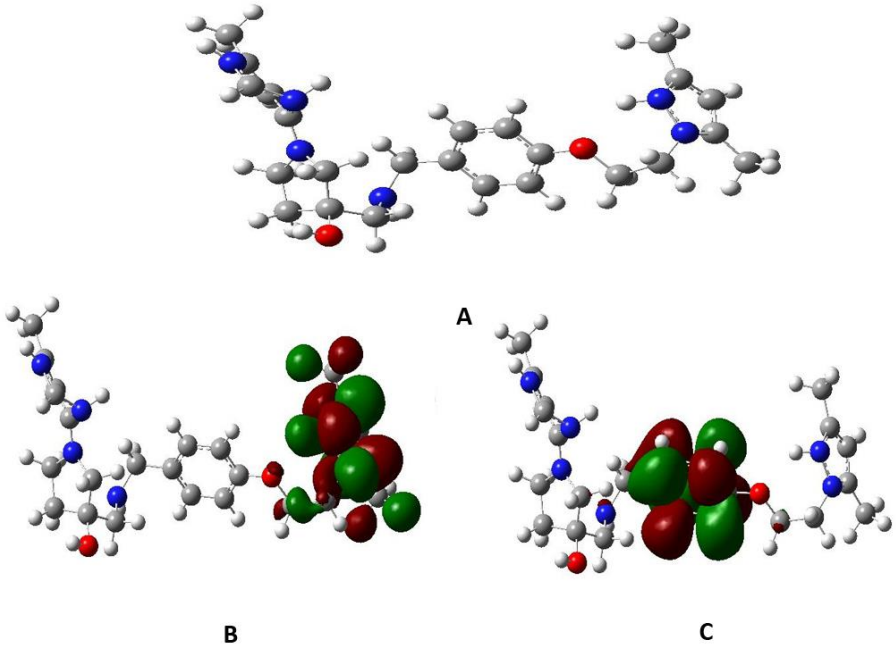


*Figure 42: Structure of Nucleoside Mimetics (3-[[[4-[2-(3,5-Dimethylpyrazol-1-yl)ethoxy]phenyl]methylamino]methyl]-1-(6-methylpyrimidin-4-yl)pyrrolidin-3-ol) and its frontier molecular orbitals; HOMO and LUMO A) Optimized geometry of Nucleoside Mimetics B) HOMO structure of Nucleoside Mimetics C) LUMO structure of Nucleoside Mimetics*

In the above figures, the positive and negative phase of the molecular orbitals is represented by different colors. The color red is used to represent the positive phase and color green is used to represent the negative phase. The atoms that are occupied by more density of HOMO electrons have a stronger ability to detach an electron, while the atoms that are occupied by more density of LUMO electrons have

the ability to gain an electronIn the case of Antineoplaston A10, the HOMO plot shows that atoms around the benzene ring are the most likely to detach an electron. This indicates that the atoms of the benzene ring are the primary electron-donors in the compound. On the other hand, the LUMO, or Lowest Unoccupied Molecular Orbital, plot shows the atoms that have the ability to gain an electron. In the case of Antineoplaston A10, the LUMO plot shows that atoms are more occupied at the lower part of the compound, indicating that these atoms are the primary electron acceptors in the compound. This suggests that the lower part of the compound is more likely to form a chemical bond with another molecule or react in some other way.

The HOMO-LUMO of cardamonin showed that electrons were aggregated at the lower part of the compound i.e. dihydro yphenyl group which illustrated that those atoms are responsible to both accepting and donating electrons. Likewise, it was found that the HOMO plot of indole derivative (5-cyclopentaneamido-1-ethyl-N-(2-methoxyethyl)-1H-indole-2-carboxamide), the electrons were aggregated at the carboxamide and indole moiety group whereas in LUMO plot, the electrons were localized at indole and pentaneamido group. Additionally, in HOMO figure in Kinase inhibitor (2-[[anilino(oxo)methyl]amino]-4,5-dimethoxybenzoic acid) and Nucleoside Mimetics (3-[[[4-[2-(3,5-Dimethylpyrazol-1-yl)ethoxy]phenyl]methylamino]methyl]-1-(6-methylpyrimidin-4-yl)pyrrolidin-3-ol), the electrons were clouded on the entire structure and pyrrolidin group respectively. Similarly, LUMO plot of Kinase inhibitor (2-[[anilino(oxo)methyl]amino]-4,5-dimethoxybenzoic acid) showed electrons were localized at dimethoxybenzoic acid moiety whereas in Nucleoside Mimetics (3-[[[4-[2-(3,5-Dimethylpyrazol-1-yl)ethoxy]phenyl]methylamino]methyl]-1-(6-methylpyrimidin-4-yl)pyrrolidin-3-ol), localized in phenyl moiety.

## 4.10 Molecular electrostatic potential (MEP)

Molecular Electrostatic Potential (MEP) is a useful tool in understanding the relationship between a molecule's structure and its physical and chemical properties. It displays information about the distribution of electrons in a molecule, as well as the positive, negative, and neutral electrostatic potential regions. This information can be represented in the form of a color-coded map, where different regions of the molecule are colored based on their electrostatic potential (Gupta and Sharma, 2006). Different values of the electrostatic potential at the surface are represented by different colors, the regions of the molecule where the electron density is highest are colored blue, and these regions are considered as potential sites for nucleophilic attack. Conversely, regions where the electron density is lowest are colored red, and these regions are considered as potential sites for electrophilic attack. The potential increases in the order red < orange < yellow < green < blue. The color code of the map is usually set in a range of values, where the deepest red color indicates the strongest repulsion and the deepest blue color indicates the strongest attraction (Karabacak *et al.,* 2015). The computer software Gauss view was used to plot the electrostatic potential surface of the title molecule using the DFT/B3LYP/6-31G basis set. Projections of these surfaces along the molecular plane are shown in the figure 59-63. This provides us a visual representation of the chemically active sites and comparative reactivity of atoms which allows us to identify the regions of the

molecule that are most likely to participate in chemical reactions, and can be useful in understanding the mechanism of action of a drug or in designing new molecules with specific properties.

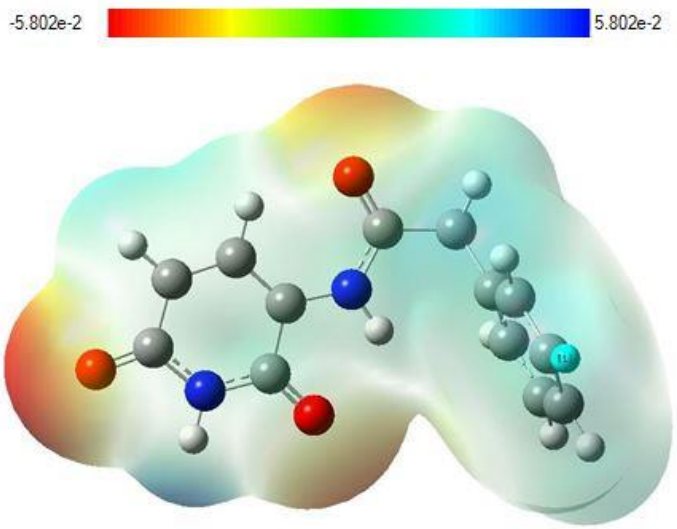


*Figure 43: Electrostatic potential 3D map of Antineoplaston A10*

In this context, the color code of the map was in the range of -5.802 a.u. (deepest red) and 5.802 a.u (deepest blue) for the compound Antineoplaston A10, blue indicating the strongest attraction and red indicating the strongest repulsion. It can be observed in the above figure: 60 that the regions having the negative potential (deepest red colored area) are the C=O groups indicated the strongest repulsion and almost all the other rest atoms indicated the strongest attraction.

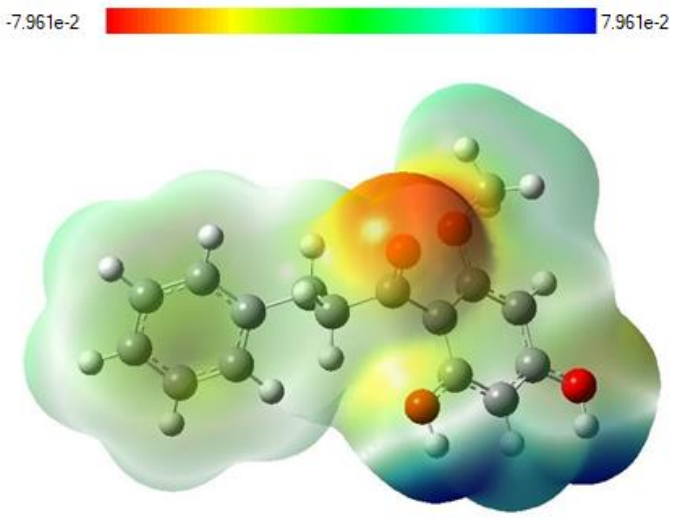


*Figure 44: Electrostatic potential 3D map of cardamonin*

The color code of the map used in the study of Cardamonin had a range of -7.961 a.u. (deepest red) to 7.961 a.u (deepest blue), with blue indicating the strongest

attraction and red indicating the strongest repulsion. It was seen that all C=O groups lied in the deepest red and yellow area means they have the negative potential hence the strongest repulsion. Similarly, other atoms were in green and blue color, the strongest attraction.

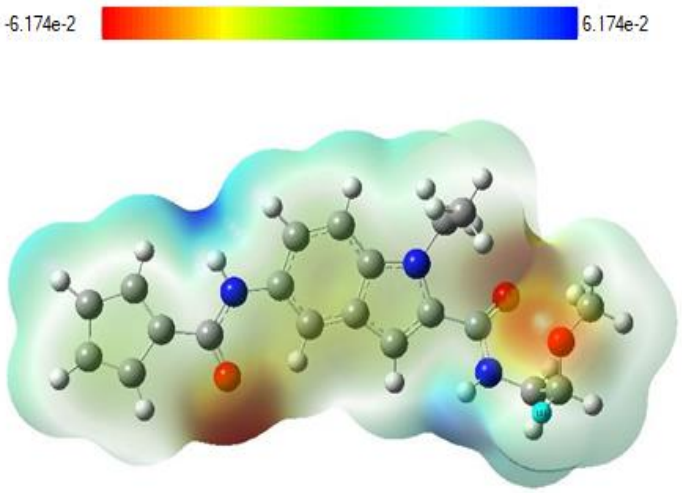


*Figure 45: Electrostatic potential 3D map of indole derivative (5-cyclopentaneamido-1-ethyl-N-(2-methoxyethyl)-1H-indole-2-carboxamide)*

The electrostatic potential map used in the indole derivative (5-cyclopentaneamido-1-ethyl-N-(2-methoxyethyl)-1H-indole-2-carboxamide) study had a color that ranged from -6.174 a.u (deepest red) to 6.174 a.u (deepest blue). Here all the C=O and Oxygen groups were on red area, resulting in negative electrostatic. Similarly, the blue region around the nitrogen indicated positive electrostatic.

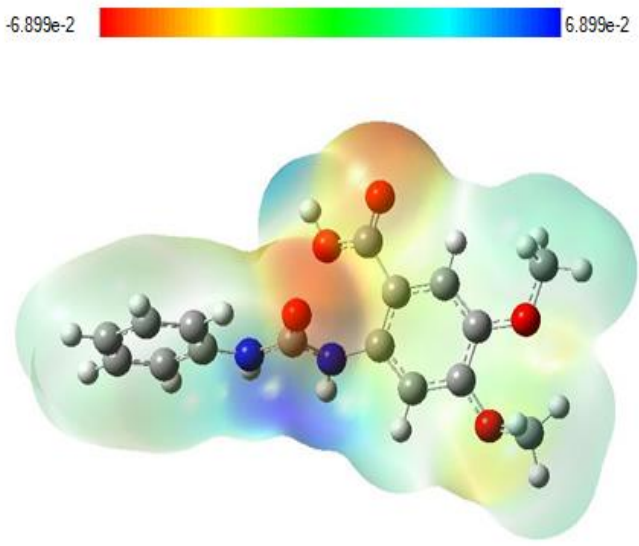


*Figure 46: Electrostatic potential 3D map of Kinase inhibitor (2-[[anilino(oxo)methyl]amino]-4,5-dimethoxybenzoic acid)*

In electrostatic potential map of Kinase inhibitor (2-[[anilino(oxo)methyl]amino]-4,5-dimethoxybenzoic acid) had the color ranged from -6.899 a.u (deepest red) and 6.899 a.u (deepest blue). Here the Oxygen groups of methoxy moiety as well as other C=O groups were on red region and yellow on other Oxygen groups, indicating the strong repulsion. Likewise, NH group of aniline were on dark blue area, meaning they had strong attraction.

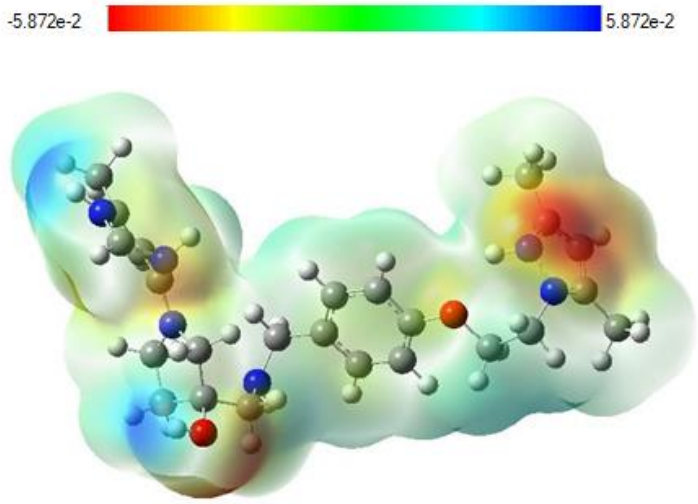


*Figure 47: Electrostatic potential 3D map of Nucleoside Mimetics (3-[[[4-[2-(3,5-Dimethylpyrazol-1-yl)ethoxy]phenyl]methylamino]methyl]-1-(6-methylpyrimidin-4-yl)pyrrolidin-3-ol)*

The Electrostatic potential map of Nucleoside Mimetics (3-[[[4-[2-(3,5-Dimethylpyrazol-1-yl)ethoxy]phenyl]methylamino]methyl]-1-(6-methylpyrimidin-4-yl)pyrrolidin-3-ol) had range from -5.872 a.u (deepest red) and 5.872 a.u (deepest blue). It was seen that the Methyl pyrimidine group were on deep red region while other oxygen atoms and all NH groups were on orange region, signifying the strongest electronegative. Likewise, deep blue color was observed around the Hydrogen groups of Pyrazole and methyl groups, signifying the strongest electropositive.

## 4.11 Infrared spectrum analysis

IR spectroscopy is a technique used to study the vibrations of chemical bonds in a molecule. The IR spectrum of a compound can provide information about the types of functional groups present in the molecule. In this study, the IR spectrum of various compounds was analyzed using the Gauss 03 program and B3LYP/631G basis set. This combination of software and basis set allows for the identification of specific vibrations, such as C-H, C-C, C-O O-H, N-H and C-N within the compound.

### 4.11.1 Vibrational Spectrum Analysis of Antineoplaston A10

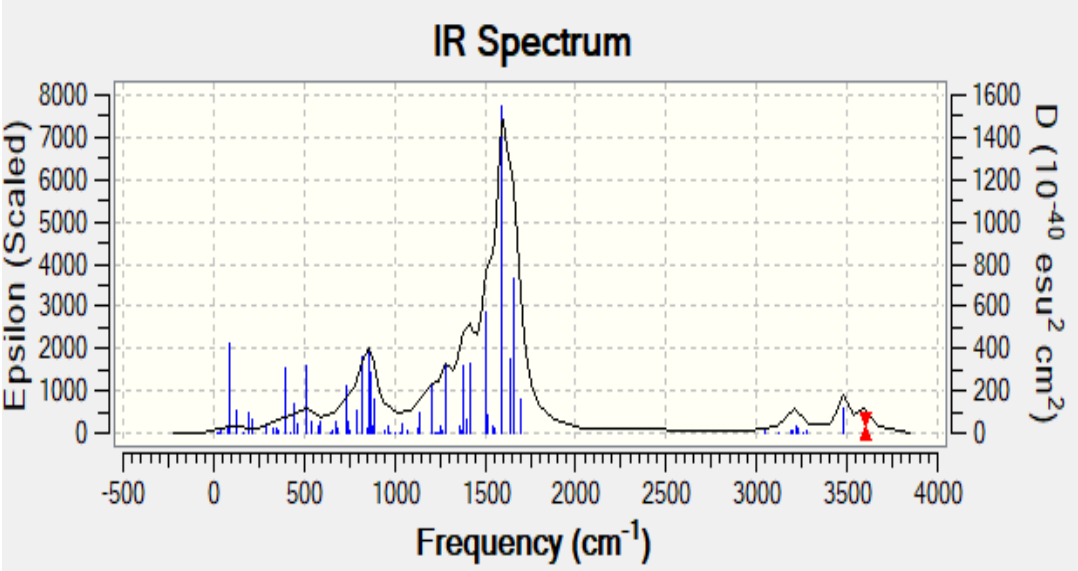


*Figure 48: FTIR spectrum of Antineoplaston A10*

**C-H, C-C , C-O , N-H, C-N Vibration**

C-H vibration of Antineoplaston A10 was observed at 3050, 3124, 3186, 3190, 3204, 3215, 3229 and 3258 $cm^{-1}$. Similarly, C-C vibration of Antineoplaston A10 was observed at 1370, 1507 and 1546, $cm^{-1}$ whereas C-O vibration occurred at 1637, 1659, 1663 and 1697 $cm^{-1}$. Likewise, N-H vibration was observed at 1375 and 1402 $cm^{-1}$. Moreover, C-N vibration was seen at 1256, 1264, 1283 and 1375 $cm^{-1}$

### 4.11.2 Vibrational Spectrum Analysis of Cardamonin

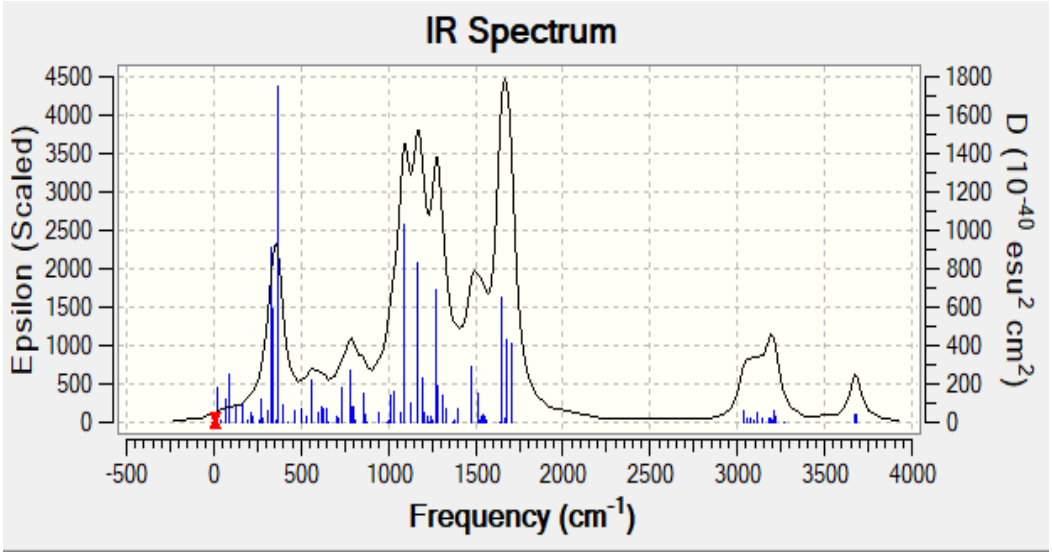


*Figure 49: FTIR spectrum of Cardamonin*

**C-H, C-C, C-O Vibration**

We observed three types of vibration in Cardamonin. The C-H vibration of Cardamonin was found to be at 3041- 3269 $cm^{-1}$. Similarly, C-C vibration was seen at 1663, 1642, 1372 and 1647$cm^{-1}$ whereas C-O vibration was observed at 1702 $cm^{-1}$

### 4.11.3 Vibrational Spectrum Analysis of indole derivative (5-cyclopentaneamido-1-ethyl-N-(2-methoxyethyl)-1H-indole-2-carboxamide)

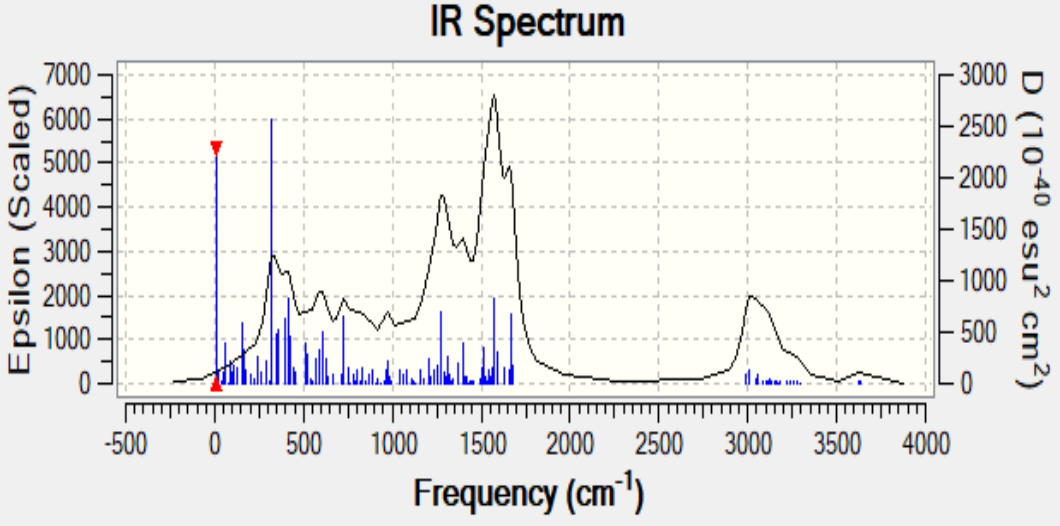


*Figure 50: FTIR spectrum of indole derivative (5-cyclopentaneamido-1-ethyl-N-(2-methoxyethyl)-1H-indole-2-carboxamide)*

**C-H , C-C , C-O, N-H, C-N Vibration**

The C-H vibration of indole derivative (5-cyclopentaneamido-1-ethyl-N-(2-methoxyethyl)-1H-indole-2-carboxamide) was observed in large range from 2990-3296 $cm^{-1}$. Furthermore, C-C vibration was seen at 1132, 1365, 1394, 1410, 1509 and 1505 $cm^{-1}$as well as C-O vibration was visualized at 1664 and 1655 $cm^{-1}$. Additionally, N-H vibration was seen at 3628, and 3638 $cm^{-1}$ whereas C-N vibration was observed at 1444, 1574 and 1590 $cm^{-1}$.

### 4.11.4 Vibrational Spectrum Analysis of Kinase inhibitor (2-[[anilino(oxo)methyl]amino]-4,5-dimethoxybenzoic acid)

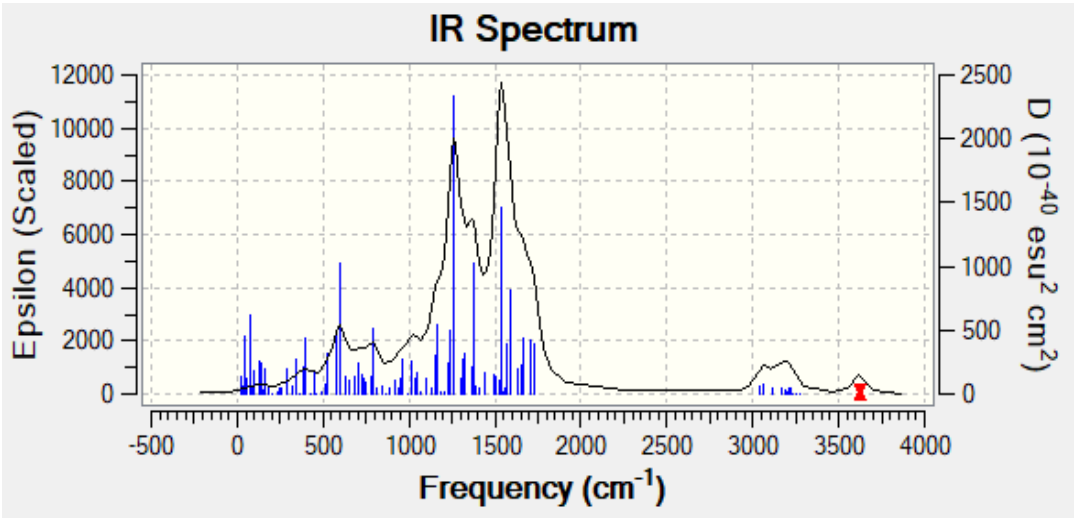


*Figure 51: FTIR spectrum of Kinase inhibitor (2-[[anilino(oxo)methyl]amino]-4,5-dimethoxybenzoic acid)*

**C-H, C-C, C-O, N-H Vibration**

The C-H vibration of Kinase inhibitor (2-[[anilino(oxo)methyl]amino]-4,5-dimethoxybenzoic acid) was observed at 3042, 3066, 3622, 3184, 3278, 3199, 3224, 3229 and 3256, $cm^{-1}$. Moreover, C-C vibration was seen at 1411, 1325, 1627, 1666 and 1664 $cm^{-1}$. Similarly, C-O vibration was observed at 1014, 1094 and 1710 $cm^{-1}$ whereas N-H vibration was visualized at 3613 and 3623 $cm^{-1}$.

### 4.11.5 Vibrational Spectrum Analysis of Nucleoside Mimetics (3-[[[4-[2-(3,5-Dimethylpyrazol-1-yl)ethoxy]phenyl]methylamino]methyl]-1-(6-methylpyrimidin-4-yl)pyrrolidin-3-ol)

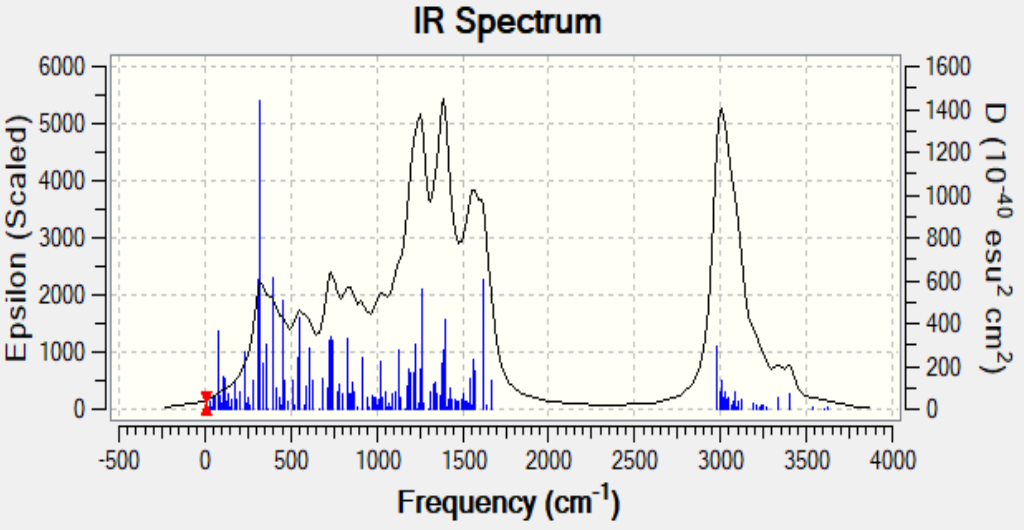


*Figure 52: FTIR spectrum of Nucleoside Mimetics (3-[[[4-[2-(3,5-Dimethylpyrazol-1-yl)ethoxy]phenyl]methylamino]methyl]-1-(6-methylpyrimidin-4-yl)pyrrolidin-3-ol)*

**C-H, C-C, N-H, C-N Vibration**

The C-H and C-C vibration of Nucleoside Mimetics (3-[[[4-[2-(3,5-Dimethylpyrazol-1-yl)ethoxy]phenyl]methylamino]methyl]-1-(6-methylpyrimidin-4-yl)pyrrolidin-3-ol) was observed at 2946, 3188, 3189, 3228, 3233, 3253 3265, 3628, $cm^{-1}$ and 1354, 1474, 1670, 1638 $cm^{-1}$ respectively. In addition, N-H vibration was seen at 3404, 3603, 3333 and 3534$cm^{-1}$ whereas C-N vibration was seen at 1385$cm^{-1}$.

# 5. SUMMARY

The current situation requires the development of alternative to antibiotics as a means of treating infections to curb the worldwide incidence of serious illnesses and death from both acute and chronic infections due to the rise of antibiotic-resistant. Drug researchers and medical professionals are concerned about the growing failure of traditional chemotherapy methods, making it imperative to find new antibiotics to combat current health issues. As a result, many researchers are exploring new techniques for discovering promising therapeutics. One approach gaining popularity in drug discovery is virtual screening, a computational technique that uses molecular docking to predict potential inhibitors of target proteins and was used in this particular study. Molecular docking was used to screen various libraries of ligands, natural products, indole derivatives, kinase inhibitors, and nucleoside mimetics to find out potential inhibitors for the target protein Dam. The lead compounds were then selected based on their Lipinski rule of five, which evaluates drugability and toxicity, mutagenicity, carcinogenicity, teratogenic potential and binding affinity with target protein and hMAT1A.

The results of the study showed that Antineoplaston A10 and Cardamonin from natural products, 5-cyclopentaneamido-1-ethyl-N-(2-methoxyethyl)-1H-indole-2-carboxamide from Indole Derivatives, 2-[[anilino(oxo)methyl]amino]-4,5-dimethoxybenzoic acid from Kinase Inhibitors and 3-[[[4-[2-(3,5-Dimethylpyrazol-1-yl)ethoxy]phenyl]methylamino]methyl]-1-(6-methylpyrimidin-4-yl)pyrrolidin-3-ol from Nucleoside Mimetics , were found to inhibit Dam and showed the highest binding energy compared to other ligands from the same library and low binding affinity with hMAT1A. Those compounds that showed higher binding affinity to hMAT1A were eliminated as they may affect liver health as many drugs are cleared through liver metabolism. Further studies using PyMOL, Discovery Studio, LIGPLOT+, and Gauss 03 revealed strong interactions between the selected compounds and their target proteins, suggesting stability in their complexes. Hence, our findings suggest that using computational methods for drug discovery, known as in silico approaches, is a useful way to sort through large libraries of potential drugs with fewer resources and in short period of time in comparison to traditional screening methods. This makes them particularly useful in addressing the current situation of increasing rates of antibiotic resistance to identify effective inhibitors or antibiotics in a timely manner, which is crucial for controlling the spread of diseases caused by multi-drug resistant strains.

# 6. CONCLUSION

The lead compounds, Antineoplaston A10 and Cardamonin from natural products, 5-cyclopentaneamido-1-ethyl-N-(2-methoxyethyl)-1H-indole-2-carboxamide from Indole Derivatives, 2-[[anilino(oxo)methyl]amino]-4,5-dimethoxybenzoic acid from Kinase Inhibitors and 3-[[[4-[2-(3,5-Dimethylpyrazol-1-yl)ethoxy]phenyl]methylamino]methyl]-1-(6-methylpyrimidin-4-yl)pyrrolidin-3-ol from Nucleoside Mimetics, that were identified in this study underwent a thorough evaluation based on ADME/Tox screening and other drug-like properties. It is assumed that the compounds that passed this screening are considered safe for use. The results of the molecular docking analysis revealed that these compounds exhibited a high binding affinity with the Dam protein, and a low affinity with the hMATA1 protein suggesting that these compounds have the potential to inhibit the Dam protein, which would hinder the pathogenic activity of the pathogens and prevent them from causing infections, while also avoiding any adverse effects on human health.

# 7. RECOMMENDATION

It is suggested that further research be conducted on the lead compounds identified, Antineoplaston A10, Cardamonin, 5-cyclopentaneamido-1-ethyl-N-(2-methoxyethyl)-1H-indole-2-carboxamide, 2-[[anilino(oxo)methyl]amino]-4,5-dimethoxybenzoic acid and 3-[[[4-[2-(3,5-Dimethylpyrazol-1-yl)ethoxy]phenyl]methylamino]methyl]-1-(6-methylpyrimidin-4-yl)pyrrolidin-3-ol, based on their physiochemical and enzyme kinetics. Further, invitro testing, toxicity testing could be done in order to further verify these potential leads as antibiotics

# REFERENCES


Abdelaziz, S. M., Aboshanab, K. M., Yahia, I. S., Yassien, M. A., & Hassouna, N. A. (2021). Correlation between the Antibiotic Resistance Genes and Susceptibility to Antibiotics among the Carbapenem-Resistant Gram-Negative Pathogens. *Antibiotics (Basel, Switzerland)*, *10*(3), 255. https://doi.org/10.3390/antibiotics10030255

Abebe, G. M. (2020). The role of bacterial biofilm in antibiotic resistance and food contamination. *International Journal of Microbiology*, *2020*, 1–10. https://doi.org/10.1155/2020/1705814

Abrahamian, E., Fox, P. C., Naerum, L., Christensen, I. T., Thøgersen, H., & Clark, R. D. (2003). Efficient generation, storage, and manipulation of fully flexible pharmacophore multiplets and their use in 3-D similarity searching. *Journal of chemical information and computer sciences*, *43*(2), 458–468. https://doi.org/10.1021/ci025595r

Acharya, C., Coop, A., Polli, J. E., & Mackerell, A. D., Jr (2011). Recent advances in ligand-based drug design: relevance and utility of the conformationally sampled pharmacophore approach. *Current computer-aided drug design*, *7*(1), 10–22. https://doi.org/10.2174/157340911793743547

Adato, O., Ninyo, N., Gophna, U., & Snir, S. (2015). Detecting horizontal gene transfer between closely related taxa. *PLOS Computational Biology*, *11*(10). https://doi.org/10.1371/journal.pcbi.1004408

Adhikari, U., & Scheiner, S. (2013). Magnitude and mechanism of charge enhancement of CH··O hydrogen bonds. *The journal of physical chemistry. A*, *117*(40), 10551–10562. https://doi.org/10.1021/jp4081788

Alekshun, M. N., & Levy, S. B. (2007). Molecular mechanisms of antibacterial multidrug resistance. Cell, *128*(6), 1037–1050. https://doi.org/10.1016/j.cell.2007.03.004

Aljanaby, A. A., & Aljanaby, I. A. (2018). Prevalence of aerobic pathogenic bacteria isolated from patients with burn infection and their antimicrobial susceptibility patterns in Al-Najaf City, iraq- a three-year cross-sectional study. *F1000Research*, *7*, 1157. https://doi.org/10.12688/f1000research.15088.1

Allen, W. J., Balius, T. E., Mukherjee, S., Brozell, S. R., Moustakas, D. T., Lang, P. T., Case, D. A., Kuntz, I. D., & Rizzo, R. C. (2015). DOCK 6: Impact of new features and current docking performance. *Journal of computational chemistry*, *36*(15), 1132–1156. https://doi.org/10.1002/jcc.23905

Alsayed, S. S., Lun, S., Bailey, A. W., Suri, A., Huang, C.-C., Mocerino, M., Payne, A., Sredni, S. T., Bishai, W. R., & Gunosewoyo, H. (2021). Design, synthesis and evaluation of novel indole-2-carboxamides for growth inhibition of *mycobacterium tuberculosis* and paediatric brain tumour cells. *RSC Advances*, *11*(26), 15497–15511. https://doi.org/10.1039/d0ra10728j

Amaning Danquah, C., Osei-Djarbeng, S., Appiah, T., Duah Boakye, Y., & Adu, F. (2020). Combating biofilm and quorum sensing: A new strategy to fight infections. *Bacterial Biofilms*. https://doi.org/10.5772/intechopen.89227

Anderl, J. N., Franklin, M. J., & Stewart, P. S. (2000). Role of antibiotic penetration limitation in Klebsiella pneumoniae biofilm resistance to ampicillin and ciprofloxacin. *Antimicrobial agents and chemotherapy, 44(7),* 1818–1824. https://doi.org/10.1128/AAC.44.7.1818-1824.2000

Anderson, M. J., Parks, P. J., & Peterson, M. L. (2013). A mucosal model to study microbial biofilm development and anti-biofilm therapeutics. *Journal of microbiological methods, 92(2),* 201–208. https://doi.org/10.1016/j.mimet.2012.12.003

Andersson, D. I., Nicoloff, H., & Hjort, K. (2019). Mechanisms and clinical relevance of bacterial heteroresistance. *Nature reviews. Microbiology*, *17*(8), 479–496. https://doi.org/10.1038/s41579-019-0218-1

Antonoplis, A., Zang, X., Wegner, T., Wender, P. A., & Cegelski, L. (2019). Vancomycin-Arginine Conjugate Inhibits Growth of Carbapenem-Resistant *E. coli* and Targets Cell-Wall Synthesis. *ACS chemical biology*, *14*(9), 2065–2070. https://doi.org/10.1021/acschembio.9b00565

Ashburn, T. T., & Thor, K. B. (2004). Drug repositioning: identifying and developing new uses for existing drugs. *Nature reviews. Drug discovery*, *3*(8), 673–683. https://doi.org/10.1038/nrd1468

Aslam, B., Wang, W., Arshad, M. I., Khurshid, M., Muzammil, S., Rasool, M. H., Nisar, M. A., Alvi, R. F., Aslam, M. A., Qamar, M. U., Salamat, M. K. F., & Baloch, Z. (2018). Antibiotic resistance: a rundown of a global crisis. *Infection and drug resistance*, *11*, 1645–1658. https://doi.org/10.2147/IDR.S173867

Aslam, B., Wang, W., Arshad, M. I., Khurshid, M., Muzammil, S., Rasool, M. H., Nisar, M. A., Alvi, R. F., Aslam, M. A., Qamar, M. U., Salamat, M. K. F., & Baloch, Z. (2018). Antibiotic resistance: a rundown of a global crisis. *Infection and drug resistance*, *11*, 1645–1658. https://doi.org/10.2147/IDR.S173867

Bagge, N., Hentzer, M., Andersen, J. B., Ciofu, O., Givskov, M., & Høiby, N. (2004). Dynamics and spatial distribution of beta-lactamase expression in Pseudomonas aeruginosa biofilms. *Antimicrobial agents and chemotherapy, 48(4)*, 1168–1174. https://doi.org/10.1128/AAC.48.4.1168-1174.2004

Baig, M. H., Ahmad, K., Roy, S., Ashraf, J. M., Adil, M., Siddiqui, M. H., Khan, S., Kamal, M. A., Provazník, I., & Choi, I. (2016). Computer Aided Drug Design: Success and Limitations. *Current pharmaceutical design*, *22*(5), 572–581. https://doi.org/10.2174/1381612822666151125000550

Balbontín, R., Rowley, G., Pucciarelli, M. G., López-Garrido, J., Wormstone, Y., Lucchini, S., García-Del Portillo, F., Hinton, J. C., & Casadesús, J. (2006). DNA adenine methylation regulates virulence gene expression in Salmonella enterica serovar Typhimurium. *Journal of bacteriology, 188*(23), 8160–8168. https://doi.org/10.1128/JB.00847-06

Baldwin R. L. (2007). Energetics of protein folding. *Journal of molecular biology*, *371*(2), 283–301. https://doi.org/10.1016/j.jmb.2007.05.078

Bartlett, J. G., Gilbert, D. N., & Spellberg, B. (2013). Seven ways to preserve the miracle of antibiotics. *Clinical infectious diseases : an official publication of the Infectious Diseases Society of America,* *56*(10), 1445–1450. https://doi.org/10.1093/cid/cit070

Bartuzi, D., Kaczor, A., Targowska-Duda, K., & Matosiuk, D. (2017). Recent advances and applications of molecular docking to G protein-coupled receptors. *Molecules*, *22*(2), 340. https://doi.org/10.3390/molecules22020340

Beaumont, C., Young, G. C., Cavalier, T., & Young, M. A. (2014). Human absorption, distribution, metabolism and excretion properties of drug molecules: A plethora of approaches. *British Journal of Clinical Pharmacology*, *78*(6), 1185–1200. https://doi.org/10.1111/bcp.12468

Bergerat, A., Guschlbauer, W., & Fazakerley, G. V. (1991). Allosteric and catalytic binding of S-adenosylmethionine to Escherichia coli DNA adenine methyltransferase monitored by 3H NMR. *Proceedings of the National Academy of Sciences of the United States of America*, *88*(15), 6394–6397. https://doi.org/10.1073/pnas.88.15.6394

Blair, J. M., Webber, M. A., Baylay, A. J., Ogbolu, D. O., & Piddock, L. J. (2015). Molecular mechanisms of antibiotic resistance. *Nature reviews. Microbiology*, *13*(1), 42–51. https://doi.org/10.1038/nrmicro3380

Blattner, F. R., Plunkett, G., 3rd, Bloch, C. A., Perna, N. T., Burland, V., Riley, M., Collado-Vides, J., Glasner, J. D., Rode, C. K., Mayhew, G. F., Gregor, J., Davis, N. W., Kirkpatrick, H. A., Goeden, M. A., Rose, D. J., Mau, B., & Shao, Y. (1997). The complete genome sequence of Escherichia coli K-12. *Science (New York, N.Y.), 277*(5331), 1453–1462. https://doi.org/10.1126/science.277.5331.1453

Blizzard, T. A., Chen, H., Kim, S., Wu, J., Bodner, R., Gude, C., Imbriglio, J., Young, K., Park, Y. W., Ogawa, A., Raghoobar, S., Hairston, N., Painter, R. E., Wisniewski, D., Scapin, G., Fitzgerald, P., Sharma, N., Lu, J., Ha, S., Hermes, J., … Hammond, M. L. (2014). Discovery of MK-7655, a β-lactamase inhibitor for combination with Primaxin®. *Bioorganic & medicinal chemistry letters, 24*(3), 780–785. https://doi.org/10.1016/j.bmcl.2013.12.101

Blondy, S., David, V., Verdier, M., Mathonnet, M., Perraud, A., & Christou, N. (2020). 5-Fluorouracil resistance mechanisms in colorectal cancer: From classical pathways to promising processes. *Cancer science*, *111*(9), 3142–3154. https://doi.org/10.1111/cas.14532

Brady, G. P., Jr, & Stouten, P. F. (2000). Fast prediction and visualization of protein binding pockets with PASS. *Journal of computer-aided molecular design*, *14*(4), 383–401. https://doi.org/10.1023/a:1008124202956

Breijyeh, Z., Jubeh, B., & Karaman, R. (2020). Resistance of Gram-Negative Bacteria to Current Antibacterial Agents and Approaches to Resolve It. *Molecules (Basel, Switzerland)*, *25*(6), 1340. https://doi.org/10.3390/molecules25061340

Buckner, J. C., Malkin, M. G., Reed, E., Cascino, T. L., Reid, J. M., Ames, M. M., Tong, W. P., Lim, S., & Figg, W. D. (1999). Phase II study of antineoplastons A10 (NSC 648539) and AS2-1 (NSC 620261) in patients with recurrent glioma. *Mayo Clinic proceedings*, *74*(2), 137–145. https://doi.org/10.4065/74.2.137

Burnett, A., Wetzler, M., & Löwenberg, B. (2011). Therapeutic advances in acute myeloid leukemia. *Journal of clinical oncology : official journal of the American Society of Clinical Oncology*, *29*(5), 487–494. https://doi.org/10.1200/JCO.2010.30.1820

Burzynski, S. R., Janicki, T. J., Weaver, R. A., & Burzynski, B. (2006). Targeted therapy with antineoplastons A10 and AS2-1 of high-grade, recurrent, and progressive brainstem glioma. *Integrative cancer therapies*, *5*(1), 40–47. https://doi.org/10.1177/1534735405285380

Caruso, J. A., Campana, R., Wei, C., Su, C.-H., Hanks, A. M., Bornmann, W. G., & Keyomarsi, K. (2014). Indole-3-carbinol and its N-alkoxy derivatives preferentially target erα-positive breast cancer cells. *Cell Cycle*, *13*(16), 2587–2599. https://doi.org/10.4161/15384101.2015.942210

Centers for Disease Control and Prevention. (2021, November 23). *2019 antibiotic resistance threats report*. Centers for Disease Control and Prevention. Retrieved February 9, 2023, from https://www.cdc.gov/drugresistance/biggest-threats.html

Cepas, V., López, Y., Muñoz, E., Rolo, D., Ardanuy, C., Martí, S., Xercavins, M., Horcajada, J. P., Bosch, J., & Soto, S. M. (2019). Relationship Between Biofilm Formation and Antimicrobial Resistance in Gram-Negative Bacteria. *Microbial drug resistance (Larchmont, N.Y.)*, *25*(1), 72–79. https://doi.org/10.1089/mdr.2018.0027

Chagas, C. M., Moss, S., & Alisaraie, L. (2018). Drug metabolites and their effects on the development of adverse reactions: Revisiting Lipinski's Rule of Five. *International journal of pharmaceutics*, *549*(1-2), 133–149. https://doi.org/10.1016/j.ijpharm.2018.07.046

Chavan, B.B., Gadekar, A.S., Mehta, P.P., Vawhal, P.K., Kolsure, A.K., Chabukswar, A.R. (2016). Synthesis and medicinal significance of chalcones—A review. *Asian Journal of Biomedical and Pharmaceutical Sciences, 6*(56), 01-07

Chen, G., Liu, Z., Zhang, Y., Shan, X., Jiang, L., Zhao, Y., He, W., Feng, Z., Yang, S., & Liang, G. (2012). Synthesis and anti-inflammatory evaluation of novel benzimidazole and imidazopyridine derivatives. *ACS Medicinal Chemistry Letters*, *4*(1), 69–74. https://doi.org/10.1021/ml300282t

Chen, L., Morrow, J. K., Tran, H. T., Phatak, S. S., Du-Cuny, L., & Zhang, S. (2012). From laptop to benchtop to bedside: structure-based drug design on protein targets. *Current pharmaceutical design*, *18*(9), 1217–1239. https://doi.org/10.2174/138161212799436386

Colovos, C., & Yeates, T. O. (1993). Verification of protein structures: Patterns of nonbonded atomic interactions. *Protein Science*, *2*(9), 1511–1519. https://doi.org/10.1002/pro.5560020916

Corbeil, C. R., Williams, C. I., & Labute, P. (2012). Variability in docking success rates due to dataset preparation. *Journal of computer-aided molecular design*, *26*(6), 775–786. https://doi.org/10.1007/s10822-012-9570-1

Cosconati, S., Forli, S., Perryman, A. L., Harris, R., Goodsell, D. S., & Olson, A. J. (2010). Virtual Screening with AutoDock: Theory and Practice. *Expert opinion on drug discovery*, *5*(6), 597–607. https://doi.org/10.1517/17460441.2010.484460

Cox, G., & Wright, G. D. (2013). Intrinsic antibiotic resistance: mechanisms, origins, challenges and solutions. *International journal of medical microbiology : IJMM, 303*(6-7), 287–292. https://doi.org/10.1016/j.ijmm.2013.02.009

da Rocha, A. B., Lopes, R. M., & Schwartsmann, G. (2001). Natural products in anticancer therapy. *Current opinion in pharmacology*, *1*(4), 364–369. https://doi.org/10.1016/s1471-4892(01)00063-7

da Silva Guerra, A. S., do Nascimento Malta, D. J., Morais Laranjeira, L. P., Souza Maia, M. B., Cavalcanti Colaço, N., do Carmo Alves de Lima, M., Galdino, S. L., da Rocha Pitta, I., & Gonçalves-Silva, T. (2011). Anti-inflammatory and antinociceptive activities of indole–imidazolidine derivatives. *International Immunopharmacology*, *11*(11), 1816–1822. https://doi.org/10.1016/j.intimp.2011.07.010

Dai, W., Ge, X., Xu, T., Lu, C., Zhou, W., Sun, D., Gong, Y., & Dai, Y. (2018). Two indole-2-carboxamide derivatives attenuate lipopolysaccharide-induced acute lung injury by inhibiting inflammatory response. *Canadian journal of physiology and pharmacology*, *96*(12), 1261–1267. https://doi.org/10.1139/cjpp-2018-0027

Davey, M. E., & O'toole, G. A. (2000). Microbial biofilms: from ecology to molecular genetics. *Microbiology and molecular biology reviews : MMBR*, *64*(4), 847–867. https://doi.org/10.1128/MMBR.64.4.847-867.2000

Del Rio, A., & Varchi, G. (2016). Molecular design of compounds targeting histone methyltransferases. *Epi-Informatics*, 257–272. https://doi.org/10.1016/b978-0-12-802808-7.00009-5

Dheda, K., Gumbo, T., Maartens, G., Dooley, K. E., McNerney, R., Murray, M., Furin, J., Nardell, E. A., London, L., Lessem, E., Theron, G., van Helden, P., Niemann, S., Merker, M., Dowdy, D., Van Rie, A., Siu, G. K., Pasipanodya, J. G., Rodrigues, C., Clark, T. G., … Warren, R. M. (2017). The epidemiology, pathogenesis, transmission, diagnosis, and management of multidrug-resistant, extensively drug-resistant, and incurable tuberculosis. *The Lancet. Respiratory medicine*, S2213-2600(17)30079-6. Advance online publication. https://doi.org/10.1016/S2213-2600(17)30079-6

Dickerson, J. E., Zhu, A., Robertson, D. L., & Hentges, K. E. (2011). Defining the role of essen`tial genes in human disease. *PLoS ONE*, *6*(11). https://doi.org/10.1371/journal.pone.0027368

Dickson, M., & Gagnon, J. P. (2004). Key factors in the rising cost of new drug discovery and development. *Nature reviews. Drug discovery*, *3*(5), 417–429. https://doi.org/10.1038/nrd1382

Dincer, S., Masume Uslu, F., & Delik, A. (2020). Antibiotic resistance in biofilm. *Bacterial Biofilms*. https://doi.org/10.5772/intechopen.92388

Docquier, J. D., & Mangani, S. (2018). An update on β-lactamase inhibitor discovery and development. *Drug resistance updates : reviews and commentaries in antimicrobial and anticancer chemotherapy*, *36*, 13–29. https://doi.org/10.1016/j.drup.2017.11.002

Donelli, G. (2015). *Biofilm-based healthcare-associated infections volume I*. Springer International Publishing.

Duan, J., Dixon, S. L., Lowrie, J. F., & Sherman, W. (2010). Analysis and comparison of 2D fingerprints: insights into database screening performance using eight fingerprint methods. *Journal of molecular graphics & modelling*, *29*(2), 157–170. https://doi.org/10.1016/j.jmgm.2010.05.008

Dudley, J. T., Deshpande, T., & Butte, A. J. (2011). Exploiting drug-disease relationships for computational drug repositioning. *Briefings in bioinformatics*, *12*(4), 303–311. https://doi.org/10.1093/bib/bbr013

Dueger, E. L., House, J. K., Heithoff, D. M., & Mahan, M. J. (2003). Salmonella DNA adenine methylase mutants elicit early and late onset protective immune responses in calves. *Vaccine*, *21*(23), 3249–3258. https://doi.org/10.1016/s0264-410x(03)00252-4

Durán-Iturbide, N. A., Díaz-Eufracio, B. I., & Medina-Franco, J. L. (2020). *in silico* ADME/tox profiling of natural products: A focus on BIOFACQUIM. *ACS Omega*, *5*(26), 16076–16084. https://doi.org/10.1021/acsomega.0c01581

Džidić, S., Šušković, J., & Kos, B. (2008). Antibiotic resistance mechanisms in bacteria: biochemical and genetic aspects. *Food Technology and Biotechnology, 46*, 11-21.

Egan, W. J., Merz, K. M., Jr, & Baldwin, J. J. (2000). Prediction of drug absorption using multivariate statistics. *Journal of medicinal chemistry*, *43*(21), 3867–3877. https://doi.org/10.1021/jm000292e

Ehmann, D. E., Jahić, H., Ross, P. L., Gu, R. F., Hu, J., Kern, G., Walkup, G. K., & Fisher, S. L. (2012). Avibactam is a covalent, reversible, non-β-lactam β-lactamase inhibitor. *Proceedings of the National Academy of Sciences of the United States of America, 109*(29), 11663–11668. https://doi.org/10.1073/pnas.1205073109

Etebu, E., and Arikekpar, I. (2016). Antibiotics: Classification and mechanisms of action with emphasis on molecular perspectives. *International Journal of*

*Applied Microbiology and Biotechnology Research, 4*(2016), 90-101. https://doi.org/10.33500/ijambr.2016.04.011

EU Regulation 528/2012. (2013). Evaluation of active substances. Benzoic acid. Product-type 03 (Veterinary hygiene). Assessment report finalised in the Standing Committee on Biocidal Products, at its meeting on 27 September 2013. pp. 1-74.

European Centre for Disease Prevention and Control. (2013, July 4). *Point prevalence survey of healthcare-associated infections and antimicrobial use in European Acute Care Hospitals 2011-2012* Retrieved February 10, 2023, from https://www.ecdc.europa.eu/en/publications-data/point-prevalence-survey-healthcare-associated-infections-and-antimicrobial-use-0

European Centre for Disease Prevention and Control (ECDC), European Food Safety Authority (EFSA), & European Medicines Agency (EMA) (2017). ECDC/EFSA/EMA second joint report on the integrated analysis of the consumption of antimicrobial agents and occurrence of antimicrobial resistance in bacteria from humans and food-producing animals: Joint Interagency Antimicrobial Consumption and Resistance Analysis (JIACRA) Report. *EFSA journal. European Food Safety Authority*, *15*(7), e04872. https://doi.org/10.2903/j.efsa.2017.4872

Ferreira, L. G., Dos Santos, R. N., Oliva, G., & Andricopulo, A. D. (2015). Molecular docking and structure-based drug design strategies. *Molecules (Basel, Switzerland)*, *20*(7), 13384–13421. https://doi.org/10.3390/molecules200713384

Ferreira, L. G., Dos Santos, R. N., Oliva, G., & Andricopulo, A. D. (2015). Molecular docking and structure-based drug design strategies. *Molecules (Basel, Switzerland)*, *20*(7), 13384–13421. https://doi.org/10.3390/molecules200713384

Fleischmann, R. D., Adams, M. D., White, O., Clayton, R. A., Kirkness, E. F., Kerlavage, A. R., Bult, C. J., Tomb, J. F., Dougherty, B. A., & Merrick, J. M. (1995). Whole-genome random sequencing and assembly of Haemophilus influenzae Rd. Science (New York, N.Y.), 269(5223), 496–512. https://doi.org/10.1126/science.7542800

Freebairn, D., Linton, D., Harkin-Jones, E., Jones, D. S., Gilmore, B. F., & Gorman, S. P. (2013). Electrical methods of controlling bacterial adhesion and biofilm on device surfaces. *Expert review of medical devices, 10(1)*, 85–103. https://doi.org/10.1586/erd.12.70

Friedberg J. W. (2011). Relapsed/refractory diffuse large B-cell lymphoma. *Hematology. American Society of Hematology. Education Program*, *2011*, 498–505. https://doi.org/10.1182/asheducation-2011.1.498

Friedman, M., Henika, P. R., & Mandrell, R. E. (2003). Antibacterial activities of phenolic benzaldehydes and benzoic acids against Campylobacter jejuni, Escherichia coli, Listeria monocytogenes, and Salmonella enterica. *Journal of*

*food protection*, *66*(10), 1811–1821. https://doi.org/10.4315/0362-028x-66.10.1811

Friesner, R. A., Banks, J. L., Murphy, R. B., Halgren, T. A., Klicic, J. J., Mainz, D. T., Repasky, M. P., Knoll, E. H., Shelley, M., Perry, J. K., Shaw, D. E., Francis, P., & Shenkin, P. S. (2004). Glide: a new approach for rapid, accurate docking and scoring. 1. Method and assessment of docking accuracy. *Journal of medicinal chemistry*, *47*(7), 1739–1749. https://doi.org/10.1021/jm0306430

Fux, C. A., Costerton, J. W., Stewart, P. S., & Stoodley, P. (2005). Survival strategies of infectious biofilms. *Trends in microbiology, 13(1)*, 34–40. https://doi.org/10.1016/j.tim.2004.11.010

García-Del Portillo, F., Pucciarelli, M. G., & Casadesús, J. (1999). DNA adenine methylase mutants of Salmonella typhimurium show defects in protein secretion, cell invasion, and M cell cytotoxicity. *Proceedings of the National Academy of Sciences of the United States of America*, *96*(20), 11578–11583. https://doi.org/10.1073/pnas.96.20.11578c

Giacomodonato, M. N., Sarnacki, S. H., Llana, M. N., & Cerquetti, M. C. (2009). Dam and its role in pathogenicity of salmonella enterica. *The Journal of Infection in Developing Countries*, *3*(07), 484–490. https://doi.org/10.3855/jidc.465

Goh, B. C., Hadden, J. A., Bernardi, R. C., Singharoy, A., McGreevy, R., Rudack, T., Cassidy, C. K., & Schulten, K. (2016). Computational methodologies for real-space structural refinement of large macromolecular complexes. *Annual Review of Biophysics*, *45*(1), 253–278. https://doi.org/10.1146/annurev-biophys-062215-011113

Gomes, M. N., Muratov, E. N., Pereira, M., Peixoto, J. C., Rosseto, L. P., Cravo, P. V. L., Andrade, C. H., & Neves, B. J. (2017). Chalcone Derivatives: Promising Starting Points for Drug Design. *Molecules (Basel, Switzerland)*, *22*(8), 1210. https://doi.org/10.3390/molecules22081210

Govindarajan, M., Karabacak, M., Suvitha, A., & Periandy, S. (2012). FT-IR, FT-Raman, ab initio, HF and DFT studies, NBO, HOMO-LUMO and electronic structure calculations on 4-chloro-3-nitrotoluene. *Spectrochimica acta. Part A, Molecular and biomolecular spectroscopy*, *89*, 137–148. https://doi.org/10.1016/j.saa.2011.12.067

Gromiha, M. M., Nagarajan, R., & Selvaraj, S. (2019). Protein structural bioinformatics: An overview. *Encyclopedia of Bioinformatics and Computational Biology,* 445-459. https://doi.org/10.1016/b978-0-12-809633-8.20278-1

Guedes, I. A., Pereira, F. S. S., & Dardenne, L. E. (2018). Empirical Scoring Functions for Structure-Based Virtual Screening: Applications, Critical Aspects, and Challenges. Frontiers in pharmacology, 9, 1089. https://doi.org/10.3389/fphar.2018.01089

Gupta, V. P., & Sharma, A. (2006). Anharmonic analysis of the Vibrational Spectra of some cyanides and related molecules of astrophysical importance.

*Spectrochimica Acta Part A: Molecular and Biomolecular Spectroscopy*, *65*(3-4), 759–769. https://doi.org/10.1016/j.saa.2006.01.006

Hasan, T.H., & AL-Harmoosh, R.A. (2020). Mechanisms of Antibiotics Resistance in Bacteria. *Systematic Reviews in Pharmacy, 11*, 817-823.

He, X., Alian, A., Stroud, R., & Ortiz de Montellano, P. R. (2006). Pyrrolidine carboxamides as a novel class of inhibitors of enoyl acyl carrier protein reductase from Mycobacterium tuberculosis. *Journal of medicinal chemistry*, *49*(21), 6308–6323. https://doi.org/10.1021/jm060715y

Heithoff, D. M., Enioutina, E. Y., Daynes, R. A., Sinsheimer, R. L., Low, D. A., & Mahan, M. J. (2001). Salmonella DNA adenine methylase mutants confer cross-protective immunity. *Infection and immunity*, *69*(11), 6725–6730. https://doi.org/10.1128/IAI.69.11.6725-6730.2001

Hellinger, W. C., & Brewer, N. S. (1991). Imipenem. *Mayo Clinic proceedings, 66*(10), 1074–1081. https://doi.org/10.1016/s0025-6196(12)61732-7

Hendlich, M., Rippmann, F., & Barnickel, G. (1997). LIGSITE: automatic and efficient detection of potential small molecule-binding sites in proteins. Journal of molecular graphics & modelling, 15(6), 359–389. https://doi.org/10.1016/s1093-3263(98)00002-3

Herman, G. E., & Modrich, P. (1982). Escherichia coli dam methylase. Physical and catalytic properties of the homogeneous enzyme. *The Journal of biological chemistry*, *257*(5), 2605–2612.

Heusipp, G., Fälker, S., & Schmidt, M. A. (2007). DNA adenine methylation and bacterial pathogenesis. International journal of medical microbiology : IJMM, 297(1), 1–7. https://doi.org/10.1016/j.ijmm.2006.10.002

Heusipp, G., Fälker, S., & Schmidt, M. A. (2007). DNA adenine methylation and bacterial pathogenesis. *International journal of medical microbiology : IJMM*, *297*(1), 1–7. https://doi.org/10.1016/j.ijmm.2006.10.002

Hobley, G., McKelvie, J. C., Harmer, J. E., Howe, J., Oyston, P. C. F., & Roach, P. L. (2012). Development of rationally designed DNA N6 adenine methyltransferase inhibitors. *Bioorganic & Medicinal Chemistry Letters*, *22*(9), 3079–3082. https://doi.org/10.1016/j.bmcl.2012.03.072

Høiby, N., Bjarnsholt, T., Givskov, M., Molin, S., & Ciofu, O. (2010). Antibiotic resistance of bacterial biofilms. *International journal of antimicrobial agents*, *35*(4), 322–332. https://doi.org/10.1016/j.ijantimicag.2009.12.011

Hopkins, A. L., & Groom, C. R. (2002). The druggable genome. *Nature Reviews Drug Discovery*, *1*(9), 727–730. https://doi.org/10.1038/nrd892

Hou, S., Yang, X., Tong, Y., Yang, Y., Chen, Q., Wan, B., Wei, R., Wang, Y., Zhang, Y., Kong, B., Huang, J., Chen, Y., Lu, T., Hu, Q., & Du, D. (2021). Structure-based discovery of 1H-indole-2-carboxamide derivatives as potent ASK1 inhibitors for potential treatment of ulcerative colitis. *European journal of medicinal chemistry*, *211*, 113114. https://doi.org/10.1016/j.ejmech.2020.113114

Huang, S. Y., Grinter, S. Z., & Zou, X. (2010). Scoring functions and their evaluation methods for protein-ligand docking: recent advances and future directions. Physical chemistry chemical physics : PCCP, 12(40), 12899–12908. https://doi.org/10.1039/c0cp00151a

Irwin J. J. (2008). Using ZINC to acquire a virtual screening library. Current protocols in bioinformatics, Chapter 14, 14.6.1–14.6.23. https://doi.org/10.1002/0471250953.bi1406s22

Jahne, M. A., Rogers, S. W., Ramler, I. P., Holder, E., & Hayes, G. (2015). Hierarchal clustering yields insight into multidrug-resistant bacteria isolated from a cattle feedlot wastewater treatment system. *Environmental monitoring and assessment*, *187*(1), 4168. https://doi.org/10.1007/s10661-014-4168-9

Jain A. N. (2003). Surflex: fully automatic flexible molecular docking using a molecular similarity-based search engine. *Journal of medicinal chemistry*, *46*(4), 499–511. https://doi.org/10.1021/jm020406h

Ji, Y., Zhang, B., Van, S. F., Horn, Warren, P., Woodnutt, G., Burnham, M. K., & Rosenberg, M. (2001). Identification of critical staphylococcal genes using conditional phenotypes generated by antisense RNA. *Science*, *293*(5538), 2266–2269. https://doi.org/10.1126/science.1063566

Johnson, W., Bergfeld, W. F., Belsito, D. V., Hill, R. A., Klaassen, C. D., Liebler, D. C., Marks, J. G., Shank, R. C., Slaga, T. J., Snyder, P. W., & Andersen, F. A. (2017). Safety assessment of benzyl alcohol, benzoic acid and its salts, and benzyl benzoate. *International Journal of Toxicology*, *36*(3_suppl). https://doi.org/10.1177/1091581817728996

Jones, G., Willett, P., Glen, R. C., Leach, A. R., & Taylor, R. (1997). Development and validation of a genetic algorithm for flexible docking. *Journal of molecular biology*, *267*(3), 727–748. https://doi.org/10.1006/jmbi.1996.0897

Jorgensen, W. L. (2009). Efficient drug lead discovery and Optimization. *Accounts of Chemical Research*, *42*(6), 724–733. https://doi.org/10.1021/ar800236t

Jørgensen, A. M., & Pedersen, J. T. (2001). Structural diversity of small molecule libraries. *Journal of chemical information and computer sciences*, *41*(2), 338–345. https://doi.org/10.1021/ci000111h

Juhas, M., Reuß, D. R., Zhu, B., & Commichau, F. M. (2014). Bacillus subtilis and escherichia coli essential genes and minimal cell factories after one decade of genome engineering. *Microbiology*, *160*(11), 2341–2351. https://doi.org/10.1099/mic.0.079376-0

Julio, S. M., Heithoff, D. M., Provenzano, D., Klose, K. E., Sinsheimer, R. L., Low, D. A., & Mahan, M. J. (2001). DNA adenine methylase is essential for viability and plays a role in the pathogenesis of *yersinia pseudotuberculosis* and *vibrio cholerae*. *Infection and Immunity*, *69*(12), 7610–7615. https://doi.org/10.1128/iai.69.12.7610-7615.2001

Kadhum, H. A., and Hasan, T. H. 2019. The Study of Bacillus Subtils Antimicrobial Activity on Some of the Pathological Isolates. *International Journal of Drug Delivery Technology, 9*(02), 193-19

Kagami, L. P., das Neves, G. M., Timmers, L. F. S. M., Caceres, R. A., & Eifler-Lima, V. L. (2020). Geo-Measures: A PyMOL plugin for protein structure ensembles analysis. *Computational biology and chemistry*, *87*, 107322. Advance online publication. https://doi.org/10.1016/j.compbiolchem.2020.107322

Kapetanovic I. M. (2008). Computer-aided drug discovery and development (CADDD): in silico-chemico-biological approach. Chemico-biological interactions, 171(2), 165–176. https://doi.org/10.1016/j.cbi.2006.12.006

Karabacak, M., Bilgili, S., & Atac, A. (2015). Molecular structure, spectroscopic characterization, HOMO and LUMO analysis of 3,3'-diaminobenzidine with DFT quantum chemical calculations. *Spectrochimica acta. Part A, Molecular and biomolecular spectroscopy*, *150*, 83–93. https://doi.org/10.1016/j.saa.2015.05.013

Katsori, A. M., & Hadjipavlou-Litina, D. (2011). Recent progress in therapeutic applications of chalcones. *Expert opinion on therapeutic patents*, *21*(10), 1575–1596. https://doi.org/10.1517/13543776.2011.596529

Khatoon, Z., McTiernan, C. D., Suuronen, E. J., Mah, T. F., & Alarcon, E. I. (2018). Bacterial biofilm formation on implantable devices and approaches to its treatment and prevention. *Heliyon*, *4*(12), e01067. https://doi.org/10.1016/j.heliyon.2018.e01067

Kitchen, D. B., Decornez, H., Furr, J. R., & Bajorath, J. (2004). Docking and scoring in virtual screening for drug discovery: methods and applications. Nature reviews. Drug discovery, 3(11), 935–949. https://doi.org/10.1038/nrd1549

Kobayashi, K., Ehrlich, S. D., Albertini, A., Amati, G., Andersen, K. K., Arnaud, M., Asai, K., Ashikaga, S., Aymerich, S., Bessieres, P., Boland, F., Brignell, S. C., Bron, S., Bunai, K., Chapuis, J., Christiansen, L. C., Danchin, A., Débarbouillé, M., Dervyn, E., … Ogasawara, N. (2003). Essential *bacillus subtilis* genes. *Proceedings of the National Academy of Sciences*, *100*(8), 4678–4683. https://doi.org/10.1073/pnas.0730515100

Kosar, B., & Albayrak, C. (2011). Spectroscopic investigations and quantum chemical computational study of (E)-4-methoxy-2-[(p-tolylimino)methyl]phenol. *Spectrochimica acta. Part A, Molecular and biomolecular spectroscopy*, *78*(1), 160–167. https://doi.org/10.1016/j.saa.2010.09.016

Kosar, B., & Albayrak, C. (2011). Spectroscopic investigations and quantum chemical computational study of (E)-4-methoxy-2-[(p-tolylimino)methyl]phenol. *Spectrochimica acta. Part A, Molecular and biomolecular spectroscopy*, *78*(1), 160–167. https://doi.org/10.1016/j.saa.2010.09.016

Kubinyi, H. (n.d.). Hydrogen bonding: The last mystery in drug design? *Pharmacokinetic Optimization in Drug Research*, 513–524. https://doi.org/10.1002/9783906390437.ch28

Küçükgüzel, Ş. G., & Şenkardeş, S. (2015). Recent advances in bioactive pyrazoles. *European Journal of Medicinal Chemistry*, *97*, 786–815. https://doi.org/10.1016/j.ejmech.2014.11.059

Lane, H. Y., Lin, C. H., Green, M. F., Hellemann, G., Huang, C. C., Chen, P. W., Tun, R., Chang, Y. C., & Tsai, G. E. (2013). Add-on treatment of benzoate for schizophrenia: a randomized, double-blind, placebo-controlled trial of D-amino acid oxidase inhibitor. *JAMA psychiatry*, *70*(12), 1267–1275. https://doi.org/10.1001/jamapsychiatry.2013.2159

Laskowski R. A. (1995). SURFNET: a program for visualizing molecular surfaces, cavities, and intermolecular interactions. Journal of molecular graphics, 13(5), 323–308. https://doi.org/10.1016/0263-7855(95)00073-9

Laskowski, R. A., & Swindells, M. B. (2011). LigPlot+: multiple ligand-protein interaction diagrams for drug discovery. Journal of chemical information and modeling, 51(10), 2778–2786. https://doi.org/10.1021/ci200227u

Laskowski, R. A., MacArthur, M. W., Moss, D. S., & Thornton, J. M. (1993). Procheck: A program to check the stereochemical quality of protein structures. *Journal of Applied Crystallography*, *26*(2), 283–291. https://doi.org/10.1107/s0021889892009944

Lazarus, B., Paterson, D. L., Mollinger, J. L., & Rogers, B. A. (2015). Do human extraintestinal Escherichia coli infections resistant to expanded-spectrum cephalosporins originate from food-producing animals? A systematic review. *Clinical infectious diseases : an official publication of the Infectious Diseases Society of America*, *60*(3), 439–452. https://doi.org/10.1093/cid/ciu785

Le Roux, F., & Blokesch, M. (2018). Eco-evolutionary Dynamics Linked to Horizontal Gene Transfer in Vibrios. *Annual review of microbiology*, *72*, 89–110. https://doi.org/10.1146/annurev-micro-090817-062148

Le, Q. P., Ueda, S., Nguyen, T. N., Dao, T. V., Van Hoang, T. A., Tran, T. T., Hirai, I., Nakayama, T., Kawahara, R., Do, T. H., Vien, Q. M., & Yamamoto, Y. (2015). Characteristics of Extended-Spectrum β-Lactamase-Producing Escherichia coli in Retail Meats and Shrimp at a Local Market in Vietnam. *Foodborne pathogens and disease*, *12*(8), 719–725. https://doi.org/10.1089/fpd.2015.1954

Leiva, R., Barniol-Xicota, M., Codony, S., Ginex, T., Vanderlinden, E., Montes, M., Caffrey, M., Luque, F. J., Naesens, L., & Vázquez, S. (2018). Aniline-Based Inhibitors of Influenza H1N1 Virus Acting on Hemagglutinin-Mediated Fusion. *Journal of medicinal chemistry*, *61*(1), 98–118. https://doi.org/10.1021/acs.jmedchem.7b00908

Levitt, D. G., & Banaszak, L. J. (1992). POCKET: a computer graphics method for identifying and displaying protein cavities and their surrounding amino

acids. Journal of molecular graphics, 10(4), 229–234. https://doi.org/10.1016/0263-7855(92)80074-n

Li, H., Peng, J., Leung, Y., Leung, K. S., Wong, M. H., Lu, G., & Ballester, P. J. (2018). The Impact of Protein Structure and Sequence Similarity on the Accuracy of Machine-Learning Scoring Functions for Binding Affinity Prediction. Biomolecules, 8(1), 12. https://doi.org/10.3390/biom8010012

Li, W., Atkinson, G. C., Thakor, N. S., Allas, U., Lu, C. C., Chan, K. Y., Tenson, T., Schulten, K., Wilson, K. S., Hauryliuk, V., & Frank, J. (2013). Mechanism of tetracycline resistance by ribosomal protection protein Tet(O). Nature communications, 4, 1477. https://doi.org/10.1038/ncomms2470

Liang, J., Edelsbrunner, H., & Woodward, C. (1998). Anatomy of protein pockets and cavities: measurement of binding site geometry and implications for ligand design. Protein science : a publication of the Protein Society, 7(9), 1884–1897. https://doi.org/10.1002/pro.5560070905

Lin, X., Li, X., & Lin, X. (2020). A Review on Applications of Computational Methods in Drug Screening and Design. *Molecules (Basel, Switzerland)*, *25*(6), 1375. https://doi.org/10.3390/molecules25061375

Lionta, E., Spyrou, G., Vassilatis, D., & Cournia, Z. (2014). Structure-based virtual screening for Drug Discovery: Principles, applications and recent advances. *Current Topics in Medicinal Chemistry*, *14*(16), 1923–1938. https://doi.org/10.2174/1568026614666140929124445

Lipinski, C. A., Lombardo, F., Dominy, B. W., & Feeney, P. J. (2001). Experimental and computational approaches to estimate solubility and permeability in drug discovery and development settings. Advanced drug delivery reviews, 46(1-3), 3–26. https://doi.org/10.1016/s0169-409x(00)00129-0

Liu, Z., Tang, L., Zhu, H., Xu, T., Qiu, C., Zheng, S., Gu, Y., Feng, J., Zhang, Y., & Liang, G. (2016). Design, synthesis, and structure–activity relationship study of novel indole-2-carboxamide derivatives as anti-inflammatory agents for the treatment of sepsis. *Journal of Medicinal Chemistry*, *59*(10), 4637–4650. https://doi.org/10.1021/acs.jmedchem.5b02006

López-López, E., Naveja, J. J., & Medina-Franco, J. L. (2019). DataWarrior: an evaluation of the open-source drug discovery tool. Expert opinion on drug discovery, 14(4), 335–341. https://doi.org/10.1080/17460441.2019.1581170

Lounnas, V., Ritschel, T., Kelder, J., McGuire, R., Bywater, R. P., & Foloppe, N. (2013). Current progress in Structure-Based Rational Drug Design marks a new mindset in drug discovery. *Computational and structural biotechnology journal*, *5*, e201302011. https://doi.org/10.5936/csbj.201302011

Low, D. A., Weyand, N. J., & Mahan, M. J. (2001). Roles of DNA adenine methylation in regulating bacterial gene expression and virulence. Infection and immunity, 69(12), 7197–7204. https://doi.org/10.1128/IAI.69.12.7197-7204.2001

Lushniak B. D. (2014). Antibiotic resistance: a public health crisis. Public health reports (Washington, D.C. : 1974), 129(4), 314–316. https://doi.org/10.1177/003335491412900402

Lyngstadaas, A., Løbner-Olesen, A., & Boye, E. (1995). Characterization of three genes in the dam-containing operon of escherichia coli. *Molecular and General Genetics MGG*, *247*(5), 546–554. https://doi.org/10.1007/bf00290345

Mah T. F. (2012). Biofilm-specific antibiotic resistance. *Future microbiology*, *7*(9), 1061–1072. https://doi.org/10.2217/fmb.12.76

Maia, R. T., & Amador, V. C. (2018). Molecular docking for detoxifying enzyme studies. *Molecular Docking*. https://doi.org/10.5772/intechopen.73920

Majeed, H. T., & Aljanaby, A. A. J. (2019). Antibiotic Susceptibility Patterns and Prevalence of Some Extended Spectrum Beta-Lactamases Genes in Gram-Negative Bacteria Isolated from Patients Infected with Urinary Tract Infections in Al-Najaf City, Iraq. *Avicenna journal of medical biotechnology*, *11*(2), 192–201.

Mallipeddi, P. L., Kumar, G., White, S. W., & Webb, T. R. (2014). Recent advances in computer-aided drug design as applied to anti-influenza drug discovery. *Current topics in medicinal chemistry*, *14*(16), 1875–1889. https://doi.org/10.2174/1568026614666140929153812

Manson, J. M., Hancock, L. E., & Gilmore, M. S. (2010). Mechanism of chromosomal transfer of Enterococcus faecalis pathogenicity island, capsule, antimicrobial resistance, and other traits. *Proceedings of the National Academy of Sciences of the United States of America*, *107*(27), 12269–12274. https://doi.org/10.1073/pnas.1000139107

Marinus, M. G. (2000).Recombination Is Essential for Viability of anEscherichia coli dam (DNA Adenine Methyltransferase) Mutant. Journal of Bacteriology Jan 2000, 182 (2) 463-468. https://doi.org/10.1128/JB.182.2.463-468.2000

Mashhoon, N., Pruss, C., Carroll, M., Johnson, P. H., & Reich, N. O. (2006). Selective inhibitors of bacterial DNA adenine methyltransferases. *SLAS Discovery*, *11*(5), 497–510. https://doi.org/10.1177/1087057106287933

McCarthy, A. J., Loeffler, A., Witney, A. A., Gould, K. A., Lloyd, D. H., & Lindsay, J. A. (2014). Extensive horizontal gene transfer during Staphylococcus aureus co-colonization in vivo. *Genome Biology and Evolution*, *6*(10), 2697–2708. https://doi.org/10.1093/gbe/evu214

Meng, X. Y., Zhang, H. X., Mezei, M., & Cui, M. (2011). Molecular docking: a powerful approach for structure-based drug discovery. Current computer-aided drug design, 7(2), 146–157. https://doi.org/10.2174/157340911795677602

Michael, G. B., Butaye, P., Cloeckaert, A., & Schwarz, S. (2006). Genes and mutations conferring antimicrobial resistance in salmonella: An update. *Microbes and Infection*, *8*(7), 1898–1914. https://doi.org/10.1016/j.micinf.2005.12.019

Miller, D. C., Lunn, G., Jones, P., Sabnis, Y., Davies, N. L., & Driscoll, P. (2012). Investigation of the effect of molecular properties on the binding kinetics of a ligand to its biological target. *MedChemComm*, *3*(4), 449. https://doi.org/10.1039/c2md00270a

Mohler, V. L., Heithoff, D. M., Mahan, M. J., Walker, K. H., Hornitzky, M. A., Shum, L. W., Makin, K. J., & House, J. K. (2008). Cross-protective immunity conferred by a DNA adenine methylase deficient Salmonella enterica serovar Typhimurium vaccine in calves challenged with Salmonella serovar Newport. *Vaccine*, *26*(14), 1751–1758. https://doi.org/10.1016/j.vaccine.2008.01.018

Morris, A. L., MacArthur, M. W., Hutchinson, E. G., & Thornton, J. M. (1992). Stereochemical quality of protein structure coordinates. *Proteins*, *12*(4), 345–364. https://doi.org/10.1002/prot.340120407

Morris, G. M., Huey, R., Lindstrom, W., Sanner, M. F., Belew, R. K., Goodsell, D. S., & Olson, A. J. (2009). AutoDock4 and AutoDockTools4: Automated docking with selective receptor flexibility. Journal of computational chemistry, 30(16), 2785–2791. https://doi.org/10.1002/jcc.21256

Morris, G. M., Huey, R., Lindstrom, W., Sanner, M. F., Belew, R. K., Goodsell, D. S., & Olson, A. J. (2009). AutoDock4 and AutoDockTools4: Automated docking with selective receptor flexibility. Journal of computational chemistry, 30(16), 2785–2791. https://doi.org/10.1002/jcc.21256

Muegge, I. (2005). PMF scoring revisited. *Journal of Medicinal Chemistry*, *49*(20), 5895–5902. https://doi.org/10.1021/jm050038s

Mulani, M. S., Kamble, E. E., Kumkar, S. N., Tawre, M. S., & Pardesi, K. R. (2019). Emerging Strategies to Combat ESKAPE Pathogens in the Era of Antimicrobial Resistance: A Review. *Frontiers in microbiology*, *10*, 539. https://doi.org/10.3389/fmicb.2019.00539

Munita, J. M., & Arias, C. A. (2016). Mechanisms of Antibiotic Resistance. *Microbiology spectrum, 4*(2), 10.1128/microbiolspec.VMBF-0016-2015. https://doi.org/10.1128/microbiolspec.VMBF-0016-2015

Munita, J. M., & Arias, C. A. (2016). Mechanisms of Antibiotic Resistance. Microbiology spectrum, 4(2), 10.1128/microbiolspec.VMBF-0016-2015. https://doi.org/10.1128/microbiolspec.VMBF-0016-2015

Ng, W. L., & Bassler, B. L. (2009). Bacterial quorum-sensing network architectures. *Annual review of genetics*, *43*, 197–222. https://doi.org/10.1146/annurev-genet-102108-134304

Ni, L., Meng, C. Q., & Sikorski, J. A. (2004). Recent advances in Therapeutic Chalcones. *Expert Opinion on Therapeutic Patents*, *14*(12), 1669–1691. https://doi.org/10.1517/13543776.14.12.1669

Nick Pace, C., Scholtz, J. M., & Grimsley, G. R. (2014). Forces stabilizing proteins. *FEBS letters*, *588*(14), 2177–2184. https://doi.org/10.1016/j.febslet.2014.05.006

Novick, R. P., & Geisinger, E. (2008). Quorum sensing in staphylococci. *Annual review of genetics*, *42*, 541–564. https://doi.org/10.1146/annurev.genet.42.110807.091640

O'Boyle, N. M., Banck, M., James, C. A., Morley, C., Vandermeersch, T., & Hutchison, G. R. (2011). Open Babel: An open chemical toolbox. Journal of cheminformatics, 3, 33. https://doi.org/10.1186/1758-2946-3-33

Okamoto, T. (2002). A change in PBP1 is involved in amoxicillin resistance of clinical isolates of helicobacter pylori. *Journal of Antimicrobial Chemotherapy*, *50*(6), 849–856. https://doi.org/10.1093/jac/dkf140

Oliver, A., Cantón, R., Campo, P., Baquero, F., & Blázquez, J. (2000). High frequency of hypermutable Pseudomonas aeruginosa in cystic fibrosis lung infection. *Science (New York, N.Y.)*, *288*(5469), 1251–1254. https://doi.org/10.1126/science.288.5469.1251

Orlikova, B., Tasdemir, D., Golais, F., Dicato, M., & Diederich, M. (2011). Dietary chalcones with chemopreventive and chemotherapeutic potential. *Genes & nutrition*, *6*(2), 125–147. https://doi.org/10.1007/s12263-011-0210-5

Ou-Yang, S. S., Lu, J. Y., Kong, X. Q., Liang, Z. J., Luo, C., & Jiang, H. (2012). Computational drug discovery. *Acta pharmacologica Sinica*, *33*(9), 1131–1140. https://doi.org/10.1038/aps.2012.109

Pang, X., & Zhou, H. X. (2017). Rate Constants and Mechanisms of Protein-Ligand Binding. *Annual review of biophysics*, *46*, 105–130. https://doi.org/10.1146/annurev-biophys-070816-033639

Peterson, S. N., & Reich, N. O. (2006). GATC flanking sequences regulate Dam activity: evidence for how Dam specificity may influence pap expression. *Journal of molecular biology*, *355*(3), 459–472. https://doi.org/10.1016/j.jmb.2005.11.003

Petit, J., Meurice, N., Kaiser, C., & Maggiora, G. (2012). Softening the Rule of Five--where to draw the line?. *Bioorganic & medicinal chemistry*, *20*(18), 5343–5351. https://doi.org/10.1016/j.bmc.2011.11.064

Piddock, L. J. V. (1995). Mechanisms of resistance to fluoroquinolones. *Drugs*, *49*(Supplement 2), 29–35. https://doi.org/10.2165/00003495-199500492-00006

Pina, A. S., Hussain, A., & Roque, A. C. (2009). An historical overview of drug discovery. *Methods in molecular biology (Clifton, N.J.)*, *572*, 3–12. https://doi.org/10.1007/978-1-60761-244-5_1

Prentis, R. A., Lis, Y., & Walker, S. R. (1988). Pharmaceutical innovation by the seven UK-owned pharmaceutical companies (1964-1985). British journal of clinical pharmacology, 25(3), 387–396. https://doi.org/10.1111/j.1365-2125.1988.tb03318.x

Price R. (2016). O'Neill report on antimicrobial resistance: funding for antimicrobial specialists should be improved. *European journal of hospital pharmacy :*

*science and practice*, *23*(4), 245–247. https://doi.org/10.1136/ejhpharm-2016-001013

Prieto, A. I., Ramos-Morales, F., & Casadesús, J. (2004). Bile-induced DNA damage in Salmonella enterica. *Genetics*, *168*(4), 1787–1794. https://doi.org/10.1534/genetics.104.031062

Pucciarelli, M. G., Prieto, A. I., Casadesús, J., & Garcı A-Del Portillo, F. (2002). Envelope instability in DNA adenine methylase mutants of Salmonella enterica. *Microbiology (Reading, England)*, *148*(Pt 4), 1171–1182. https://doi.org/10.1099/00221287-148-4-1171

Puiu, R. A., Dolete, G., Ene, A.-M., Nicoară, B., Vlăsceanu, G. M., Holban, A. M., Grumezescu, A. M., & Bolocan, A. (2017). Properties of biofilms developed on medical devices. *Biofilms and Implantable Medical Devices*, 25–46. https://doi.org/10.1016/b978-0-08-100382-4.00002-2

Pushpakom, S., Iorio, F., Eyers, P. A., Escott, K. J., Hopper, S., Wells, A., Doig, A., Guilliams, T., Latimer, J., McNamee, C., Norris, A., Sanseau, P., Cavalla, D., & Pirmohamed, M. (2019). Drug repurposing: progress, challenges and recommendations. *Nature reviews. Drug discovery*, *18*(1), 41–58. https://doi.org/10.1038/nrd.2018.168

Rajan, S., Baek, K., & Yoon, H. S. (2013). C-H…O hydrogen bonds in FK506-binding protein-ligand interactions. *Journal of molecular recognition : JMR*, *26*(11), 550–555. https://doi.org/10.1002/jmr.2299

Ramachandran, G. N., & Sasisekharan, V. (1968). Conformation of polypeptides and proteins. *Advances in protein chemistry*, *23*, 283–438. https://doi.org/10.1016/s0065-3233(08)60402-7

Rarey, M., Kramer, B., Lengauer, T., & Klebe, G. (1996). A fast flexible docking method using an incremental construction algorithm. *Journal of molecular biology*, *261*(3), 470–489. https://doi.org/10.1006/jmbi.1996.0477

Redgrave, L. S., Sutton, S. B., Webber, M. A., & Piddock, L. J. (2014). Fluoroquinolone resistance: mechanisms, impact on bacteria, and role in evolutionary success. Trends in microbiology, 22(8), 438–445. https://doi.org/10.1016/j.tim.2014.04.007

Revelle, L. K., D'Avignon, D. A., & Wilson, J. A. (1996). 3-[(Phenylacetyl)amino]-2,6-piperidinedione hydrolysis studies with improved synthesis and characterization of hydrolysates. *Journal of pharmaceutical sciences*, *85*(10), 1049–1052. https://doi.org/10.1021/js960120y

Reygaert W. C. (2018). An overview of the antimicrobial resistance mechanisms of bacteria. *AIMS microbiology*, *4*(3), 482–501. https://doi.org/10.3934/microbiol.2018.3.482

Reygaert W. C. (2018). An overview of the antimicrobial resistance mechanisms of bacteria. *AIMS microbiology*, *4*(3), 482–501. https://doi.org/10.3934/microbiol.2018.3.482

Roberts M. C. (2005). Update on acquired tetracycline resistance genes. FEMS microbiology letters, 245(2), 195–203. https://doi.org/10.1016/j.femsle.2005.02.034

Ruiz-Carmona, S., Alvarez-Garcia, D., Foloppe, N., Garmendia-Doval, A. B., Juhos, S., Schmidtke, P., Barril, X., Hubbard, R. E., & Morley, S. D. (2014). rDock: a fast, versatile and open source program for docking ligands to proteins and nucleic acids. *PLoS computational biology*, *10*(4), e1003571. https://doi.org/10.1371/journal.pcbi.1003571

Saini, T., Kumar, S., & Narasimhan, B. (2015). Central Nervous System Activities of Indole Derivatives: An Overview. *Central nervous system agents in medicinal chemistry*, *16*(1), 19–28. https://doi.org/10.2174/1871524915666150608103224

Salloum, S., Tawk, M., & Tayyara, L. (2020). Bacterial resistance to antibiotics and associated factors in two hospital centers in Lebanon from January 2017 to June 2017. *Infection prevention in practice*, *2*(2), 100043. https://doi.org/10.1016/j.infpip.2020.100043

Sánchez-Romero, M. A., Olivenza, D. R., Gutiérrez, G., & Casadesús, J. (2020). Contribution of DNA adenine methylation to gene expression heterogeneity in*salmonella enterica*. *Nucleic Acids Research*, *48*(21), 11857–11867. https://doi.org/10.1093/nar/gkaa730

Sander, T., Freyss, J., von Korff, M., & Rufener, C. (2015). DataWarrior: an open-source program for chemistry aware data visualization and analysis. Journal of chemical information and modeling, 55(2), 460–473. https://doi.org/10.1021/ci500588j

Schreiber, G., Haran, G., & Zhou, H. X. (2009). Fundamental aspects of protein-protein association kinetics. *Chemical reviews*, *109*(3), 839–860. https://doi.org/10.1021/cr800373w

Schwarz, S., Kehrenberg, C., Doublet, B., & Cloeckaert, A. (2004). Molecular basis of bacterial resistance to chloramphenicol and florfenicol. *FEMS microbiology reviews, 28*(5), 519–542. https://doi.org/10.1016/j.femsre.2004.04.001

Seeliger, D., & de Groot, B. L. (2010). Ligand docking and binding site analysis with PyMOL and Autodock/Vina. Journal of computer-aided molecular design, 24(5), 417–422. https://doi.org/10.1007/s10822-010-9352-6

Shapiro, A. B., Gao, N., Jahić, H., Carter, N. M., Chen, A., & Miller, A. A. (2017). Reversibility of Covalent, Broad-Spectrum Serine β-Lactamase Inhibition by the Diazabicyclooctenone ETX2514. ACS infectious diseases, 3(11), 833–844. https://doi.org/10.1021/acsinfecdis.7b00113

Sharma, D., Misba, L., & Khan, A. U. (2019). Antibiotics versus biofilm: An emerging battleground in Microbial Communities. *Antimicrobial Resistance & Infection Control*, *8*(1). https://doi.org/10.1186/s13756-019-0533-3

Sippl M. J. (1993). Recognition of errors in three-dimensional structures of proteins. *Proteins*, *17*(4), 355–362. https://doi.org/10.1002/prot.340170404

Sippl M. J. (1995). Knowledge-based potentials for proteins. *Current opinion in structural biology*, *5*(2), 229–235. https://doi.org/10.1016/0959-440x(95)80081-6

Sippl, M. J. (1993). Recognition of errors in three-dimensional structures of proteins. *Proteins: Structure, Function, and Genetics*, *17*(4), 355–362. https://doi.org/10.1002/prot.340170404

Sixty-eighth world health assembly. (n.d.) *Sixty-eighth world health assembly - world health organization*.. Retrieved February 10, 2023, from https://apps.who.int/gb/ebwha/pdf_files/WHA68-REC1/A68_R1_REC1-en.pdf?ua=1

Sliwoski, G., Kothiwale, S., Meiler, J., & Lowe, E. W. (2013). Computational methods in drug discovery. *Pharmacological Reviews, 66*(1), 334-395. https://doi.org/10.1124/pr.112.007336

Sobolev, O. V., Afonine, P. V., Moriarty, N. W., Hekkelman, M. L., Joosten, R. P., Perrakis, A., & Adams, P. D. (2020). A Global Ramachandran Score Identifies Protein Structures with Unlikely Stereochemistry. *Structure (London, England : 1993)*, *28*(11), 1249–1258.e2. https://doi.org/10.1016/j.str.2020.08.005

Sohns, J. M., Bavendiek, U., Ross, T. L., & Bengel, F. M. (2017). Targeting Cardiovascular Implant Infection: Multimodality and Molecular Imaging. *Circulation. Cardiovascular imaging, 10(12)*, e005376. https://doi.org/10.1161/CIRCIMAGING.117.005376

Sousa, S. F., Fernandes, P. A., & Ramos, M. J. (2006). Protein-ligand docking: current status and future challenges. Proteins, 65(1), 15–26. https://doi.org/10.1002/prot.21082

Spellberg, B., & Gilbert, D. N. (2014). The future of antibiotics and resistance: a tribute to a career of leadership by John Bartlett. Clinical infectious diseases : an official publication of the Infectious Diseases Society of America, 59 Suppl 2(Suppl 2), S71–S75. https://doi.org/10.1093/cid/ciu392

Spellberg, B., Srinivasan, A., & Chambers, H. F. (2016). New Societal Approaches to Empowering Antibiotic Stewardship. JAMA, 315(12), 1229–1230. https://doi.org/10.1001/jama.2016.1346

Stapleton, P. D., & Taylor, P. W. (2002). Methicillin resistance in Staphylococcus aureus: Mechanisms and modulation. *Science Progress*, *85*(1), 57–72. https://doi.org/10.3184/003685002783238870

Stein, R. A., & Chirilă, M. (2014). Characteristics of foodborne hazard and diseases: Pathogenesis and virulence. *Encyclopedia of Food Safety*, 166–182. https://doi.org/10.1016/b978-0-12-378612-8.00061-5

Stewart, P. S., & Costerton, J. W. (2001). Antibiotic resistance of bacteria in biofilms. *Lancet (London, England)*, *358*(9276), 135–138. https://doi.org/10.1016/s0140-6736(01)05321-1

Tan, J. J., Cong, X. J., Hu, L. M., Wang, C. X., Jia, L., & Liang, X. J. (2010). Therapeutic strategies underpinning the development of novel techniques for the treatment of HIV infection. *Drug discovery today*, *15*(5-6), 186–197. https://doi.org/10.1016/j.drudis.2010.01.004

Teillant, A., Gandra, S., Barter, D., Morgan, D. J., & Laxminarayan, R. (2015). Potential burden of antibiotic resistance on surgery and cancer chemotherapy antibiotic prophylaxis in the USA: a literature review and modelling study. *The Lancet. Infectious diseases*, *15*(12), 1429–1437. https://doi.org/10.1016/S1473-3099(15)00270-4

Trott, O., & Olson, A. J. (2010). AutoDock Vina: improving the speed and accuracy of docking with a new scoring function, efficient optimization, and multithreading. *Journal of computational chemistry*, *31*(2), 455–461. https://doi.org/10.1002/jcc.21334

Vasudevan, R. (2014). Biofilms: Microbial cities of scientific significance. *Journal of Microbiology & Experimentation*, *1*(3). https://doi.org/10.15406/jmen.2014.01.00014

Veber, D. F., Johnson, S. R., Cheng, H. Y., Smith, B. R., Ward, K. W., & Kopple, K. D. (2002). Molecular properties that influence the oral bioavailability of drug candidates. *Journal of medicinal chemistry*, *45*(12), 2615–2623. https://doi.org/10.1021/jm020017n

Veerachamy, S., Yarlagadda, T., Manivasagam, G., & Yarlagadda, P. K. (2014). Bacterial adherence and biofilm formation on medical implants: a review. *Proceedings of the Institution of Mechanical Engineers. Part H, Journal of engineering in medicine, 228(10)*, 1083–1099. https://doi.org/10.1177/0954411914556137

Venkatachalam, C. M., Jiang, X., Oldfield, T., & Waldman, M. (2003). LigandFit: a novel method for the shape-directed rapid docking of ligands to protein active sites. *Journal of molecular graphics & modelling*, *21*(4), 289–307. https://doi.org/10.1016/s1093-3263(02)00164-x

Wallace, A. C., Laskowski, R. A., & Thornton, J. M. (1995). LIGPLOT: a program to generate schematic diagrams of protein-ligand interactions. *Protein engineering*, *8*(2), 127–134. https://doi.org/10.1093/protein/8.2.127

Wang, X., Song, K., Li, L., & Chen, L. (2018). Structure-based drug design strategies and challenges. *Current Topics in Medicinal Chemistry*, *18*(12), 998–1006. https://doi.org/10.2174/1568026618666180813152921

Waring M. J. (2010). Lipophilicity in drug discovery. *Expert opinion on drug discovery*, *5*(3), 235–248. https://doi.org/10.1517/17460441003605098

Watt, M. M., Collins, M. S., & Johnson, D. W. (2013). Ion-π interactions in ligand design for anions and main group cations. *Accounts of chemical research*, *46*(4), 955–966. https://doi.org/10.1021/ar300100g

WHO. (2021). *Comprehensive review of the WHO Global Action Plan on Antimicrobial Resistance* (Vol. 1, Issue September).

WHO Association Media Centre. (2015). Sixty-Eighth World Health Assembly. *World Health Organization,* May, 18–26. http://www.who.int/mediacentre/events/governance/wha/en/

WHO Geneva. (2017). Global action plan on antimicrobial resistance. *World Health Organization,* 1–28.

Wiederstein, M., & Sippl, M. J. (2007). Prosa-web: Interactive web service for the recognition of errors in three-dimensional structures of proteins. *Nucleic Acids Research*, *35*(Web Server). https://doi.org/10.1093/nar/gkm290

Wiederstein, M., & Sippl, M. J. (2007). Prosa-web: Interactive web service for the recognition of errors in three-dimensional structures of proteins. *Nucleic Acids Research*, *35*(Web Server). https://doi.org/10.1093/nar/gkm290

Williams, P., & Cámara, M. (2009). Quorum sensing and environmental adaptation in Pseudomonas aeruginosa: a tale of regulatory networks and multifunctional signal molecules. *Current opinion in microbiology*, *12(2)*, 182–191. https://doi.org/10.1016/j.mib.2009.01.00

Wilson, D. N., Hauryliuk, V., Atkinson, G. C., & O'Neill, A. J. (2020). Target protection as a key antibiotic resistance mechanism. *Nature Reviews Microbiology*, *18*(11), 637–648. https://doi.org/10.1038/s41579-020-0386-z

World Health Organization. (2020, October 19). *10 threats to Global Health in 2018*. Medium. Retrieved February 10, 2023, from https://medium.com/who/10-threats-to-global-health-in-2018-232daf0bbef3

World Health Organization. (n.d.). *Global action plan on antimicrobial resistance*. World Health Organization. Retrieved February 7, 2023, from https://www.who.int/publications-detail-redirect/9789241509763

World Health Organization. (n.d.). *Global action plan on antimicrobial resistance*. World Health Organization. Retrieved February 10, 2023, from https://www.who.int/publications-detail-redirect/9789241509763

World Health Organization. (n.d.). *Ten health issues who will tackle this year*. World Health Organization. Retrieved February 10, 2023, from https://www.who.int/news-room/spotlight/ten-threats-to-global-health-in-2019

Wu, S., Liu, J., Liu, C., Yang, A., & Qiao, J. (2020). Quorum sensing for population-level control of bacteria and potential therapeutic applications. *Cellular and molecular life sciences : CMLS,* *77*(7), 1319–1343. https://doi.org/10.1007/s00018-019-03326-8

Ye, Y.-N., Hua, Z.-G., Huang, J., Rao, N., & Guo, F.-B. (2013). CEG: A database of essential Gene Clusters. *BMC Genomics*, *14*(1). https://doi.org/10.1186/1471-2164-14-769

Yuan, S., Chan, H. C. S., & Hu, Z. (2017). Using pymol as a platform for computational drug design. *WIREs Computational Molecular Science*, *7*(2). https://doi.org/10.1002/wcms.1298

Zarb, P., Coignard, B., Griskeviciene, J., Muller, A., Vankerckhoven, V., Weist, K., Goossens, M. M., Vaerenberg, S., Hopkins, S., Catry, B., Monnet, D. L., Goossens, H., & Suetens, C. (2012). The european centre for disease prevention and control (ECDC) pilot point prevalence survey of healthcare-associated infections and antimicrobial use. *In Eurosurveillance* (Vol. 17, Issue 46). https://doi.org/10.2807/ese.17.46.20316-en

Zhang, X., Peng, C., Zhang, G., & Gao, F. (2015). Comparative analysis of essential genes in prokaryotic Genomic Islands. *Scientific Reports*, *5*(1). https://doi.org/10.1038/srep12561

Zhang, Y., Wu, J., Ying, S., Chen, G., Wu, B., Xu, T., Liu, Z., Liu, X., Huang, L., Shan, X., Dai, Y., & Liang, G. (2016). Discovery of new MD2 inhibitor from chalcone derivatives with anti-inflammatory effects in LPS-induced acute lung injury. *Scientific reports*, *6*, 25130. https://doi.org/10.1038/srep25130

Zhong, P., Wu, L., Qian, Y., Fang, Q., Liang, D., Wang, J., Zeng, C., Wang, Y., & Liang, G. (2015). Blockage of ROS and NF-κB-mediated inflammation by a new chalcone L6H9 protects cardiomyocytes from hyperglycemia-induced injuries. *Biochimica et biophysica acta*, *1852*(7), 1230–1241. https://doi.org/10.1016/j.bbadis.2015.02.011

Zhou, P., Huang, J., & Tian, F. (2012). Specific noncovalent interactions at protein-ligand interface: implications for rational drug design. *Current medicinal chemistry*, *19*(2), 226–238. https://doi.org/10.2174/092986712803414150

Zimdahl, R. L. (2015). Antibiotics. *Six Chemicals That Changed Agriculture*, 165–182. https://doi.org/10.1016/b978-0-12-800561-3.00009-2